JYVÄSKYLÄ STUDIES IN COMPUTING
199

M. G. S. Sriyananda

Analysis and Performance of FBMC Techniques with Application to Relay Networks

JYVÄSKYLÄN YLIOPISTO

JYVÄSKYLÄ STUDIES IN COMPUTING 199

M. G. S. Sriyananda

Analysis and Performance of FBMC Techniques with Application to Relay Networks

Esitetään Jyväskylän yliopiston informaatioteknologian tiedekunnan suostumuksella
julkisesti tarkastettavaksi Mattilanniemen A-rakennuksen salissa MaA103
marraskuun 5. päivänä 2014 kello 13.

Academic dissertation to be publicly discussed, by permission of
the Faculty of Information Technology of the University of Jyväskylä,
in Mattilanniemi, hall MaA103, on November 5, 2014 at 13 o'clock.

UNIVERSITY OF JYVÄSKYLÄ

JYVÄSKYLÄ 2014

Analysis and Performance of FBMC Techniques with Application to Relay Networks

JYVÄSKYLÄ STUDIES IN COMPUTING 199

M. G. S. Sriyananda

Analysis and Performance of FBMC Techniques with Application to Relay Networks

UNIVERSITY OF JYVÄSKYLÄ

JYVÄSKYLÄ 2014

Editors
Timo Männikkö
Department of Mathematical Information Technology, University of Jyväskylä
Pekka Olsbo, Ville Korkiakangas
Publishing Unit, University Library of Jyväskylä

URN:ISBN:978-951-39-5661-5
ISBN 978-951-39-5661-5 (PDF)

ISBN 978-951-39-5660-8 (nid.)
ISSN 1456-5390

Jyväskylä University Printing House, Jyväskylä 2014

ABSTRACT

Sriyananda, M. G. S.
Analysis and Performance of FBMC Techniques with Application to Relay Networks
Jyväskylä: University of Jyväskylä, 2014, 142 p.
(Jyväskylä Studies in Computing
ISSN 1456-5390; 199)
ISBN 978-951-39-5660-8 (nid.)
ISBN 978-951-39-5661-5 (PDF)
Finnish summary
Diss.

Filter Bank Multicarrier (FBMC) technique is recognized as one of the potential scheme that is capable of resolving some of the major problems associated with other multicarrier communication techniques like Orthogonal Frequency Division Multiplexing (OFDM). Basic design principles are used for that purpose, recognizing FBMC scheme as an extension to OFDM as well as a separate transmission technique. In addition, increase of throughput in a spectrally efficient manner over other wireless transmission systems is one of the supplementary main aspects addressed by this scheme. This is considered as a crucial objective in order to meet the demand arisen from the ever increasing number of users, upcoming applications and rapidly evolving services. Starting from verification of basic formulation, performance of causal multirate FBMC technique is investigated. Properties of self-interference are comprehensively studied in the first part of the presentation. The performance is evaluated under different fading channel and synchronization conditions. Using the characteristics of self-interference, approximate closed-form expression for bit error rate (BER) is presented in general. Analysis for the Nakagami-*m* channel is presented in the form of asymptotic expressions. The study is extended to analyze the performance over Decode-and-Forward (DF) relay system operated under asymmetric and asynchronous channel conditions. Three main performance measures, viz. BER, outage probability and capacity are used for the performance evaluation. For this purpose, relevant closed-form expressions are also derived. The analysis on the DF FBMC relay system is further extended to synchronous asymmetric scenarios with diversity reception and a maximal-ratio combining (MRC) based receiver is used. The study is made more realistic by considering the correlation effect among antennas. The same three performance measures are used for the study and their approximate closed-form expressions are also developed.

Keywords: Antenna correlation, Asymmetric, Asymptotic, Asynchronous, BER, Causal, Diversity reception, Ergodic capacity, FBMC, Multipath channel, Nakagami-*m*, OFDM, Outage probability, Rayleigh, Relay, Rician, Symmetric, Synchronous

Author	M. G. S. Sriyananda Department of Mathematical Information Technology Faculty of Information Technology University of Jyväskylä FINLAND
Supervisors	Professor R. M. A. P. Rajatheva Department of Communications Engineering Faculty of Information Technology and Electrical Engineering University of Oulu FINLAND
	Professors T. Hämäläinen and T. Ristaniemi Department of Mathematical Information Technology Faculty of Information Technology University of Jyväskylä FINLAND
Reviewers	Professor M. Renfors Department of Electronics and Communications Engineering Faculty of Computing and Electrical Engineering Tampere University of Technology FINLAND
	Professor C. F. Bader SUPELEC Campus of Rennes Brittany FRANCE
Opponent	Professor M. S. Elmusrati Department of Computer Science Faculty of Technology University of Vaasa FINLAND

PREFACE

The study presented in this thesis was carried out at the Department of Mathematical Information Technology, Faculty of Information Technology, University of Jyväskylä, Finland, during the period January 2012 - September 2013. I sincerely acknowledge the Doctoral Program in Computing and Mathematical Sciences (COMAS) for funding this research work. In addition, I thank the Department of Mathematical Information Technology for provision of top-up grants for some of the expenses in several occasions.

I would like to express my profound gratitude and appreciation to my thesis supervisor, Professor Nandana Rajatheva, for his invaluable guidance within the remote collaboration overcoming many of the barriers arisen due to distance between two institutes. Discussions with him, his suggestions and advices paved the way for me to explore widely on literary work creating an automatic thrust towards the forefront the current research under minimum academic supervision.

I specially thank Professor Timo Hämäläinen for hosting me and facilitating my doctoral studies. I gratefully appreciate his encouragements and efforts to support me in numerous ways. Precious contributions rendered by Professor Tapani Ristaniemi to improve and finalize my thesis are highly valued. In addition, I thank both of them for their coordinating functions at certain phases of this investigation comprising the final review process. Giving me opportunity to establish my own remote collaboration is a actually precarious but prudent decision of them which led to a very fruitful research study.

It is a great pleasure and privilege for me to have Professor Markku Renfors from the Tampere University of Technology and Professor Faouzi Bader from the SUPELEC as the reviewers. I am obliged for their endeavors to look at this venture in separate perspectives giving me meticulous and constructive comments to uplift the quality of this thesis at multiple stages of the review process. I am very glad to defend this dissertation against Professor Mohammed Elmusrati from the University of Vaasa while admiring his role as the opponent.

It is a privilege for me to experience the cooperation of the faculty members those who got involved in making this effort a success in numerous ways. Further, I was contented with the assistance of the non-academic staff of the Faculty of Information Technology in various means in a quicker and courteous manner where the services of different secretaries and coordinators can be highlighted with much recognition. I would also like to convey my warmest regards to my colleagues and friends in our faculty for creating a gentle and soothing working atmosphere which I benefited a lot during the stay in Finland for my doctoral studies.

I always respect my genuine teachers, mentors and advisors with utmost honor. They are among the visionaries those who contributed very generously for my advancements since my childhood consisting the era of my early education with the pure intention of gifting and shaping up a valuable global citizen who can serve the world in a gentle and humanitarian way. To be on realistic, they had

no narrow, personal or commercial aspects in rendering that invaluable service.

I extend my sincere and deepest gratitude to my parents and the elder brother for their love and support given throughout my life including this difficult period and the activities I have engaged in. The strong foundation laid by them for my life has always been a great strength not only to face, tolerate and fortify myself against all the foreseen risks and dangers but also to overcome many of the obstacles and barriers.

October 16, 2014 M. G. S. Sriyananda

LIST OF ACRONYMS

Acronym	Definition / Interpretation
AF	Amplify-and-Forward
A-OFDM	Asymmetric-Orthogonal Frequency Division Multiplexing
ARQ	Automatic Repeat Request
AWGN	Additive White Gaussian Noise
BER	Bit Error Rate
BICM-OFDM	Bit-interleaved Coded Modulation-Orthogonal Frequency Division Multiplexing
BPSK	Binary Phase-shift Keying
CDMA	Code Division Multiple Access
CF	Compress-and-Forward
CFO	Carrier Frequency Offset
CI-OFDM	Carrier Interferometry-Orthogonal Frequency Division Multiplexing
CMFB	Cosine-modulated Filter Bank
CMFIRBFB	Cosine-Modulated Finite-Impulse Response Biorthogonal Filter Bank
COFDM	Coded Orthogonal Frequency Division Multiplexing
CoMP	Coordinated Multi-Point
CP	Cyclic Prefix
CP-OFDM	Cyclic Prefix-Orthogonal Frequency Division Multiplexing
CSI	Channel State Information
DF	Decode-and-Forward
DFT	Discrete Fourier Transform
DS-CDMA	Direct Sequence-Code Division Multiple Access
DSRC	Dedicated Short Range Communications
DWMT	Discrete Wavelet Multitone
EGC	Equal-gain Combining
FBMC	Filter Bank Multicarrier
FDE	Frequency-domain Equalization
FDM	Frequency Division Multiplexing
FFT	Fast Fourier Transform
FH-OFDM	Frequency Hopping-Orthogonal Frequency Division Multiplexing
FMT	Filtered Multitone Modulation
FTN	Faster than Nyquist
HDTV	High Definition Television
ICI	Intercarrier Interference, Interchannel Interference
ICSI	Intercarrier and Intersymbol Interference, Interchannel Interference and Intersymbol Interference
IDFT	Inverse Discrete Fourier Transform

Acronym	Definition / Interpretation
IFFT	Inverse Fast Fourier Transform
IOTA	Isotropic Orthogonal Transform Algorithm
ISI	Intersymbol Interference
ITU	International Telecommunication Union
LED	Light Emitting Diode
LTE	Long Term Evolution
mMAC	Multihop Medium Access Control
MB-OFDM	Multiband-Orthogonal Frequency Division Multiplexing
MC-CDMA	Multicarrier-Code Division Multiple Access
MIMO	Multiple-Input Multiple-Output
MRC	Maximal-ratio combining
nG	nth Generation (1G = First Generation, ... , 5G = Fifth Generation)
NPR	Near Perfect Reconstruction
OFDM	Orthogonal Frequency Division Multiplexing
OFDMA	Orthogonal Frequency Division Multiple Access
OFDM-CDMA	Orthogonal Frequency Division Multiplexing-Code Division Multiple Access
OFDM-DMT	Orthogonal Frequency Division Multiplexing-Discrete Multitone
OQAM	Offset Quadrature Amplitude Modulation
PAPR	Peak-to-Average Power Ratio
PC-OFDM	Post-coded Orthogonal Frequency Division Multiplexing
PCSI	Perfect Channel State Information
PDF	Probability Density Function
PLC	Power Line Communication
PSK	Phase-shift Keying
QAM	Quadrature Amplitude Modulation
RQ	Repeat Request
SC-FDE	Single-Carrier Frequency-Domain Equalization
SIMO	Single Input Multiple Output
SINR	Signal-to-Interference-Plus-Noise Ratio
SISO	Single-Input Single-Output
SNR	Signal-to-Noise Ratio
TDD-CDMA	Time Division Duplexing-Code Division Multiple Access
UAV	Unmanned Areal Vehicle
UHDTV	Ultra High Definition Television
VHDTV	Very High Definition Television
V-OFDM	Vector-Orthogonal Frequency Division Multiplexing
WAVE	Wireless Access in Vehicular Environments
W-OFDM	Wavelet-based Orthogonal Frequency Division Multiplexing
ZF	Zero Forcing

LIST OF SYMBOLS AND NOTATIONS

1 Common Symbols, Variables and Notations

Symbol	**Definition / Interpretation**
a_{k_F}	Data symbol on subcarrier k_F in an OFDM transmission
a_m	Data symbol on subcarrier m in an OFDM transmission
$a_{m,n}$	Real data symbol n on subcarrier m
$a_{m',n'}$	Real data symbol n' on subcarrier m'
$a_{m'',n''}$	Real data symbol n'' on subcarrier m''
$\hat{a}'_{m,n}$	An element of estimated real data symbol alphabet for the desired symbol $a_{m,n}$
B_λ	λ^{th} filter coefficient
d_{r_x}	Relative antenna spacing between adjacent antennas at the destination in number of wavelengths
E_b	Energy per bit
$\hbar$	Index for a hop
h_C	Quasi-static Rician channel coefficient
h_{Cl}	Quasi-static Rician channel coefficient for the path l
h_l	Quasi-static channel coefficient for the path l
$h_{\ell,l}$	Quasi-static channel coefficient for the path l for the antenna ℓ
$h_l(t)$	Channel coefficient of the path l at time t
h_N	Quasi-static Nakagami-m channel coefficient
h_{Nl}	Quasi-static Nakagami-m channel coefficient for the path l
h_R	Quasi-static Rayleigh channel coefficient
h_{Rl}	Quasi-static Rayleigh channel coefficient for the path l
$\overline{h}_C$	Average fading power of Rician channel coefficients
$\overline{h}_N$	Average fading power of Nakagami-m channel coefficients
$\overline{h}_R$	Average fading power of Rayleigh channel coefficients
j	$\sqrt{-1}$
k	Discrete domain index for time
k_F	Index for channel tap or IDFT / DFT point in OFDM implementation
$\mathcal{K}_C$	Rician K factor
$\mathcal{K}_{RK}$	Rician K factor in square form
l	Index for a delayed path and a delay step
ℓ	Index for a receive antenna
L	Number of independent paths
L_F	Length of the filter
$L_\hbar$	Number of independent paths for the hop $\hbar$
$\mathcal{L}$	Number of diversity receive antennas
m	Index for subcarriers
m'	Index for subcarriers
m''	Index for subcarriers

Symbol	Definition / Interpretation
m_N	Nakagami shape factor
M	Half of the total number of subcarriers ($2M =$ Total number of subcarriers)
n	Time domain index for real data symbols
n'	Time domain index for real data symbols
n''	Time domain index for real data symbols
n_F	Time domain index for the data symbol that has completed the full filter length
N_F	Number of FFT points and total number of subcarriers for OFDM
p_x	Row-index of the receive antenna correlation matrix
q_x	Column-index of the receive antenna correlation matrix
r	Index used for the Taylor series expansion
$\mathrm{SINR}_{\hbar,th}$	Threshold signal-to-interference-plus-noise ratio for the outage probability of the hop $\hbar$
t	Continuous domain variable for time
T_s	Signaling interval
$\mathbb{Z}^+$	Set of positive integers (including 0)
γ_C	Signal-to-noise ratio value per symbol for Rician channel coefficients
γ_l	Signal-to-noise ratio value per symbol for channel coefficients on the path l
γ_N	Signal-to-noise ratio value per symbol for a Nakagami-m channel coefficients
γ_R	Signal-to-noise ratio value per symbol for Rayleigh channel coefficients
$\overline{\gamma}_C$	Average signal-to-noise value per symbol for the Rician channel
$\overline{\gamma}_N$	Average signal-to-noise value per symbol for the Nakagami-m channel
$\overline{\gamma}_R$	Average signal-to-noise value per symbol for the Rayleigh channel
ϵ	Subcarrier frequency offset
θ_{r_x}	Mean angle of arrival
λ	Index for the filter coefficients
Λ	Overlapping factor
$\sigma_{a_{m,n_F}}$	Variance of the binary symmetric symbol sequence related to a_{m,n_F}
σ_m	Standard deviation to the additive white Gaussian noise on subcarrier m (for OFDM)
$\sigma^2_{r_x}$	Destination angle spread
τ	Small time shift
$\tau_l(t)$	Propagation delay of the path l at time t
$\cdot_{AC}$	A signal or a value after filtering with antenna correlation
$\cdot_{As}$	A value given by an asymptotic expression
$\cdot_{\mathcal{L}}$	A node with $\mathcal{L}$ diversity receive antennas

2 Mathematical Functions and Distributions

Symbol	Definition / Interpretation
$\mathrm{Ei}\left(\cdot\right)$	Exponential integral function
$f\left(x;\mu,\sigma^2\right)$	Probability density function of random variable x in a Gaussian distribution with mean μ and variance σ^2
$f_{h_C}\left(\cdot\right)$	Rician probability density function of variable h_C
$f_{h_N}\left(\cdot\right)$	Nakagami-m probability density function of variable h_N
$f_{h_R}\left(\cdot\right)$	Rayleigh probability density function of variable h_R
$f_{\mathrm{SINR}_{\hbar,m}}\left(\cdot\right)$	Probability density function of sum of two equally weighted gamma variables $\mathrm{SINR}_{\hbar,m}$ related to the transformed Rayleigh channel
$f_{\mathrm{SINR}_{\hbar mh\epsilon}}\left(\cdot\right)$	Probability density function of weighted gamma variable $\mathrm{SINR}_{\hbar mh\epsilon}$ related to the transformed Rayleigh channel
$f_{\mathrm{SINR}_{\ell,\hbar,m}}\left(\cdot\right)$	Probability density function of weighted gamma variable $\mathrm{SINR}_{\ell,\hbar,m}$ related to the transformed Rayleigh channel
$f_{\alpha_{\hbar,w,m,\epsilon}}\left(\cdot\right)$	Probability density function of weighted gamma variable $\alpha_{\hbar,w,m,\epsilon}$ related to the transformed Rayleigh channel
$f_{\alpha_{w,m,\epsilon}}\left(\cdot\right)$	Probability density function of weighted gamma variable $\alpha_{w,m,\epsilon}$ related to the transformed Rayleigh channel
$f_{\gamma_C}\left(\cdot\right)$	Probability density function of signal-to-noise ratio value per symbol γ_C for the Rician channel
$f_{\gamma_{Cl}}\left(\cdot\right)$	Probability density function of signal-to-noise ratio value per symbol on the path l γ_{Cl} for the Rician channel
$f_{\gamma_l}\left(\cdot\right)$	Probability density function of signal-to-noise ratio value per symbol γ_l
$f_{\gamma_N}\left(\cdot\right)$	Probability density function of signal-to-noise ratio value per symbol γ_N for the Nakagami-m channel
$f_{\gamma_{Nl}}\left(\cdot\right)$	Probability density function of signal-to-noise ratio value per symbol on the path l γ_{Nl} for the Nakagami-m channel
$f_{\gamma_R}\left(\cdot\right)$	Probability density function of signal-to-noise ratio value per symbol γ_R for the Rayleigh channel
$f_{\gamma_{Rl}}\left(\cdot\right)$	Probability density function of signal-to-noise ratio value per symbol on the path l γ_{Rl} for the Rayleigh channel
$f_{\gamma_{\Omega_{NL}}}\left(\cdot\right)$	Probability density function in form of Taylor series expansion of squared variable for the Nakagami-m channel with the parameter Ω_{NL}
$f_{\gamma_{\Omega_{RL}}}\left(\cdot\right)$	Probability density function of squared variable for the transformed Rayleigh channel with the parameter Ω_{RL}
$J_0\left(\cdot\right)$	Zero-order Bessel function
$\mathcal{N}\left(\mu,\sigma^2\right)$	A Gaussian distribution with mean μ and variance σ^2
$Q(\cdot)$	Gaussian Q-function
$\Gamma\left(\cdot\right)$	Gamma function
$\Gamma\left(\cdot,\cdot\right)$	Incomplete gamma function
$\delta\left(\cdot\right)$	Dirac delta function

Symbol	Definition / Interpretation
$\delta_{\cdot,\cdot}$	Kronecker delta function

3 Mathematical Operators and Notations

Symbol	Definition / Interpretation
$\operatorname{diag}\{\cdot\}$	Diagonal matrix
$\mathbb{E}[\cdot]$	Expectation operator
$\Im\{\cdot\}$	Operator to extract the imaginary part of a complex valued argument
$\min\{\cdot\}$	The minimum in a set of elements
$\Pr(\cdot)$	Probability of an event
$\Re\{\cdot\}$	Operator to extract the real part of a complex valued argument
$\cdot^T$	Matrix transpose
$\cdot^*$	Complex conjugate
$\cdot!$	Factorial value
$\lvert\cdot\rvert$	Absolute value
$\cdot \sim \cdot$	Distributed according to
$\cdot \in \cdot$	Is an element of
$\hat{\cdot}$	Estimated parameter, value or symbol
$\geq$	Greater than or equal
$\leq$	Less than or equal
$\triangleq$	Is defined as

LIST OF FIGURES

CONTENTS

1 INTRODUCTION

Even though wireless transmission and associated technologies are said to be in mature stages of their life cycles at the moment, thirst for new technologies and higher throughputs has not abated. Now they are extensively connected to most of the infrastructure facilities and they are inseparable from day-to-day activities. Services and operations are enriched with many interdisciplinary applications and cross-functionalities. Even though the massive boom of the past may be over, researchers and developers are still looking for new technologies to improve the existing systems evolving through generations.

1.1 Wireless World

Today's mobile phones are not devices merely used for personal communications. Now they are handheld intelligent computers capable of handling multimedia applications and remotely controlled functionalities. Capability of communication is just one of their features, although a mandatory infrastructure facility. There are many stationary and mobile devices connected in parallel to networks through the wireless interface. These are expected to be even more efficient, user friendly, sophisticated and smarter than is the case now. They will be able to satisfy these expectations by acquiring and / or using remote resources with the aid of sound backing of wireless connectivity. Those resources are in demand and may involve cloud-based processing and functionalities with intelligence and storage. Certain tasks can be processed very quickly and in a smarter manner in remote centralized or distributed systems. Devices may take inputs (e.g., instructions, data) and deliver outputs to respective destinations. This scenario is valid for data storage as well. This results in exchange of data and information that is not confined to man-to-man communication only but includes also man-to-machine, machine-to-man and between machines communications. Most of the appliances and instruments would be networked empowering the concept of "Internet of Things". It is clear that machines also contribute towards the needs of mobility and higher throughputs. Due to this, demand for ubiquitous and heterogeneous networks facilitating the use of those services has massively grown. The trends are on the increase, and there is no any sign of their diminution.

According to current trends and usage patterns, most of the wireless traffic is originated from indoor environments and there is a possibility of increase in that. In that case, most of the transmit signal power is consumed to penetrate buildings and manmade structures. Due to that reason, development of more and more indoor wireless solutions and technically efficient methodologies for short range communications are being highly encouraged rather than enhancements for medium to long range outdoor base stations ever before.

Usually a new generation of wireless telecommunication system is commercially launched in every decade. 1G systems (Nordic Mobile Telephone) were introduced in 1981 and 2G systems were deployed in 1992. 3G and 4G systems were made available for general public in 2001 and 2011 respectively. These technologies have their stages of maturity and decline at some time or another during their life cycles, and it is still not clear whether it would be possible to introduce a truly new generation by 2020. As yet, there is no widely available or accepted concrete and clearly defined set of goals for 5G. But, compared with 4G and LTE networks, 5G is expected to achieve 1,000 times the system capacity, and 25 times the average mobile cell throughput. In addition, energy efficiency, data rate, and spectral efficiency are to be 10 times as the previous generation offering seamless and universal communications anywhere, at any time using different mobile or stationary wireless devices. These different types of network nodes are designed to handle various transmission power levels and data processing capabilities while supporting different radio access technologies.

There is a precisely identified set of candidates for the physical layer structure. This includes massive or large scale multiple-input multiple-output (MIMO), dense small cells, virtual MIMO, multi-tier antenna arrays (including virtual arrays), cognitive and self-configurable techniques, millimeter wave communications, faster than Nyquist (FTN) signaling techniques [1], different types of cooperative communication technologies like relays, interference alignment techniques and multirate filter bank multicarrier (FBMC) transmission techniques. Visible-light communications powered by LED (light emitting diode) sources is another strong candidate for the physical layer air interface, especially an attractive transmission technique for medium to short range and indoor applications, where white LEDs and different types of photodiodes are used as signal transmitters and signal receivers respectively. Currently a single LED system is capable of supporting data rates up to 3.5 gigabytes per second. Device-to-device communication is an upcoming concept where devices close to each other are facilitated to communicate without going through the main network infrastructure, leading to higher efficiency improving spectrum reuse in densely populated scenarios which are the most challenging scenarios due to the spectrum constraints.

There are several design challenges that are being addressed with a considerable support from the upcoming physical layer transmission techniques. The problems of reduction of end-to-end latency, interference and mobility management and flexible use of uplink and downlink resources are also expected to be addressed by some of them.

The future air interface transmission techniques are designed to provide infrastructure facilities for enhanced consumer devices like Very High Definition Television (VHDTV), Ultra High Definition Television (UHDTV) and multiview 3D High Definition Television (HDTV) and for industrial services like business process outsourcing under adverse transmission medium conditions which include higher moving speeds in densely congested wireless environments. More generally, they are to be coexisted and supported by many of the big data related functionalities and numerous emerging smart concepts (e.g., smart grid, smart homes, smart cities and e-health) directly or indirectly including some of the associated applications. Apparently some of the techniques like CoMP (coordinated multipoint), beamforming, relay and some concepts of different cooperative communication strategies used or suggested to be used for versions of 4G are going to be incorporated as enhancing or supportive associated techniques for 5G as well. Data streams traveling through heterogeneous networks are to be supported by different types of backhaul links. For the purpose of achieving the due cost and flexibility of 5G infrastructure facilities, more software-based implementations and virtualization of some network resources are required leading to multiple virtual core networks customized to needs of particular applications.

Since the radio spectrum is a scarce resource, improvements in physical layer throughput enhancement techniques are always in demand where the limit of theoretical channel capacity can be considered as the bound. But in real life activities related to wireless interface is bounded by many factors. These factors include economical, technical and social parameters like return on investment, operational or transmission cost per bit, implementation complexity, technical compatibility of associated technologies and end user demand.

On the other hand there is an inevitable necessity for a reduction in the consumption of fossil fuels. That can be partially answered with moderated consumption of energy generated by them in the sectors of both wire and wireless communication. This constraint can be realized by efficient use of resources combined with the reduction in the overall system complexity. At present, almost all the telecommunication devices with their manufacturing processes, including research and development activities are powered by energy generated by fossil fuels. There is a global trend in all the sectors of engineering, including the telecommunication sector to satisfy all the technical requirements in a greener manner, making a better tomorrow for all the living beings in this planet.

1.2 Wireless Channel

The performance of any communication system over radio channel is a basic element that is looked into when selecting a specific transmission technique for any application or large-scale deployment. It is usually evaluated in terms of average signal-to-noise ratio (SNR), outage probability and bit error probability (alternatively bit error rate (BER)) [2]. Except for a few specific applications related to air interface transmission techniques, fading, shadowing, reflection, refraction, scattering, diffraction and the like processes are considered as unfavorable phenomena when occurring in radio interface. In addition, channel capacity is limited by available bandwidth as well [3]-[5]. Effects due to path loss, the Doppler spread and multipath propagation [6]-[10] are also to be accounted when providing solutions for problems associated with any type of communication technique. These effects are capable of generating additional forms of interferences like intersymbol interference (ISI), intercarrier interference (ICI) and a combination of intercarrier and intersymbol interference (ICSI) [11]. In other words channel characteristics are dependent on multipath fading, the rate of time variation and frequency selectivity. Due to these reasons, air interface is still identified as one of the bottlenecks in mobile and wireless communication, basically in terms of capacity and reliability.

There are four types of fading. They are determined by the bandwidth and symbol period of the transmit signal. When the signal bandwidth is smaller than the coherence bandwidth of the channel, the channel is said to be flat-faded or frequency-flat. Otherwise it is said to exhibit frequency-selective fading. When the symbol period is much shorter than the coherence time, the channel is defined as slow fading. Otherwise, the channel is regarded as fast fading [8], [9]. Frequency-selective fading is seen in high-data rate transmissions. This is due to the wider bandwidth of the transmit signal than bandwidth over which the frequency response of a wireless channel has a constant gain and linear phase. In other words, this is a phenomenon caused by the time dispersion of the transmit symbol within the channel.

1.2.1 Multipath Propagation

Multipath propagation is one of the main phenomenon in a wireless channel. Different replicas of the transmit signal are received through different paths and have distinct properties like distance and attenuation strengths. The delays and the channel coefficient values vary, generating delay and Doppler spreads. The most important parameters of a channel are coherence bandwidth and coherence time [8], [9]. Coherence bandwidth is a statistical measure of the range of frequencies over which a channel can be considered to be flat. Or coherence bandwidth may be the approximate maximum bandwidth or frequency interval over which a comparable or correlated amplitude fading is likely to be experienced by two frequencies of a signal. Again, this is reciprocal to the multipath spread. A multipath channel can be modeled [6], [10] as

$$h\left(\tau, t\right) = \sum_{l=0}^{L-1} h_{l}\left(t\right) \delta\left(\tau - \tau_{l}\left(t\right)\right), \tag{1.1}$$

where $h\left(\tau, t\right)$ is the baseband equivalent channel impulse response of the multipath channel at time t due to an impulse applied at time $t - \tau$. $\delta\left(\cdot\right)$ is the Dirac delta function. In other words, $h(\tau, t)$ is the channel response at time t, due to an impulse applied at time $t - \tau$. τ is a small time shift. $h_l(t)$ and $\tau_l(t)$ are the channel coefficient and the propagation delay of the path l. A multipath channel under quasi-static fading can be represented by

$$h(\tau, t) = \sum_{l=0}^{L-1} h_l \delta(\tau - \tau_l). \tag{1.2}$$

The channel response can be frequency-dependent due to the phase differences of each path with distinct delays. There may be constructive or destructive contributions to the total signal, due to these replicas of the transmit signal, leading to rapid fluctuations of the resultant signal at the receiver [7]. However in the case of modeling, uniform power delay profile is considered. In this case average power of each tap is held as constant and that is the same for all the taps in the delay profile. But in this presentation, in order make the comparisons more fair and realistic, the total power associated with the profile is set to unity.

1.2.2 Intersymbol Interference

Basically, signals arriving through delayed paths as copies of the transmit signal are not helpful for signal detection. They are identified as ISI and make the communication systems less reliable. Most of the times these replicas have less signal power than does the first-arrive signal. Here ISI is a form of signal distortion where one symbol interferes with the subsequent symbols. Further, ISI is a resultant of multipath propagation and frequency-selective fading of the wireless channel [7].

The other main reason for ISI is the transmission of signal through a band-limited channel. In this situation, the frequency response above a certain frequency known as the cutoff frequency is zero. Signals passed outside the band are removed, leading to a new pulse shape for the receive signal. A symbol can be spread over the subsequent symbol periods, due to a change in its pulse shape. Apart from the loss incurred due to the change of the shape of the first symbol, other symbols can also be subjected to severe interference. When a message is transmitted through such channel, the spread pulse of each individual symbol will interfere with the subsequent symbols. Pulse shaping can be used to avoid interference caused by bandwidth limitation. If a channel frequency response is flat and the shaping filter is with a finite bandwidth, it is possible to communicate without generating any ISI at all.

In the design of the transmit and receive filters, attempts are always made to minimize the effects of ISI in general, irrespective of their causes. Other widely used remedial methods to compensate ISI include the use of adaptive equalizers. Channel codes (error correction codes) can also be used to combat ISI [12] or to improve the link performance in the case of imperfect channel equalization. Some communication techniques, mainly in the family of multicarrier communication techniques, are, by design alone, quite robust against ISI. Unfortunately, FBMC is highly susceptible in this respect.

1.2.3 Doppler Effect

The Doppler effect is caused by a shift in the receive signal frequency from that of the original transmit frequency due to differences in relative velocities. The Doppler shift range across the bandwidth of the signal is known as the Doppler spread. The value of the Doppler spread can be considered as a measure of how rapidly the channel impulse response varies in time. Typically, the reason for that is the relative movement between the source and the destination nodes. The coherence time of a channel denotes the period of time within which the channel fading remains correlated above a predetermined threshold. The coherence time is inversely proportional to the Doppler spread [8], [13]. Thus, a slowly fading channel has a large coherence time and a fast fading channel has a small coherence time.

1.3 OFDM and FBMC Systems

Multicarrier communication techniques are among the most successful air interface transmission techniques. Amongst them, orthogonal frequency division multiplexing (OFDM) is identified as the dominant technique in the sphere of broadband wireless communication. Both the techniques of OFDM and those of filter bank multicarrier (FBMC) were selected for this study. That is after considering the, characteristics of many multicarrier communication techniques and other factors, like applicability, usage, deployment and the potential, in order to deal with higher throughputs under complicated and congested air interface conditions. In both techniques, a wide-band frequency-selective channel is divided into an equivalent set of narrow-band frequency-flat orthogonal subchannels while increasing the system throughput compared to conventional non-orthogonal single channel techniques. This is achieved by splitting the input high-rate data stream into a number of substreams. These are transmitted in parallel over a number of subcarriers. Interference between closely-spaced subcarriers is prevented by the property of orthogonality maintained among them; they are even allowed to overlap each other, resulting in very highly spectrum-efficient communication architectures against non-orthogonal techniques.

OFDM or, more precisely, cyclic prefix-orthogonal frequency division multiplexing (CP-OFDM) [6], [14]-[18] is a family of multicarrier transmission techniques enriched with many inherent properties. Efficient use of spectrum, robustness against frequency-selective fading, resistance to both ISI and ICI (with the aid of guard intervals and cyclic prefixes) and capability of being implemented using Fast Fourier Transform (FFT) techniques can be highlighted as some of the key merits of it. The critical and limiting drawbacks of OFDM, however, include higher peak-to-average power ratio (PAPR), higher sensitivity for carrier frequency offset (CFO) errors, larger number of side lobes with non negligible power levels, inevitable overhead due to cyclic prefixes (or guard intervals) and extra time consumed due to guard intervals. Due to these considerations, OFDM is still a commendable and impressive topic where any sort of discussion on transmission techniques takes place. FBMC, which is also known as orthogonal frequency division multiplexing / offset quadrature amplitude modulation (OFDM / OQAM) [11], [19]-[21] is a result of endeavors to overcome the inherent demerits associated with OFDM. Neither guard intervals nor cyclic prefixes are needed by design. Comparatively higher throughput is expected to be maintained with a continuous and efficient transmission. Another main advantage is much more efficient use of spectrum with lower spectral leakages or reduced amount of power associated with side lobes, where the robustness against ICI is increased due to that. FBMC is supported by some theories of multirate techniques [22], [23] and theories of well-localized filter design [19], [24]-[28]. Therefore, the success of this particular category of communication techniques is strongly dependent on aforementioned associated technologies. For this reason, it is very important to study their developments while exploring how to integrate them to FBMC.

1.4 Motivation and Problem Definition

There are two types of challenges and problems related to any kind of communication technique, namely, general problems and challenges and specific problems and challenges. One of the prominent challenges in the first category is the ever-increasing demand for higher throughputs and bandwidths. One typical example is the rise in that demand due to 8K UHDTV mobile transmissions. It is still questionable how efficiently a real time 8K UHDTV mobile transmission can be supported through the existing or proposed wireless transmission techniques. Scarcity of the available spectrum and limitations associated with the channel capacity can be considered as the main reasons behind this technical barriers. Another challenge is created by the necessity for more energy-efficient and greener systems for wireless communications. That is because the percentage of the total global energy consumption by air interface communication techniques, especially in the sector of wireless mobile communication, is not negligible. Now they are significant energy consumers, basically of fossil fuels. There are many other emerging applications and needs with a propensity to create general problems and challenges in the sphere of wireless communication. So there are two options: either to improve the existing technology or to introduce a new technology to meet the requirements. Irrespective of all the causes, one of the most extensively addressed conventional motivation can be stated in a traditional way. That is the increasing number of users while increasing data rates. Here the tradeoff is to be properly managed. However, that topic is also kept away from the main streams of this study.

Existing air interface multicarrier communication techniques are being heavily investigated for further enhancements in their performance in the physical layer. But increase of system complexity with the solutions is another problem.

Simpler techniques with higher performance are always preferred. In this study, it is tried to keep the solutions as simple as possible while attempting to improve performance. Among the number of considerations motivating this study are the following:

- Irrespective of the position in the life cycle of a particular technique, the associated problems can be addressed at different scales, with the expectation of making them easier to manage in this way. That also applies to OFDM, which, from the research point of view, is in the latter stages of its life cycle. This is an example of how to handle technique-specific problems and challenges on the same footing.

- FBMC may be considered as an extended version of OFDM or a completely separate category of communication techniques. Most importantly, there are plenty of similarities between these two technologies. Many studies have been carried out in relation to FBMC. But still better solutions are required for the problems associated with them. These problems include inability to handle frequency offsets (CFOs due to Doppler spread or synchronization errors), problems related to PAPR and overhead due to guard intervals or cyclic prefixes. There is also a need to avoid spectral leakages, which is associated with the OFDM family of multicarrier communication techniques.

- Insight knowledge on any communication technique, including that on their susceptibility for various types of interferences is needed for all the related consecutive work. This is not only to improve the technology but to gain some information that is very important in selecting a particular technique for applications. In this respect, OFDM has been heavily investigated, but there is still a significant amount of work to be done in relation to FBMC.

- It is important to note that interference is a key problem for any form of communication technique. Therefore, as the first step, more attention is paid to identify the characteristics of interferences in FBMC. That is done in the expectation of being able to use that information for later improvements.

- Once any communication technique is developed, it is necessary to have insight knowledge on its performance. It is to be tested at least for the basic channel models under different fading and synchronization conditions.

- In addition, the preference for less computationally complex and efficient symbol detection, symbol recovery and interference management schemes is also taken into account as much as possible.

- There are some areas containing many important associated techniques, concepts and conditions. These include relays, coding and channel equalization concepts. They are to be further investigated.

Some of the problems that can be identified and are related to these communication techniques are addressed within this study.

- Higher throughputs are always in demand. Orthogonal subcarriers are used to support high data rates in a spectrum-efficient manner. This is the case for both OFDM and FBMC.

- Basic FBMC models are developed to be operated in asynchronous multipath channel environments. Most of the publications include certain assumptions made at different stages where the reasoning out for the assumptions are also made available. Here the intention is to formulate a basic causal FBMC transmitter and receiver setup operated under asynchronous conditions without any assumptions for corroborative simulations. But for derivation of analytical expressions, a reasonable set of assumptions are made while safeguarding the core concepts and theories. The setup is customized to a well-accepted subcarrier filter.

- It would be much better to have detailed, more accurate performance information that doesn't include any assumptions or a set of assumptions with concrete justifications that can be used for further related developments.

- Lack of theoretical and analytical developments related to this is an apparent factor. These are very important in verifying the accuracy of the technique and for consecutive related enhancements.

1.5 Limitations and Assumptions

This study is subject to several limitations and assumptions unless specifically stated otherwise.

I. The channel and the parameters related to antenna correlation are assumed to be perfectly known at the receiver.
II. Free space propagation models (e.g., Hata model), which are used to address issues like distance and Doppler shifts, are not taken into account.
III. Modeled channel and antenna correlation properties are taken as realistic factors.
IV. Issues related to PAPR are not considered.
V. Data flow is assumed to be unidirectional and data rates are considered to be constant throughout the operation of the system. No feedback mechanisms are considered (i.e., at least no repeat request (RQ) or automatic repeat request (ARQ) schemes are considered).
VI. Delays for two consecutive channel taps are assumed to be equivalent to single or multiplies of sample intervals.
VII. A uniform power delay profile is considered.

VIII. Unless otherwise it is specifically mentioned, no interferences from external sources are considered.

1.6 Thesis Outline and Contributions

The foremost objective of this study is to analyze and investigate the performance of an FBMC technique and some of the associated concepts related to wireless communication. Out of the many FBMC techniques, one that is supported by multirate principles and customized to well-established PHYDYAS subcarrier filter (See APPENDIX 1.2) is identified as a potential example for that. This is the same way as it is used in standard OFDM/OQAM technique. The FBMC technique and some of the concepts associated with it are subjected to further investigations. Greater attention is paid on addressing the problems related to basic formulations (e.g., resolving incompatibilities associated with some of the existing formulations related to asynchronous operation), inherent self-interference and performance over different fading channel environments. Those contributions, together with relevant background information are arranged as shown below.

1.6.1 Thesis Outline

A chapter by chapter summary of this thesis is outlined, highlighting the importance, organization of each of them and the gradual development of the entire technical presentation.

- **Chapter 2 :** The basic models for OFDM and FBMC systems with relevant background information are presented. In the case of FBMC, a complete formulation for a causal asynchronous system (causal system in the presence of time and frequency offsets) customized to a subcarrier filter that can be operated under different channel and synchronization conditions is discussed.

- **Chapter 3 :** A comprehensive analysis of self-interference is presented. Different asynchronous conditions in a communication system are taken into account in this presentation. Interference is categorized into two forms, based on the way they are created, and their probabilistic properties are also studied. Numerical results are presented for a selected set of scenarios.

- **Chapter 4 :** Performance of a basic FBMC system over different fading channels under different synchronization conditions is dealt in this chapter. Performances of two types of receivers where the first one is based on the minimum Euclidean distance and the other one is based on the channel equalization principles are tested. Closed-form expressions for the additive white Gaussian noise (AWGN) and Rayleigh channels followed by an asymptotic error rate analysis for the Nakagami-m channel are given. Simulation and numerical results for all of them for a set of scenarios are made available.

- **Chapter 5 :** Integration of the merits of FBMC with relay concepts is aimed by this chapter. An asymmetric and asynchronous decode-and-forward (DF) FBMC relay system is modeled as a pilot example. Here three basic and the most prominently used performance measures namely, BER, outage probability and ergodic capacity, are used to evaluate the relay performance. Closed-form expressions for all of them are derived, first for the individual hops and then end-to-end wireless link. Both simulation and analytical results are made available.

- **Chapter 6 :** The concepts of FBMC, DF relay and diversity reception are integrated with the expectation of investigation of combined merits associated with them and the overall system performance. A asymmetric and asynchronous DF FBMC relay system is modeled while considering the antenna correlation properties. BER, outage probability and ergodic capacity are used for this investigation. Closed-form analytical expressions are derived for all of them. Both simulation and analytical results are used to evaluate the end-to-end performance.

- **Chapter 7 :** The thesis is concluded and suggestions for future studies are made.

1.6.2 Contributions

This study makes several contributions in the analysis and performance evaluation of air interface communication techniques. Even though an FBMC technique is selected for this study, many of the approaches and derivations presented here can be applied to and are compatible with many of the multicarrier communication techniques.

- A basic formulation both in continuous and discrete formats for a causal multirate asynchronous FBMC system operated in a multipath channel is made available.

- Complete and comprehensive analysis is done on self-interference in an FBMC system under different synchronization conditions that can be applicable to the scenarios with delayed paths. Properties of interference are also studied in detail.

- Using the properties of self-interference, a set of closed-form expressions is derived and a mechanism for performance measures is established. A more precise discussion on their use in deriving closed-form expressions for BER in the forms of general and asymptotic formulations is carried out. For this, a set of scenarios is selected for different channel models under different fading and synchronization conditions. Applicability of minimum Euclidean distance based receiver for signal detection and interference cancellation is also concisely explored.

- The performance of an FBMC system in connection with relay concepts is presented. For that purpose, the performance of an asymmetric and asynchronous DF relay system using three performance measures, viz. BER, outage probability and capacity, is discussed. The necessary closed-form expressions are derived for that.

- The investigation on DF FBMC relay system is further extended considering scenarios with diversity reception. The performance of an asymmetric DF relay system using the same performance measures is discussed. Correlation effect among antennas is also taken into account. Closed-form expressions for all the performance measures are presented.

2 OFDM AND FBMC TECHNIQUES

OFDM is identified as a currently widely-used and prominent wireless communication technique. It has a clearly identified capacity for use in a more sophisticated manner with the help of associated technologies and techniques. But due to certain limitations associated with it and with the upcoming requirements, it has been completed to search for alternative transmission techniques for the physical layer communication. FBMC can be introduced as a potential candidate that is capable of ameliorating certain drawbacks associated with OFDM. There is a detailed discussion in this chapter on both these techniques, including their merits and demerits, applications and developments, basic formulation and signal models used within this study. In certain classifications, OFDM is identified as a member of the FBMC family with rectangular pulse shaping. On the other hand, FBMC is often identified as an extension of OFDM with pulse shaping. Here it is assumed that a rectangular pulse shape is the default shape of a pulse and that in FBMC the pulse shaping is done with the aid of subcarrier filters. Therefore, it is clear that there is a strong inter-relationship between them.

2.1 Introduction

The preliminary preparation work for OFDM started in the 1870s with an attempt to increase capacity by using frequency division multiplexing (FDM) based transmission techniques [29]. That was the era of Alexander Graham Bell. However the work done in [30] is commonly considered as the basis for both OFDM and FBMC techniques in general.

In focusing on to the other inventions related to OFDM, the development of a slightly overlapped carrier technique was seen with the introduction of the N2 carrier technique in the 1960s [29]. Usage of double sideband amplitude modulation could be observed in that connection. The main problem associated with that technique is its higher susceptibility for ISI with increased speed of time-division multiplexing transmission. Wider bandwidth always gives rise to frequency-selective fading and then pulse dispersion. Fine-grained FDM addressing those problems and concentrating on the data in less-faded subchannels was introduced. The idea was to equalize the narrow subchannels, using a complex analytic model, by multiplication with an inverse complex number. That is the groundbreaking pioneering piece of work for the OFDM (basic or default OFDM) technique used today. Other than N2 carrier systems, that had been introduced in mid-1960s, there had been many historical milestones, with OFDM as the prominent communication technique [31]. Nevertheless, it seems that OFDM still has not come to an end. This particular technique of communication is still being considered and recommended for upcoming systems and applications. It is very hard to find a perfect competitor or a substitute capable of outperforming it with clear-cut results covering all the scenarios. It appears that OFDM is an old technique used in modern systems. The technique itself and its related technologies have been extensively investigated mainly for wired and wireless interfaces of communication systems in many areas, including optical communication [32]-[34], with the expectation of achieving higher throughputs under difference channel conditions.

Apart form [30], the history of FBMC goes back as far as 1971 when filter banks were used for the synthesis and analysis of multicarrier signals [35]. In the initial approach, filter banks were suggested to be used in order to assist OFDM. In addition, signal design criteria and equalization algorithms are derived and explained. A differential phase modulation scheme is also presented where equalization could be obviated. But later on FBMC transmission techniques are studied and developed as alternatives or extensions for the family of OFDM techniques, thus deviating from the main stream. In that case, today they are considered either as extended versions of OFDM or as a separate family of multicarrier communication techniques.

There are some fundamentally important historical milestones common to both techniques. The Kineplex system is a military transmission technique with parallel transmission of 20 tones. It is modulated by differential 4-Phase-shift keying (4-PSK) without filtering the resulting overlapped channels. It was proposed in 1957 [36] and is similar to the basic OFDM. The tones can be placed at frequency intervals and they are capable of separation at the receiver by a bank of filters. The property of orthogonality is also used in it [37]. Therefore it is also recognized as a relatively bandwidth efficient communication system. In this particular concept, orthogonal signals are generated using sine and cosine waves yielding to an optimal spectral efficiency and a simple coding scheme in frequency domain.

Both OFDM and FBMC techniques are discussed in this chapter. First, the OFDM technique is introduced in detail. The main advantages and disadvantages associated with it are also brought in to attention. Some of the major applications of OFDM and some of the recent developments related to it are briefly presented. Its basic formulation is also made available. That is followed by an introduction to FBMC. Current trends, applications and renascent developments related to it are discussed. Both a continuous and a discrete time formulation for a basic FBMC system are presented. The chapter then is concluded, summarizing and highlighting the main points.

2.2 OFDM Technique

Some remarkable developments and a publication done in 1966 by Robert W. Chang are considered as the invention of basic OFDM transmission technique [30]. It was introduced as a methodology to transmit signals simultaneously over a band-limited channel, with no ICI and ISI, by dividing the main frequency-selective channel into a number of parallel, frequency-flat subchannels. That led to frequency-flat fading for the narrow subchannels where those channels are expected to be orthogonal. But there is another claim for this innovation as a military system [38]. The emphasis on inverse discrete Fourier transform (IDFT) and discrete Fourier transform (DFT) paved way toward the development of OFDM [35]. The addition of cyclic prefix (CP) is another important development related to OFDM [39]. The introduction of cyclic extension contributes towards maintaining orthogonality in a more efficient manner.

The basic OFDM [6] transmission technique is increasingly supported by many of the associated technologies [18]. There is a considerable number of derivations and variants that were developed based on the same principles. Some of these are major improvements while others are minor. In most of the cases, the target being addressed has been a some sort of problem: attempts were made to improve throughput, have multiuser support or establish link reliability. Some of them are still highly competitive, showing characteristics of potential candidates for air interface transmission techniques for the next generation wireless communications. Further, OFDM is used or considered for other sectors of communication, including wire lines, underwater acoustics and optical communications. Thus, there are numerous ongoing attempts to increase the usability OFDM.

2.2.1 Merits and Demerits of OFDM Technique

The main advantages of basic OFDM, specifically over other communication techniques or some of the key features where this particular transmission technique is brought to the forefront of wireless communications, can be summarized as follows:

I. Robustness or capability of withstanding against different channel conditions including tolerance or persistence to frequency-selective fading. In other words, there is a considerable robustness against phenomenon caused by multipath propagation like ISI and fading where there is a greater tolerance to symbol delays.

II. Due to easy adaptability to severe fading conditions and inherant properties of OFDM, no complex time-domain equalization schemes are needed.

III. Robustness against narrow-band co-channel interference.

IV. Robustness against the time synchronization errors.
V. Higher spectral or bandwidth efficiency as compared to other modulation schemes, spread spectrum techniques, single carrier techniques and non-orthogonal multicarrier transmission techniques.
VI. Easy, efficient and low complexity implementation using FFT.
VII. Unlike in the case of FDM, sub-channel receiver filters are not required for the basic OFDM.
VIII. Performance can be easily enhanced by integrating supportive signal processing mechanisms and techniques like diversity schemes and coding schemes.

There are some main disadvantages associated with the OFDM transmission technique and principles. These can be considered as some of the major reasons for searching alternative transmission techniques for the physical layer communication interfaces:

I. Higher PAPR and related problems. Therefore linear transmitter circuitries are required. But they have poor power efficiency.
II. Higher susceptibility for frequency synchronization problems like greater sensitivity for the Doppler shift and / or CFO.
III. Loss of throughput transfer efficiency caused by CP / guard interval.
IV. Additional processing power needed to handle the CP / guard interval.

2.2.2 Variants of OFDM Technique

There are many sub-categories and variants in the OFDM family of technologies. The following are some of the key variants or derivations that are based on the OFDM principles:

- **MC-CDMA** : Multicarrier-code division multiple access (MC-CDMA) is a multiple access technique based on the principles of code division multiple access (CDMA) and OFDM. Therefore, this is categorized as a hybrid technique as well [40], [41]. When it is compared to basic OFDM, very competitive performance results can be shown. Better throughput performance and stability of transmission can be achieved due to subcarrier diversity. Spreading is used to accommodate users. This technique can be pronounced as a precoding scheme in single user cases, and also as multiuser CDMA scheme.

- **BICM-OFDM** : Bit-interleaved coded modulation-orthogonal frequency division multiplexing (BICM-OFDM) is capable of competitively perform against standard OFDM [42]. Using the concatenation of a convolutional encoder, an interleaver, and a memoryless mapper, coding is performed along the frequency axis over the subcarriers of a single OFDM symbol. Since operations related to error control coding and decoding are done before the transmitter and after the receiver accordingly, according to certain classifications this scheme is not being recognized as a variant of OFDM.

- **OFDM-CDMA** : This is also a hybrid technology [43] containing properties of CDMA and OFDM. In orthogonal frequency division multiplexing-code division multiple access (OFDM-CDMA), a Walsh-Hadamard code is used to spread data bits in parallel to each other in time domain and summed together. Then they are transmitted as OFDM steams using subcarriers.

- **V-OFDM** : Vector-orthogonal frequency division multiplexing (V-OFDM) is designed to combat frequency nulls. This technique is a bridge between OFDM and single-carrier frequency-domain equalization (SC-FDE) [44]. In contrast to OFDM, V-OFDM is capable of converting an ISI channel into an ISI-free vector channel while using channel matrices instead of channel coefficients in one-tap equalization increasing the diversity order. V-OFDM has a smaller PAPR and lesser sensitivity to CFO than OFDM has.

For the completeness of this presentation, information on SC-FDE is presented [44]. Main principle in SC-FDE is that the IFFT is moved to the end of the receive chain rather than operating at the transmitter, to create a multicarrier waveform as in OFDM. It is clear that, subcarriers are not available within the air interface which is the main reason that SC-FDE is not considered as a variant of OFDM or an multicarrier transmission technique. Here the equalization is done frequency domain avoiding high complexity in time domain equalization. Low PARR and less sensitive to the CFO related problems are among the main advantageous compared to OFDM.

Some of the variants of OFDM result from minor changes to the main or default category. A few of them are presented bellow.

- **MB-OFDM** : Multiband-orthogonal frequency division multiplexing (MB-OFDM) is also known as frequency hopping-orthogonal frequency division multiplexing (FH-OFDM). In the multibanding approach, the spectrum is divided into several sub-bands. The transmit OFDM symbols are time-interleaved across the subbands. The transmitter and receiver architectures for this system are very similar to that of a conventional wireless OFDM. The main difference is that a time-frequency kernel is used by a MB-OFDM system to specify the center frequency for the transmission of each OFDM symbol [45].

- **CI-OFDM** : In carrier interferometry-orthogonal frequency division multiplexing (CI-OFDM), orthogonal carrier interferometry spreading codes are used so that each information symbol is spread across all subcarriers [46].

- **A-OFDM** : In asymmetric-orthogonal frequency division multiplexing (A-OFDM), part of the IFFT operation is shifted from the transmitter to the receiver [47]. The ratio of the shifted complexity is flexible and adaptive to the transceiver's capability, power supply and duplex requirement. It comes with an improved CFO sensitivity and frequency diversity and with reduced PAPR.

- **PC-OFDM** : In post-coded orthogonal frequency division multiplexing (PC-OFDM) systems, frequency diversity is introduced by spreading the information symbols across all the subcarriers in an efficient manner significantly reducing the overall computation cost of the system. These computational savings are achieved from two sources: 1) smaller size Inverse Fast Fourier Transform (IFFT) and FFT are used while replacing frequency domain precoding, and 2) the special structure of encoding matrices is exploited resulting in O(N) operations instead of O(N^2) operations [48].

- **COFDM** : The information to be transmitted is split over a large number of carriers in such a way that the signaling rate in each of them becomes significantly lower than the assumed channel coherence bandwidth. In other words, the signal is conditioned to ensure that the modulated symbols will be much longer than the echo delay spread. In coded orthogonal frequency division multiplexing (COFDM), provided that a guard interval is inserted between successive symbols, ISI is no longer generated by multipath propagation [49]. Even though CP is almost always used in OFDM systems, this can be introduced as a version of CP-OFDM as well.

2.2.3 Applications and Recent Developments

This survey is limited to applications and developments where the OFDM transmission technique is used. They are the most recent, upcoming or which are likely to appear in future. Many of the already well-established applications are purposely omitted. In relation to wireless communication technologies, there are recent progressive developments in the areas of vehicular communication, cognitive radio, massive or large-scale MIMO, interference alignment, multi-tier transmission architectures, CoMP, self-learning and physical layer security (Relay communication concepts is another prominent area, which is discussed separately.).

Special emphasis is placed on the use of OFDM in vehicular environments, where separate standardizations like IEEE 802.11p are also available for that. There is an enhancement for this standard, wireless access in vehicular environments (WAVE), aiming at applications related to intelligent transportation systems. These applications include data exchange between high-speed vehicles and between vehicles and the roadside infrastructure operated in 5.9 GHz band (5.85-5.925 GHz). In [50], channel estimation for OFDM in time-variant wireless propagation channels is considered while paying attention to the requirements and recommendations made by IEEE 802.11p as challenges for this highly mobile environment. A dynamic equalization scheme is proposed in [51]: it is to be operated on top of the existing dedicated short range communications (DSRC) technology. It is capable of providing a significant improvement for the packet error rate of data transmissions without changing the DSRC standard.

Cognitive radio is another application that has a high chance to be integrated and deployed with the existing wireless communication systems. A resource allocation framework is proposed based on the bandwidth-power product minimization in [52], which is an effective metric in evaluating the spectral resource consumption in a cognitive radio environment. Compared to classical power adaptive optimization using iterative water-filling scheme, a considerable improvement in spectral efficiency could be achieved by using this framework. A joint cross-layer and sensing design is presented in [53]. It is suggested to share the spectrum, with primary users, using cognitive radio technology in a downlink transmission of an orthogonal frequency division multiple access (OFDMA) based secondary system. In addition, the same joint design framework is used to optimize a system utility where the power allocation is adapted and the subcarrier assignment across the secondary users is based on both the channel state information (CSI) and raw sensing information.

An OFDM-based downlink transmission scheme for large-scale multiuser MIMO wireless systems is presented in [54]. The large degrees-of-freedom availability in this system is exploited to achieve low PAPR. Multiuser precoding, OFDM modulation and PAPR reduction are jointly handled as a convex optimization problem. One key challenge in realizing practical large-scale OFDM MIMO systems is created by high-dimensional channel estimation in mobile multipath channels. As a solution for that, time-frequency training OFDM transmission scheme for large-scale MIMO systems is proposed in [55]. At the receiver, a time-frequency joint channel estimation method is used to track the channel variation.

Interference alignment is another emerging area with guaranteed results and a huge potential to grow further. Covering a variety of indoor and outdoor measurement scenarios, results of the first experimental study on interference alignment in measured MIMO-OFDM interference channels are made available in [56]. In [57], opportunistic resource allocation and interference alignment are considered for interference management that can be used for OFDMA-based macro or femto cells by utilizing fading fluctuations across frequency channels in different ways. The interactions and the trade-offs between these two strategies are investigated in the paper.

The essential need of designing much more power-efficient communication systems can be supported in numerous ways. The fundamental power-delay tradeoff in point-to-point OFDM systems under imperfect CSI quality and non-ideal circuit power is analyzed in [58]. The dynamic backpressure algorithm is for cases where the determination of the rate and power control actions by the transmitter is based on instantaneous channel state information and queue state information. The problem of joint allocation of subchannels, transmission power, and phase duration in the relay-enhanced bidirectional MIMO-OFDM networks is studied in [59]. Green resource allocation schemes with reduced computational complexity are proposed to jointly allocate subchannels, power, and phase duration for user equipments in connection with direct and two-hop communications.

OFDM combined with the CoMP transmission technique is proposed to improve the performance of receivers located at the cell border. An optimal set of training sequences that can be used with the CoMP-OFDM design based on the Zadoff-Chu sequences that is capable of minimizing the mutual interference is presented in [60]. It is robust to the variations in multiple CFOs as well. Subsequently, a maximum likelihood based estimator, a robust multi-CFO estimation scheme, for simultaneous estimation of multiple CFOs is also presented. A resource allocation scheme, with (or without) adaptive modulation for CoMP with multiuser MIMO-OFDM, is suggested in [61]. In that scheme, practical linear pre- and post-processing techniques are used to cancel inter-user interference and to decompose a single user MIMO channel into parallel non-interfering spatial layers. The transmit power is allocated to spatial layers, with (or without) adaptive modulation, under the total base station power constraint and the per-base station power constraint.

Intelligent systems and machines with self-learning capabilities are being rapidly developed and deployed in almost all the sectors of engineering. A decentralized framework for dynamic spectrum assignment in multicell OFDMA networks is presented in [62]. Each cell is allowed to autonomously decide the frequency resources that are to be used by it. The procedure incorporates concepts from self-organization and machine learning in multiagent systems. A discrete stochastic approximation algorithm for time synchronization in OFDM systems is given in [63]. It is shown that this scheme can be effectively used to achieve a significant reduction in computational complexity compared to brute force maximum-likelihood methods for OFDM synchronization. Recursive self-learning capability can be identified as its most important property.

Physical layer security is one area that has been researched only in the recent past. A physical-layer transmission scheme was designed to achieve low probability of interception in cooperative systems [64]. Cooperative systems have two major differences in comparison with the previous solutions. The first one is that each relay node may have only one antenna that cannot provide antenna array redundancy for signal randomization, and the second one is that there may be timing errors due to the asynchronous nature of cooperative systems. Based on those differences, a distributed differentially-encoded OFDM transmission scheme with deliberate signal randomization to prevent eavesdropping is proposed. The scheme is capable for exploiting the available spatial and frequency diversities in asynchronous cooperative systems. Resource allocation for energy-efficient secure communication in an OFDMA downlink network is studied in [65]. The problem is modeled as a nonconvex optimization problem that takes into account the sum-rate-dependent circuit power consumption, multiple antenna eavesdropper, artificial noise generation and different quality of service requirements, including a minimum required secrecy sum-rate and a maximum tolerable secrecy outage probability. The power, secrecy data rate, and subcarrier allocation policies are optimized for maximization of the energy efficiency of secure data transmission.

Due to their attractive properties, applications of OFDM are not limited to air interface only. Their performance limits technical capabilities are being enhanced constantly. Some applications related to non-wireless communication and a radar application might also be mentioned for the completeness of this presentation. These can be found in the areas of underwater acoustic communication, power line communication (PLC), optical communication and passive radar. Significant progress is being made in point-to-point underwater acoustic communications. Interest is shown on the application of these techniques in multiuser communications. For example, a time-asynchronous multiuser reception approach for OFDM is suggested in [66]. PLC is another attractive application for OFDM. An approach to mitigate the periodic impulsive noise before synchronization of the OFDM based PLC system is given in [67]. OFDM and its variants are commonly used for optical communication. Information-theoretic results for asymmetrically-clipped optical OFDM in an intensity-modulated direct detection optical communication system is given in [68]. Passive use of worldwide interoperability for microwave access OFDM waveforms for synthetic aperture radar ground imaging is promoted in [69]. This is a suggestion to use OFDM for radar applications.

2.2.4 Basic Formulation

Basic OFDM [70], [71] consisting of N_F subcarriers (N_F-point IDFT / DFT) is considered where the block diagram is shown in Figure 1. First the source bit stream is mapped to modulation symbols from a complex constellation such as PSK or quadrature amplitude modulation (QAM). Then an OFDM symbol is generated by taking the IDFT of N_F modulation symbols.

Let $\left\{a_0, a_1, \ldots, a_m, \ldots, a_{N_F-1}\right\}$ be a block of N_F data symbols after the serial-to-parallel conversion. The IDFT of the data block is,

$$d_m = \sum_{k_F=0}^{N_F-1} a_{k_F} e^{j\frac{2\pi k_F m}{N_F}}, \quad m = 0, 1, \cdots, N_F - 1. \tag{2.1}$$

These time-domain samples are considered as the time-domain OFDM symbol $\{d_m, m = 0, 1, \cdots, N_F - 1\}$. In order to mitigate the effects of ISI caused by the channel delay spread, each time-domain OFDM symbol is preceded by a CP. That is simply a repetition of the last set of time samples. If the length of the CP is at least longer than the maximum delay spread of the multipath fading channel then the ISI can be completely mitigated. Because of the CP, the linear convolution of transmitted symbols with channel is transformed to a circular convolution. Then the output of DFT demodulation is the multiplication of the frequency-domain OFDM symbol $\mathbf{a} = \left(a_0, a_1, \ldots, a_m, \ldots, a_{N_F-1}\right)^T$ and the channel response in the frequency domain can be given as,

$$\mathbf{r} = \mathbf{H}\mathbf{a} + \mathbf{w}, \tag{2.2}$$

where $\mathbf{H} = \text{diag}\left\{H_0, H_1, \cdots, H_m, \cdots, H_{N_F-1}\right\}$. $\text{diag}\{\cdot\}$ is used to represent a diagonal matrix.

$$H_m = \sum_{l=0}^{L-1} h_l(t) e^{-j\frac{2\pi l m}{N_F}}, \tag{2.3}$$

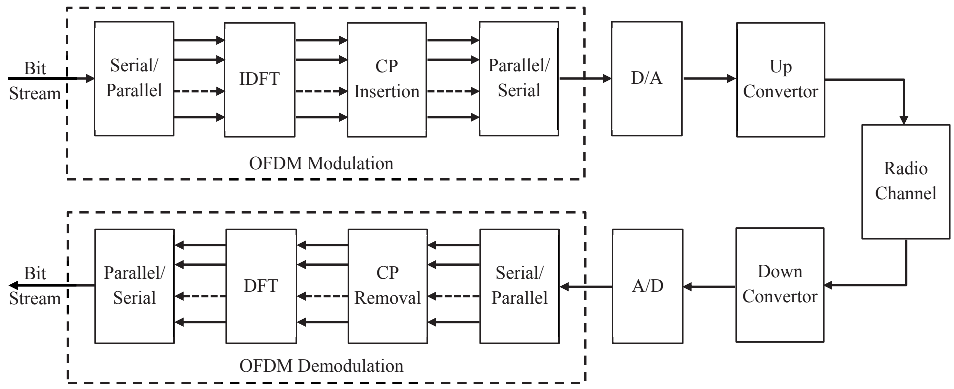

FIGURE 1 Block diagram of an OFDM system

is the complex channel frequency response at subcarrier m and $\mathbf{w}$ is the AWGN vector. The channel response for the elementary path l of the frequency-selective fading channel within the same duration is denoted by $h_l(t)$. Channel order is given by L. Since slow fading is considered, for a given symbol frame, the path gain can be assumed as $h_l = h_l(t)$. When w_m is the AWGN component, the element m of $\mathbf{r}$ which is the receive signal r_m on subcarrier m can be expressed as,

$$r_m = H_m a_m + w_m, \quad 0 \leq m \leq N_F - 1. \tag{2.4}$$

2.3 FBMC Technique

In order to get the advantages of having filters for the subcarriers [35], there have been many developments related to FBMC. In most of the FBMC techniques, identical filters are used for all the subcarriers in the transmit and receive sides. But this is not a compulsory requirement. If the orthogonality property is disregarded, the only indispensable prerequisite for a generic FBMC design is to have suitable localization filters of any kind for the subcarriers at either sides [20].

2.3.1 Merits and Demerits of FBMC Technique

Due to the disadvantages and limitations associated with existing multicarrier communication techniques in the family of OFDM techniques, FBMC is considered as a possible alternative technique to them. The specific reasons for considering it against OFDM are listed below.

I. Higher spectral or bandwidth efficiency as compared to other modulation schemes, spread spectrum and transmission techniques. The orthogonal subcarrier design is one of the reasons for that.

II. Unlike in OFDM, no guard intervals and cyclic prefixes are needed. Higher throughput and a continuous efficient transmission can be supported. In addition, no additional processing power is needed to handle guard intervals and cyclic prefixes.
III. Due to well-localized filter design, much more efficient use of spectrum with lower spectral leakages can be ensured. This is achieved due to reduced amount of power associated with side lobes (relatively low amplitudes associated with them). The robustness against ICI is also increased.
IV. In the case of FBMC, performance can be easily enhanced by integration of some of the compatible supportive signal-processing mechanisms like diversity schemes, and coding schemes.
V. FBMC is capable of outperforming certain specific application areas of OFDM and related techniques [20]. Almost perfect carrier synchronization is needed for the uplink of an OFDMA network for the signals from different nodes. In FBMC, signal separation is done through filtering. There is no such critical need for perfect synchronization or for perfect timing synchronization between users (One empty subcarrier is proposed as a guardband between two asynchronous users.). In cognitive radios, due to the filtering capability of FBMC, this is a better choice for filling in the spectrum holes.

Some critical disadvantages and demerits which are associated with the FBMC technique can also be pointed out. These are among the main obstacles behind the rapid progression of this sophisticated communication technique.

I. Self-interference generated during the asynchronous modes of operations and / or under multipath channel conditions in terms of ICI, ISI, and ICSI.
II. Excessive complexity and sometimes even non-compatibility with some of the receiver processing techniques when trying to find solutions to self-interference, multipath interference or CFO-related problems.
III. Comparatively high complexity can be seen in the both transmit and receive sides of an FBMC implementation. Even higher processing power is needed for receiver processing based on the type of scheme that is used to treat problems related to the receive signal. Because most of the receiver processing techniques are to be implemented in subcarrier level.
IV. A high sensitivity for the Doppler shift and / or CFO can be observed. But performance of the FBMC technique is slightly better compared to OFDM with the same subcarrier spacing.
V. PAPR related problems are the same as for OFDM.
VI. Additional modifications are needed to support some of the well-established concepts. In the case of higher-order modulation schemes, if binary phase-shift keying (BPSK) is regarded as the default modulation scheme for FBMC, FBMC / OQAM can be viewed as a variant. Similarly, there are some possibilities for more variants and subcategories of FBMC.
VII. Since FBMC is a combination of different concepts, already developed solutions for many of the problems cannot be directly applied as they are. Customized solutions are needed for them.

2.3.2 Variants of FBMC Technique

There are some variants and subcategories for FBMC as well. OFDM / OQAM [72] (OQAM / OFDM, OFDM-OQAM, OQAM-OFDM) which is also known as FBMC / OQAM [73] (OQAM / FBMC, FBMC-OQAM, OQAM-FBMC) is identified as most closest variant of FBMC. In these variant schemes, the usual QAM is replaced by OQAM. There are no cyclic prefixes. This is with a higher bandwidth efficiency than the standard OFDM. In QAM-OFDM, orthogonality of the transmitted subcarrier signals is achieved using rectangular pulses, whereas in OQAM-OFDM it is achieved by employing pulses with a sharper time-frequency localization. Orthogonality property becomes more visible under ideal channel conditions and cannot be ensured in frequency-selective fading channels. Complicated equalization is needed to mitigate the effect of interchannel interference (ICI). How ever single tap subcarrier wise equalization is found to be sufficient for a signal reception with a acceptable level of quality if the subcarrier spacing is similar to the corresponding OFDM system.

All the members in the OFDM family with subcarrier filters like MB-OFDM [45] are recognized as variants of FBMC. Their approach is considered as pulse shaping for OFDM.

Even though some of the multicarrier transmission techniques do not have the exact form of the filter bank technique that is used for this study, they can be considered as members of the FBMC family of techniques. In any case, they are very close to the technique that is used for this study. In other words they are enriched with highly compatible technical characteristics to the FBMC family.

- **CMFB** : Cosine-modulated filter bank (CMFB) a special case of FBMC utilizing real subband and high-rate signals. An analysis of the post-combiner equalizers used to compensate for channel distortion in cosine-modulated-based transmultiplexer systems is presented in [74], where that kinds of equalizers are used in multicarrier modulation systems with cosine-modulated filter banks for signal modulation and demodulation. Closed-form expressions for optimum post-combiner transfer functions are derived under the assumption that the number of subcarriers in the system is large enough for each subcarrier to be approximated by a constant complex gain. These transfer functions with finite impulse response are closely related to the filters in CMFB analysis and synthesis blocks. A reduced complexity post-combiner structure also presented increasing the speed of convergence followed by a convergence analysis for the post combiner.

- **W-OFDM** : In wavelet-based orthogonal frequency division multiplexing (W-OFDM), Fourier-based complex exponential carriers of the OFDM technique are replaced with a set of orthonormal wavelets reducing the interference [75]. In comparison with the standard OFDM, certain types of wavelets are capable of reducing the power of ISI and ICI, which arise from loss of orthogonality between the carriers due to the multipath wireless channel (This is not the Wideband OFDM).

- **DWMT** : The discrete wavelet multitone technique (DWMT) [76] is one of the closest technique to OFDM which can be adopted as the modulation scheme. Its side lobe attenuation is stronger than that of the OFDM modulation leading to much lower adjacent channel leakages, making it suitable for applications with dynamically allocated spectrum. The DWMT system is realized using *M*-band wavelet filter bank. The *M*-band wavelet filter bank is composed of a set of wavelet filters with longer impulse responses than its counterpart in DFT.

- **FMT** : The filtered multitone modulation (FMT) technique is another member of the family of multicarrier communication techniques related to FBMC. This is also categorized as an OFDM technique due to the deployment of subchannel shaping filters. Because this is based on a FFT implementation followed by low-rate subcarrier filtering. Non-overlapped subcarriers in the frequency domain are aimed by the design of the subcarrier filters and the choice of the subcarrier spacing in subdivision of the spectrum into a number of subcarriers. Avoidance of ICI and low ISI contributions are achieved by this way. An investigation was carried out on best attainable performance for FMT [77] in time-variant frequency-selective fading channels with an optimal maximum-likelihood detector. The performance limits were derived by extending the matched filter bounding technique to this multichannel context. In that technique, exact calculation of the average and the distribution of the matched filter error rate bound are presented. Problems of accuracy and ill-conditioning in the implementation of the exact method are overcome by a numerical procedure. An analytical treatment for the diversity effect on performance as a function of the time-frequency selectivity of the channel was also carried out. It was found that FMT is a diversity transform that is capable of yielding coding gains and time-frequency diversity gains as a function of the subcarrier spacing and the subchannel filter shape.

- **CMFIRBFB** : A cosine-modulated finite-impulse response biorthogonal filter bank (CMFIRBFB) system is presented in [78] where the system is capable of achieving perfect reconstruction with a given analysis or synthesis prototype filter. More freedom is given for the choice of prototype filters where unmatched transmit and receive filter pairs can be used.

According to certain categorizations and analyses, all the aforementioned variants are the same where FBMC is often considered as a broader term, including OFDM / OQAM, FMT and others. However, it is important to note that any kind of classification is conditional upon the basis used for that.

2.3.3 Applications and Recent Developments

The same application areas are common for OFDM and FBMC. The information available in connection to developments and applications related to FBMC is less than that for OFDM. There are a number of reasons for that.

I. In the past, there was no precisely defined stable system model for FBMC. Some of them had been confined to multirate techniques only with the assumption of ideal filters. They couldn't be operated in an asynchronous multipath channels.
II. Even now, different models, can be selected according to their features and requirements. But their performances are not the same. Now, a family of FBMC techniques can be identified. Otherwise it can be stated that there are various models form FBMC, which are eventually equivalent with the OFDM/OQAM model or extended versions of it.
III. Compared to OFDM, there is an additional complexity associated with FBMC.
IV. Many FBMC systems and associated theoretical derivations come with assumptions that cannot be considered as general assumptions. They are valid for some selected scenarios and configurations only.
V. So far there hasn't been any attractive simple receiver that can be used to eliminate different types of interferences. Most of the developments are either excessively complicated, customized to a particular configuration or with approximations. They are not compatible with other scenarios.
VI. FBMC is not yet strong enough to replace OFDM. FBMC is only a candidate for its replacement.
VII. Even the form of FBMC technique analyzed in this study, which is one of the most widely used current versions, system characteristics are strongly influenced by the properties of subcarrier filters and by the way they are used with polyphase implementation. Each and every FBMC technique is with its unique interference and has other characteristics based on the filters used and on the way they are used. Therefore, thorough and customized studies should be done on self-interference (ICI, ISI or ICSI) and other performance, even when there has been only a minor change in the filter or associated mechanisms of integration.

Some of the information on already investigated applications and development related to FBMC can be presented. Outcomes of a performance evaluation of the downlink of asynchronous OFDM and FBMC cellular radio communication systems are presented on comparative basis in [79]. An expression for the interference caused by the timing synchronization errors in the neighboring cells under multipath channel conditions is addressed. Expressions are derived for average error rates of OFDM and FBMC systems while considering the frequency correlation fading in a case of a block subcarrier assignment scheme.

OFDM is identified as an undesirable solution for certain applications such as cognitive radios and uplink of multiuser multicarrier systems, where a subset of subcarriers is allocated to each user [20]. Shortcomings of OFDM in relation to numerous applications are addressed, and it is shown that FBMC could be a more effective solution in these cases. Inherent frequency selectivity is regarded as a vital characteristic as it enables high-quality radio-scene analysis necessary for successful deployment of dynamic spectrum access in the context of cognitive radio technology. FBMC is identified as an effective scheme that can be successfully operated under frequency-selective channels [80]. Also a mechanism for construction of a transmitter-receiver pair using synthesis and analysis filter banks of different sizes is presented. By using this method, notable computational complexity savings over a wide range of practical user bandwidth allocations can be achieved compared to the conventional implementation, which consist of equally-sized filter banks that give rise to low-complexity synthesis of spectrally well-localized FBMC uplink waveforms. A resource allocation algorithm to perform uplink frequency allocation and power allocation among non-cooperative multicells, with multiuser per cell, in cognitive radio systems supported by FBMC is presented in [81]. Maximization of the total information rate of multiple users in one cell is considered for the Rayleigh channel, with path loss subject to the power constraint on each user. The multiple access channel technique is proposed to support the solution. From the perspective of effectiveness, the proposed algorithm is compared against a frequency-division multiple-access technique based resource allocation scheme and the proposed scheme is capable of outperforming that. A design and implementation of a filter bank multicarrier spread-spectrum system for use as the control channel in cognitive radio networks is presented in [82]. Any cognitive radio network requires an effective control channel that can operate under various modes of activity by primary users. Carrier and timing acquisition and tracking methods as well as a blind channel estimation method are developed for the proposed control channel.

FBMC is tested for multihop vehicular networks as well and it is found that FBMC is capable of achieving twenty times smaller end-to-end data packet delivery delays and relatively lower packet drop probabilities [83]. In this paper it is highlighted that FBMC offers a much higher performing alternative to OFDM for networks that dynamically share the spectrum among multiple nodes. Suitability of FBMC as an alternative form of dynamic spectrum access is also examined on a comparative basis. Special pulse-shaping filters of the FBMC used in physical layer are investigated to find out about their reliability for high-rate data-packet transmission. It is shown that FBMC is capable of achieving at least an order-of-magnitude performance improvement over OFDM in several aspects, which include packet transmission delays, channel access delays and effective data transmission rate available to each node in static, indoor settings. Using measurements of power spectral density and high data-rate transmissions, it is shown that, where OFDM cannot, FBMC can distinguish all the receive symbols without any errors. FBMC is tested for a vehicular network setup, and it is found that an order-of-magnitude performance improvement can be achieved by it over large distances.

There are some other upcoming applications related to non-wireless communication and associated with FBMC. Orthogonal frequency-division multiplexing / discrete multi-tone (OFDM-DMT) is proposed as a suitable communication technique for PLC schemes. By considering many associated drawbacks such as bad frequency localization and spectrum efficiency loss due to CP, the

Hermitian symmetric version of OFDM-OQAM modulation is presented as an alternative to OFDM-DMT. It is much better in terms of spectral efficiency with no CP and comparatively better with its good time-frequency localization. Analysis of the tradeoff between spectrum efficiency and interference of these two schemes in terms of transmission capacity and giving a reference SNR threshold with respect to the corresponding channel environment is presented in [84]. In case of PLC networks, windowed OFDM is the retained modulation in the HomePlug Audio Video specification, the current standard implemented in most of the in-home PLC systems. Nevertheless, OFDM-OQAM is presented as a viable alternative to that [85]. Results of comparisons between these two schemes, in terms of capacity and throughput, are given. This is an indication that the baseband version of OFDM-OQAM is a serious candidate for efficiently improving data rates in PLC networks.

2.3.4 Basic Formulation

As in [11], continuous and discrete time formulations for a complete causal asynchronous single-input single-output (SISO) multirate basic FBMC communication system consisting $2M$ subcarriers are presented. Here the causal models are developed by considering real life implementations. Further it is customized to PHYDYAS filter, [24]-[26], [86]. Here the causal models are developed by considering real life implementations avoiding certain possible drawbacks associated with non-causal models. Same way as in [11], for the purpose of clarity of accurate use of certain mathematical operations both continuous and discrete domain formulations are made available.

Continuous Domain Formulation

In the process of continuous domain system formulation, $\beta_{m,n}(t)$ at time t relating to symbol time instance n on subcarrier m and $\beta_{m',n'}(t)$ relating to any symbol time instance n' on subcarrier m' are defined as

$$\beta_{m,n}(t) \quad = \quad \sqrt{2}p(t-n\tau_s)e^{j2\pi mF_st}e^{j\psi_{m,n}}, \tag{2.5}$$

where $\psi_{m,n} = \frac{\pi}{2}(m+n)$. $\beta_{m',n'}(t)$ and $\psi_{m',n'}$ are obtained by replacing m with m' and n with n' in $\beta_{m,n}(t)$ and $\psi_{m,n}$ respectively, where $n,\ n' \in \mathbb{Z}^+$. Set of positive integers is given by $\mathbb{Z}^+$ $(0 \in \mathbb{Z}^+)$. When signaling interval is denoted by T_s, signaling frequency F_s is denoted by $F_s = \frac{1}{T_s}$ and $\tau_s = \frac{1}{2F_s}$. $p(t)$ is the normalized subcarrier filter (see APPENDIX 1.2, Eq. (A1.3)). The receive filter is also the same as the transmit filter. PHYDYAS [24]-[26] and IOTA (Isotropic Orthogonal Transform Algorithm) [27], [28] filters are among the most suitable to be used for multicarrier communication techniques. The PHYDYAS NPR (near perfect reconstruction) filter, spectral leakages of which are reduced (comparatively lesser amount of power for the side lobes), is used for this study. Now the transmit signal with real-valued data symbol $a_{m,n}$ can be given as

$$\begin{aligned} s(t) &= \sum_{m=0}^{2M-1}\sum_{n=0}^{\infty} a_{m,n}\beta_{m,n}(t) \\ &= \sqrt{2}\sum_{m=0}^{2M-1}\sum_{n=0}^{\infty} a_{m,n}p(t-n\tau_s)e^{j2\pi mF_s t}e^{j\psi_{m,n}}. \end{aligned} \quad (2.6)$$

Then the asynchronous signal on path l with delay τ_l and the subcarrier frequency offset ϵ without noise,

$$s(t-\tau_l,\epsilon) = \sqrt{2}\sum_{m=0}^{2M-1}\sum_{n=0}^{\infty} a_{m,n}p(t-\tau_l-n\tau_s)e^{j2\pi(m+\epsilon)F_s(t-\tau_l)}e^{j\psi_{m,n}}. \quad (2.7)$$

$r(t,l,\epsilon)$ is the asynchronous receive signal in an AWGN channel,

$$r(t,l,\epsilon) = s(t-\tau_l,\epsilon)+\eta(t). \quad (2.8)$$

The channel noise after the process of subchannel filtering is given by $\eta(t)$. Then the receive signal after filtering is given as $v(m',n',l,\epsilon)=\int_0^{\infty}\beta^*_{m',n'}(t)r(t,l,\epsilon)\,dt$, where $\cdot^*$ is used to denote complex conjugate. It is further simplified to,

$$\begin{aligned} v(m',n',l,\epsilon) &= 2\sum_{m=0}^{2M-1}\sum_{n=0}^{\infty} a_{m,n}e^{j\left(\psi_{m,n}-\psi_{m',n'}\right)}e^{-j2\pi(m+\epsilon)F_s\tau_l}\int_0^{\infty}p\left(t-n'\tau_s\right) \\ &\quad .\, p(t-\tau_l-n\tau_s)e^{j2\pi F_s(m-m'+\epsilon)t}+\eta(t)\,dt. \end{aligned} \quad (2.9)$$

The signal containing a desired data symbol $a_{m,n}$ is expressed as

$$\begin{aligned} v_a(m,n,l,\epsilon) &= 2a_{m,n}e^{-j2\pi(m+\epsilon)F_s\tau_l}\int_0^{\infty}p(t-n\tau_s) \\ &\quad .\, p(t-\tau_l-n\tau_s)e^{j2\pi F_s(\epsilon)t}\,dt, \end{aligned} \quad (2.10)$$

with $m=m'$ and $n=n'$. $v_a(m,n,l,\epsilon)$ in (2.10) is a component of $v(m',n',l,\epsilon)$. In that case and with $l=0,\tau_l=\tau_0=0$ and $\epsilon=0$, the desired symbol can be recovered through estimated symbol as $\hat{a}_{m,n}=\Re\{v_a(m,n,0,0)\}=a_{m,n}$. $\Re\{\cdot\}$ is the real part of a complex-valued argument. $\beta_{m,n}(t-\tau_l,\epsilon)$ is an extension of (2.5) and it is apparent in asynchronous mode of operation where

$$\beta_{m,n}(t-\tau_l,\epsilon) = \sqrt{2}p(t-\tau_l-n\tau_s)e^{j2\pi(m+\epsilon)F_s(t-\tau_l)}e^{j\psi_{m,n}}. \quad (2.11)$$

Real-valued inner product of $\beta_{m,n}(t-\tau_l,\epsilon)$ and $\beta^*_{m',n'}(t)$ is constituted to an orthonormal basis of its span under synchronous conditions $(\tau_l=0,\epsilon=0)$ as given by

$$\Re\left\{\int_{t=0}^{\infty}\beta_{m,n}\left(t\right)\beta^{*}_{m',n'}\left(t\right)dt\right\} = \delta_{m,m'}\delta_{n,n'}, \tag{2.12}$$

where Kronecker delta function is denoted by $\delta_{.,.}$.

If communication takes place through a multipath channel containing L paths with path delays of τ_l and subcarrier frequency offset ϵ and noise $\eta\left(t\right)$, the receive signal immediately before filtering $u\left(t,\epsilon\right)$ is given by

$$u\left(t,\epsilon\right) = \sum_{l=0}^{L-1}h_l s\left(t-\tau_l,\epsilon\right)+\eta\left(t\right). \tag{2.13}$$

Then the receive signal after filtering $y\left(m',n',\epsilon\right)=\int_0^{\infty}\beta^{*}_{m',n'}\left(t\right)u\left(t,\epsilon\right)dt$ can be expressed as

$$\begin{aligned} y\left(m',n',\epsilon\right) &= 2\sum_{m=0}^{2M-1}\sum_{n=0}^{\infty}a_{m,n}e^{j\left(\psi_{m,n}-\psi_{m',n'}\right)}\sum_{l=0}^{L-1}h_l e^{-j2\pi(m+\epsilon)F_s\tau_l}\int_0^{\infty}p\left(t-n'\tau_s\right) \\ &\quad .\ p(t-\tau_l-n\tau_s)e^{j2\pi F_s(m-m'+\epsilon)t}+\eta\left(t\right)dt. \end{aligned} \tag{2.14}$$

Path delays are measured with respect to the first path, and h_l is the channel coefficient.

Discrete Domain Formulation

Discrete time formulation is developed for an asynchronous communication system in the same way as in [11] for a complete causal asynchronous basic FBMC communication system of $2M$ subcarriers. $\beta_{m,n}\left[k\right]$ and $\beta_{m',n'}\left[k\right]$ at time k are given as

$$\beta_{m,n}\left[k\right] = \sqrt{2}p[k-nM]e^{j\frac{2\pi m}{2M}\left(k-\frac{L_F-1}{2}\right)}e^{j\psi_{m,n}}, \tag{2.15}$$

$\beta_{m',n'}\left[k\right]$ is obtained by replacing m with m' and n with n' in $\beta_{m,n}\left[t\right]$.

$p[k]$ (see APPENDIX 1.2, Eq. (A1.5)) is the discrete domain normalized subcarrier filter. The transmit signal $s\left[k\right]$ at time k containing real-valued data symbol $a_{m,n}$ can be expressed as

$$\begin{aligned} s\left[k\right] &= \sum_{m=0}^{2M-1}\sum_{n=0}^{\infty}a_{m,n}\beta_{m,n}\left[k\right] \\ &= \sqrt{2}\sum_{m=0}^{2M-1}\sum_{n=0}^{\infty}a_{m,n}p[k-nM]e^{j\frac{2\pi m}{2M}\left(k-\frac{L_F-1}{2}\right)}e^{j\psi_{m,n}}. \end{aligned} \tag{2.16}$$

Then $s\left[k-l,\epsilon\right]$, the asynchronous signal with delay l and subcarrier frequency offset ϵ is

$$s\,[k-l,\epsilon] \;=\; \sqrt{2}\sum_{m=0}^{2M-1}\sum_{n=0}^{\infty} a_{m,n}p[k-l-nM]e^{j\frac{2\pi(m+\epsilon)}{2M}\left(k-l-\frac{L_F-1}{2}\right)}e^{j\psi_{m,n}}. \quad (2.17)$$

The asynchronous receive signal in an AWGN channel before filtering is equivalent to

$$r\,[k,l,\epsilon] \;=\; s\,[k-l,\epsilon]+\eta\,[k]. \quad (2.18)$$

The channel noise after going through the subchannel filtering process is given by $\eta\,[k]$. The receive signal after filtering $v\,[m',n',l,\epsilon] = \sum_{k=0}^{\infty}\beta^*_{m',n'}\,[k]\,r\,[k,l,\epsilon]$ is shown by

$$\begin{aligned} v\left[m',n',l,\epsilon\right] \;&=\; 2\sum_{m=0}^{2M-1}\sum_{n=0}^{\infty} a_{m,n}e^{j\left(\psi_{m,n}-\psi_{m',n'}\right)}e^{-j\frac{2\pi(m+\epsilon)}{2M}l}\sum_{k=0}^{\infty}p\left[k-n'M\right] \\ &\quad .\,p[k-l-nM]e^{j\frac{2\pi}{2M}(m-m'+\epsilon)\left(k-\frac{L_F-1}{2}\right)}+\eta\,[k]. \end{aligned} \quad (2.19)$$

With $m=m'$ and $n=n'$, the signal containing a specific data symbol $a_{m,n}$ can be expressed as

$$\begin{aligned} v_a[m,n,l,\epsilon] \;&=\; 2a_{m,n}e^{-j\frac{2\pi(m+\epsilon)}{2M}l}\sum_{k=0}^{\infty}p[k-nM] \\ &\quad .\,p[k-l-nM]e^{j\frac{2\pi}{2M}(\epsilon)\left(k-\frac{L_F-1}{2}\right)}. \end{aligned} \quad (2.20)$$

In that case, with $l=0,\epsilon=0$, $\hat{a}_{m,n}=\Re\{v_a[m,n,0,0]\}=a_{m,n}$.
The function $\beta_{m,n}\,[k-l,\epsilon]$,

$$\beta_{m,n}[k-l,\epsilon] \;=\; \sqrt{2}p[k-l-nM]e^{j\frac{2\pi(m+\epsilon)}{2M}\left(k-\frac{L_F-1}{2}-l\right)}e^{j\psi_{m,n}}, \quad (2.21)$$

is an extensions of (2.15), and it is apparent in the asynchronous mode of operation. Under synchronous conditions $(l=0,\epsilon=0)$ the real-valued inner product of $\beta_{m,n}\,[k-l,\epsilon]$ and $\beta_{m',n'}\,[k]$ in (2.22) is constituted to an orthonormal basis of its span, giving a successful symbol recovery:

$$\Re\left\{\sum_{k=0}^{\infty}\beta_{m,n}\,[k]\beta^*_{m',n'}\,[k]\right\} \;=\; \delta_{m,m'}\delta_{n,n'}. \quad (2.22)$$

If the communication takes place through a multipath channel containing L independent paths with a path delay l, subcarrier frequency offset ϵ and noise $\eta\,[k]$, the receive signal immediately before filtering and the same receive signal after filtering $y\,[m',n',l,\epsilon]=\sum_{k=0}^{\infty}\beta^*_{m',n'}\,[k]\,u\,[k,l,\epsilon]$ can be expressed as

$$u\left[k,\epsilon\right] \;=\; \sum_{l=0}^{L-1} h_l s\left[k-l,\epsilon\right] + \eta\left[k\right], \tag{2.23}$$

and

$$\begin{aligned} y\left[m',n',\epsilon\right] &= 2\sum_{m=0}^{2M-1}\sum_{n=0}^{\infty} a_{m,n} e^{j\left(\psi_{m,n}-\psi_{m',n'}\right)} \sum_{l=0}^{L-1} h_l e^{-j\frac{2\pi(m+\epsilon)}{2M}l} \sum_{k=0}^{\infty} p\left[k-n'M\right] \\ &\quad .\; p[k-l-nM] e^{j\frac{2\pi}{2M}(m-m'+\epsilon)\left(k-\frac{L_F-1}{2}\right)} + \eta\left[k\right], \end{aligned} \tag{2.24}$$

respectively, where path delays are measured with respect to the first path.

2.4 Summary and discussion

Both the OFDM and FBMC techniques were introduced in detail. Most importantly, the reasons behind selecting them as the potential communication techniques for future communication applications were discussed. Their distinct features and associated drawbacks were also presented. Some of the major applications of OFDM and recent developments related to it were also briefly presented. In the case of FBMC, most of the available developments were discussed. It was found that FBMC is still in the early stage of its life cycle and that there are some inherent technical barriers, such as complexity, for rapid development. The basic conventional formulation used in this study for OFDM was also made available. In the case of FBMC, both continuous and discrete time formulations for a basic causal multirate FBMC system that can be operated under different fading conditions in a multipath channel were presented.

3 SELF-INTERFERENCE IN FBMC

This part of study sets out to conduct a comprehensive analysis on self-interference of a causal multirate FBMC system supported by one of the most well localized subcarrier filters. Two types of self-interferences under different synchronization conditions are investigated: interference generated from a desired symbol to other symbols and interference generated from any symbol to a particular symbol. The knowledge of these interferences is highly useful for transmitter and receiver developments leading towards interference-free reliable wireless transmission. Also their probability density functions are provided. Numerical results for asynchronous mode, with offsets in time, frequency, time-frequency and synchronous mode, are discussed.

3.1 Introduction

Interference is one of the crucial impairments that can be identified in any communication system irrespective of the medium of transmission. It is extensively influenced by the characteristics of the propagation medium. A medium of preparation can be anything including vacuum space. Here a medium of preparation can be anything including vacuum space. It is not expected to be a single medium all the times. It can be a mixture of different mediums. Usually, communication systems are designed to perform in an error-free manner under perfect conditions and without AWGN. Further, they are tested in transmission mediums or channels under different fading, synchronization and propagation conditions. Different types of interferences are generated due to the randomness of the propagation channels and the limitedness of radio spectrum, making it harder for the receiver to detect signals. The situation is much worse under asynchronous conditions with time and frequency offsets. There are basically two types interferences that can be generated without any contribution from signals transmitted from other transmitters. They are ICI, which is common in multicarrier communication systems, and ISI, which can be common in all types of communication systems. The general impression is that if there is only a CFO the type of interference is ICI and if there are delayed paths the type of interference is ISI. Co-channel and adjacent channel interferences are interferences which are generated by other sources.

ICI in a multicarrier communication system is higher when there is a relative movement between the transmitter and the receiver. There are several solutions for this. One is to use a bank of parallel subcarrier filters. If the condition is due to CFO, then the answer is to have an estimation of the frequency offset to be able to correct it. Employment of an equalization technique is another successful solution. There are number of optimum or sub-optimum equalizers. A suitable equalization technique can be selected by considering implementation complexity and the required amount of performance. A linear equalizer based on the minimum mean square error criterion can be applied in frequency domain in order to reduce the effect of ICI [12].

Multipath propagation is the typical reason for ISI. If the modulated symbol duration is big enough compared to the delay spread the channel, an equivalent ISI-free channel can be expected. This phenomenon is connected to the transmission rate and to the shape of the pulse as well. Equalization is the most commonly used solution for this. Receivers can be developed with various linear and nonlinear equalization techniques. In linear equalizers, efforts are made on detecting the current symbol while attempting to linearly suppress the interference from the other symbols. Complex algorithms are used for the same purpose for nonlinear equalizers. Two main types of equalizers can be identified based on the type of approach. Symbol by symbol equalization is carried out in equalizers such as the decision feedback equalizer, and symbol sequences are used in equalizers of the maximum likelihood sequence estimation equalizer type.

In most of the well-established multicarrier transmission techniques, the prominent or paramount need is to maintain orthogonality among all the subcarriers. In failing to do so, ICI is generated, leading to significant performance degradation. In high mobility conditions especially, a severe ICI due to Doppler spread can be observed. Results of numerous studies evaluating the BER performance of the OFDM family of technologies with ICI or by estimating the CFO are available [87]-[89]. On the other hand, capacity to bring the performance to an acceptable level in multipath channels by converting ISI into ISI-free channels through the efficient use of CP is one of the main reasons for the popularity of OFDM. The process is naturally supported by long symbol durations, and significant time delay spreads are associated with it. This can be considered as a special feature of this family and cannot be commonly applied to many of the other techniques while maintaining the same data rate and spectral efficiency. However the performance of an OFDM receiver can be degraded, due to timing-synchronization errors with the introduction of ICI and ISI. Many studies of considerable importance that are related to this problem have been carried out. Most of the developments related to OFDM can be taken as the baseline for performance comparisons and enhancements of FBMC.

The properties of self-interference in FBMC are not exactly the usual ICI or ISI, where they consist of characteristics of multirate transmission techniques.

Self-interference is spread through two-dimensional time-frequency space and, naturally, it is highly affected by the characteristics of subcarrier filters. Since the signal before filtering is inaudible for processing, generally it is corrupted and very complicated to process and the exact time-frequency domain relationship cannot be established by a simple transformation operation. The situation is even worse under asynchronous conditions. Even though there are some well-localized filters, they are not strong enough to handle the asynchronous and multipath conditions common in any kind of communication channel. On the other hand, it should be possible to integrate the filters into the system, using multirate techniques in order to maintain the throughput of the system. There have been many attempts to integrate equalization techniques to FBMC through different approaches, with the objective to mitigate different types of interferences [90]-[95]. But how easily a much better scheme can be developed for FBMC is still quite doubtful due to the aforementioned reasons and characteristics of self-interference. Therefore it is necessary to carry out all kinds of analyses on self-interference of each specific FBMC technique customized to a particular subcarrier filter. The analyses should be detailed enough, with clear insight information, without approximations and carried out under different synchronization conditions. Only the results obtained in this way can be used for the subsequent or latter development related to this particular communication technique.

Efficient use of spectrum through reduction of ICI of OFDM under different conditions is discussed and analyzed in [16], [96]. In [97], influence of interference is presented as an average of the Gaussian complementary distribution function. Pulse shaping is identified as one of the most straightforward approaches to combat ICI in any communication system. Insight knowledge on interferences is the key element gained through different analyses. In the case of FBMC, results of numerous investigations of SISO setups [98],[99] and cellular networks [79] are also available. Knowledge about the behavior of self-interference under different conditions is quite essential for all the enhancements and to find solutions for the existing problems related to this particular communication technique. However, the available presentations are not general enough to be easily understood. In contrast to all the other communication techniques, multirate-technique assisted FBMC systems are highly susceptible for self-interference. The situation is still much worse in the asynchronous mode of operation in the presence of time and frequency offsets, even without a channel.

One of the most common form of modeling self-interference is to identify and separate it from the receive information data signal [21], [83]. But this is confined to modeling purposes only. It is an apparent fact that such a clear separation cannot be observed in actual receive signal. Always the effect of self-interference is taken into account in subsequent derivations. External interferences arisen within a cellular network are modeled and presented in [79], [81]. In that case also, the interference components are separately identified and added to the receive information signal. A separate, detail and continuous formulation process is followed to derive the receive signal in this presentation where self-interference is naturally taken into account which is similar to the method followed in [90].

An analysis on the behavior of a causal multirate FBMC system under synchronous and asynchronous operational conditions is presented within this chapter, without considering the effect of channels. A discrete time formulation for that is also made available. Analysis is carried out by categorizing interferences into two types. These are generated in the system during the process of signal detection. They are followed by numerical and simulation results for selected set of scenarios for both synchronous and asynchronous modes of operations. Finally entire outcome of this investigation is summarized.

3.2 Interference Analysis

Interference in a system can be analyzed under two categories: i.e., interference generated from a particular data symbol to other symbols and interference generated from other symbols to a certain symbol. Here, the second category is presented to increase the clarity and comprehensiveness of this analysis. The symbols that have been sent completely through the transmit filter are intended to be recovered or considered as the desired data symbols. This interference is spread through time-frequency dimensions in an ICI / ISI combined format.

For simplicity, $v\,[m', n', l, \epsilon]$ in (2.19) without AWGN is considered. It can be identified as a composition (3.1) of a receive signal with the desired information symbol $v_a[m, n, l, \epsilon]$ and interferences generated to other symbols $v_I[m', n', l, \epsilon]$. These are are given by (2.20) and (3.2), respectively.

$$\begin{aligned} \textit{Receive Signal After Filtering} &= \textit{Signal with Desired Symbol} + \textit{Self-Interference} \\ v\left[m', n', l, \epsilon\right] &= v_a\left[m', n', l, \epsilon\right] + v_I\left[m', n', l, \epsilon\right] \end{aligned} \tag{3.1}$$

Equation (2.20) is obtained with $m = m'$ and $n = n'$. Parameters are set to $m \neq m'$ and $n \neq n'$ (simultaneously) for $v_I[m', n', l, \epsilon]$ (two cases $m \neq m'$ with $n = n'$ which is for pure ICI and $m = m'$ with $n \neq n'$ which is for pure ISI are also included),

$$\begin{aligned} v_I\left[m', n', l, \epsilon\right] &= 2\sum_{\substack{m=0 \\ m\neq m'}}^{2M-1}\sum_{\substack{n=0 \\ n\neq n'}}^{\infty} a_{m,n} e^{j\left(\psi_{m,n}-\psi_{m',n'}\right)} e^{-j\frac{2\pi(m+\epsilon)}{2M}l} \sum_{k=0}^{\infty} p\left[k - n'M\right] \\ &\quad .\, p[k - l - nM] e^{j\frac{2\pi}{2M}(m-m'+\epsilon)\left(k-\frac{L_F-1}{2}\right)}. \end{aligned} \tag{3.2}$$

3.2.1 Interference by a Desired Symbol

In this category, interferences caused to any other symbol $a_{m',n'}$ by $a_{m,n}$ during the process of detection under asynchronous conditions are considered. A single component of interference generated to any $a_{m',n'}$ by $a_{m,n}$ with $(m \neq m')$ and $(n \neq n')$ is presented as

$$v_I\left[m',n',m,n,l,\epsilon\right] = 2a_{m,n}e^{j\left(\psi_{m,n}-\psi_{m',n'}\right)}e^{-j\frac{2\pi(m+\epsilon)}{2M}l}\sum_{k=0}^{\infty}p\left[k-n'M\right] \\ .\, p[k-l-nM]e^{j\frac{2\pi}{2M}(m-m'+\epsilon)\left(k-\frac{L_F-1}{2}\right)}. \quad (3.3)$$

Total of all interferences in the system due to this detection is given by (3.2) (two cases, $m \neq m'$ with $n = n'$ and $m = m'$ with $n \neq n'$, are also included). By observing (3.3) and [96], it can be noted that each $\Re\{v_I[m',n',m,n,l,\epsilon]\}$ in (3.2) is with a $\Re\{v_I[m',n',m,n,l,\epsilon]\} \sim \mathcal{N}\left(0,\sigma_I^2[m',n',m,n,l,\epsilon]\right)$. An independently and identically distributed (i.i.d.) Gaussian distribution, with mean μ and variance σ^2, is represented by $\mathcal{N}\left(\mu,\sigma^2\right)$. The probability density function (PDF) for a random variable x in a Gaussian distribution is represented by $f\left(x;\mu,\sigma^2\right)$. The variance $\sigma_I^2[m',n',m,n,l,\epsilon]$ is presented by

$$\sigma_I^2\left[m',n',m,n,l,\epsilon\right] = \left|\Re\left\{2e^{j\left(\psi_{m,n}-\psi_{m',n'}\right)}e^{-j\frac{2\pi(m+\epsilon)}{2M}l}\sum_{k=0}^{\infty}p\left[k-n'M\right]\right.\right. \\ \left.\left. .\, p[k-l-nM]e^{j\frac{2\pi}{2M}(m-m'+\epsilon)\left(k-\frac{L_F-1}{2}\right)}\right\}\right|^2. \quad (3.4)$$

The total interference (3.2) is in a $\Re\{v_I[m',n',l,\epsilon]\} \sim \mathcal{N}\left(0,\sigma_I^2[m',n',l,\epsilon]\right)$. Since individual interference components are uncorrelated, the variance of total interferences $\sigma_I^2[m',n',l,\epsilon]$ is given as

$$\sigma_I^2\left[m',n',l,\epsilon\right] = \sum_{\substack{m=0\\ m\neq m'}}^{2M-1}\sum_{\substack{n=0\\ n\neq n'}}^{\infty}\sigma_I^2\left[m',n',m,n,l,\epsilon\right]. \quad (3.5)$$

Similarly, it can be shown that $\Im\{v_I[m',n',m,n,l,\epsilon]\}$ and $\Im\{v_I[m',n',l,\epsilon]\}$ are also in the Gaussian distributions. $\Im\{\cdot\}$ is the imaginary part of a complex-valued argument.

3.2.2 Interference to a Desired Symbol

In this section interference generated by any real-valued symbol $a_{m'',n''}$ related to time instance n'' on subcarrier m'' to $a_{m,n}$ during the process of detection of an asynchronous transmission is studied. A single component of interference generated to any $a_{m',n'}$ by $a_{m'',n''}$ is presented as

$$v_{I''}\left[m',n',m'',n'',l,\epsilon\right] = 2a_{m'',n''}e^{j\left(\psi_{m'',n''}-\psi_{m',n'}\right)}e^{-j\frac{2\pi\left(m''+\epsilon\right)}{2M}l}\sum_{k=0}^{\infty}p\left[k-n'M\right] \\ .\, p\left[k-l-n''M\right]e^{j\frac{2\pi}{2M}(m''-m'+\epsilon)\left(k-\frac{L_F-1}{2}\right)}, \quad (3.6)$$

where $\psi_{m'',n''} = \frac{\pi}{2}(m'' + n'')$. In the case of detection of $a_{m,n}$ parameters are set to $(m'' \neq m, n'' \neq n, m = m')$ and $(n = n')$. The sum of all interferences to a desired symbol $v_{I''}[m', n', l, \epsilon]$,

$$v_{I''}\left[m', n', l, \epsilon\right] = 2 \sum_{\substack{m''=0 \\ m' \neq m''}}^{2M-1} \sum_{\substack{n''=0 \\ n' \neq n''}}^{\infty} a_{m'',n''} e^{j\left(\psi_{m'',n''} - \psi_{m',n'}\right)} e^{-j\frac{2\pi(m''+\epsilon)}{2M} l} . \sum_{k=0}^{\infty} p\left[k - n'M\right] p\left[k - l - n''M\right] . e^{j\frac{2\pi}{2M}(m''-m'+\epsilon)\left(k - \frac{L_F-1}{2}\right)}, \quad (3.7)$$

that is available with the recovered desired symbol $a_{m,n}$ can be obtained by setting $(m = m')$ and $(n = n')$ (two cases, $m'' \neq m$ with $n'' = n$ and $m'' = m$ with $n'' \neq n$, are also included). This interference is to be eliminated for an effective signal recovery. In contrast to the analysis presented in 3.2.1, other than the instance $m'' = m$, all the symbols given by $a_{m'',n''}$ are with incomplete filter lengths where they cannot be recovered meaningfully at this particular time instance. In other words, they are purely considered as a set of meaningless symbols where only the interference is strengthened with them. With the use of a separate indexing scheme, the interference caused to any symbol, even to the symbols that are not intended to be recovered at a particular time instance or the non-desired symbols can be presented leading to a more general, complete and fair analysis. Considering (3.6) and [96], it can be observed that each $\Re\{v_{I''}[m', n', m'', n'', l, \epsilon]\}$ shown by (3.6) is with a $\Re\{v_{I''}[m', n', m'', n'', l, \epsilon]\} \sim \mathcal{N}\left(0, \sigma^2_{I''}[m', n', m'', n'', l, \epsilon]\right)$. The variance $\sigma^2_{I''}[m', n', m'', n'', l, \epsilon]$ is available in

$$\sigma^2_{I''}\left[m', n', m'', n'', l, \epsilon\right] = \left| \Re\left\{ 2e^{j\left(\psi_{m'',n''} - \psi_{m',n'}\right)} e^{-j\frac{2\pi(m''+\epsilon)}{2M} l} \sum_{k=0}^{\infty} p\left[k - n'M\right] . \; p\left[k - l - n''M\right] e^{j\frac{2\pi}{2M}(m''-m'+\epsilon)\left(k - \frac{L_F-1}{2}\right)} \right\} \right|^2 . \quad (3.8)$$

Therefore the total interference at the receiver for a desired symbol (3.7) is in $\Re\{v_{I''}[m', n', l, \epsilon]\} \sim \mathcal{N}\left(0, \sigma^2_{I''}[m', n', l, \epsilon]\right)$. The variance of the total interference generated by other symbols $\sigma^2_{I''}[m', n', l, \epsilon]$ is given by

$$\sigma^2_{I''}\left[m', n', l, \epsilon\right] = \sum_{\substack{m''=0 \\ m' \neq m''}}^{2M-1} \sum_{\substack{n''=0 \\ n' \neq n''}}^{\infty} \sigma^2_{I''}\left[m', n', m'', n'', l, \epsilon\right], \quad (3.9)$$

where individual interference components are uncorrelated. Similarly, it can be shown that $\Im\{v_{I''}[m', n', m'', n'', l, \epsilon]\}$ and $\Im\{v_{I''}[m', n', l, \epsilon]\}$ are also in Gaussian distributions.

3.3 Numerical Results

A basic FBMC system with 64 subcarriers is used to obtain numerical results. A normalized PHYDYAS filter is used as both transmit and receive subcarrier filters (APPENDIX 1.2). A symbol transmitted in subcarrier 32 is selected as the desired symbol. Here the time shift $l = 1$ is equivalent to $1/256L_F$. Interference values between -0.0001 to 0.0001 are neglected. It is important to note that not only the magnitude but also the sign of the receive interference component is also important. If the sign can be accurately identified, also the signal can be more precisely estimated.

3.3.1 Interference by a Desired Symbol

In this section, interference generated to any other symbol $a_{m',n'}$ by a desired symbol $a_{m,n}$ is presented. Parameters are set to $m \neq m'$ and $n \neq n'$ for the symbols other than the desired symbol. For the purpose of detection of a desired symbol, they are set to $m = m'$ and $n = n'$. As in [98] and [99], but without approximations, interference generated under the synchronous case $(l = 0, \epsilon = 0)$ is presented in Figure 2. Real and imaginary parts are shown in Figure 2 - (a) and (b). The results for $(l = 1, \epsilon = 0.01)$ are shown in Figure 3. The variances of total interferences for the scenarios $(l = 0, \epsilon = 0)$, $(l = 1, \epsilon = 0)$, $(l = 0, \epsilon = 0.01)$ and $(l = 1, \epsilon = 0.01)$ are 3.0171×10^{-07}, 0.0106, 0.0160 and 0.0499, respectively (Interference values in the range of -0.0001 to 0.0001 are also taken into account.). Particular probability distributions are shown in Figure 4.

3.3.2 Interference to a Desired Symbol

Interference generated by any other symbol $a_{m'',n''}$ to a desired symbol $a_{m,n}$ is presented in this section. Here the parameters are set to $m'' \neq m$, $n'' \neq n$, $m = m'$ and $n = n'$. It should be noted that interferences are presented at the location of the interference-causing symbol. This is done for the presentation purposes only, and should not be misunderstood as detected symbols or interferences at those locations. Interference generated under the synchronous case $(l = 0, \epsilon = 0)$ is presented in Figure 5. Similarly, the results for an asynchronous configuration $(l = 1, \epsilon = 0.01)$ are shown in Figure 6. The variances of total interferences for the cases $(l = 0, \epsilon = 0)$, $(l = 1, \epsilon = 0)$, $(l = 0, \epsilon = 0.01)$ and $(l = 1, \epsilon = 0.01)$ can be observed or calculated to be 3.0171×10^{-07}, 0.0173, 0.0160 and 0.0577, respectively (Interferences in the range of -0.0001 to 0.0001 are also accounted.). The respective probability distributions are shown in Figure 7. In the case of OFDM, this type of interferences is being extensively analyzed under different transmission conditions in [14], [97].

Real	*n*-6	*n*-5	*n*-4	*n*-3	*n*-2	*n*-1	*n*	*n*+1	*n*+2	*n*+3	*n*+4	*n*+5	*n*+6	
***m*-2**	0.00013	0	0	0	-0.00013	0	0	0	-0.00013	0	0	0	0.00013	***m*-2**
***m*-1**	0	0	0	0	0	0	0	0	0	0	0	0	0	***m*-1**
m	0.000203	0	0	0	-0.0002	0	1	0	-0.0002	0	0	0	0.000203	***m***
***m*+1**	0	0	0	0	0	0	0	0	0	0	0	0	0	***m*+1**
***m*+2**	0.00013	0	0	0	-0.00013	0	0	0	-0.00013	0	0	0	0.00013	***m*+2**
	n-6	*n*-5	*n*-4	*n*-3	*n*-2	*n*-1	*n*	*n*+1	*n*+2	*n*+3	*n*+4	*n*+5	*n*+6	

(a)

Imag	*n*-6	*n*-5	*n*-4	*n*-3	*n*-2	*n*-1	*n*	*n*+1	*n*+2	*n*+3	*n*+4	*n*+5	*n*+6	
***m*-2**	0	0.00059	0	0.00059	0	0	0	0	0	-0.00059	0	-0.00059	0	***m*-2**
***m*-1**	0	-0.00131	0.005362	-0.04288	0.124974	-0.2058	0.239277	-0.2058	0.124974	-0.04288	0.005362	-0.00131	0	***m*-1**
m	0	0.0023	0	0.066755	0	0.564448	0	-0.56445	0	-0.06675	0	-0.0023	0	***m***
***m*+1**	0	-0.00131	-0.00536	-0.04288	-0.12497	-0.2058	-0.23928	-0.2058	-0.12497	-0.04288	-0.00536	-0.00131	0	***m*+1**
***m*+2**	0	0.00059	0	0.00059	0	0	0	0	0	-0.00059	0	-0.00059	0	***m*+2**
	n-6	*n*-5	*n*-4	*n*-3	*n*-2	*n*-1	*n*	*n*+1	*n*+2	*n*+3	*n*+4	*n*+5	*n*+6	

(b)

FIGURE 2 Interference by $a_{m,n}$ in synchronous operation : **(a)** real and **(b)** imaginary components

Real	*n*-6	*n*-5	*n*-4	*n*-3	*n*-2	*n*-1	*n*	*n*+1	*n*+2	*n*+3	*n*+4	*n*+5	*n*+6	
***m*-2**	-0.00012	0.000111	0	0	0.000107	0	0	0	0	0	-0.00014	0	-0.00014	***m*-2**
***m*-1**	0	-0.00031	0.001204	-0.00896	0.024353	-0.03716	0.039904	-0.03163	0.017704	-0.00566	0.000658	-0.00013	0	***m*-1**
m	-0.00018	0.000623	-0.00078	0.017108	-0.00869	0.127934	-0.97473	-0.1203	0.009943	-0.01205	0.000889	-0.00036	-0.00021	***m***
***m*+1**	0	-0.00043	-0.00158	-0.01275	-0.03712	-0.05943	-0.06627	-0.05414	-0.03098	-0.00997	-0.00116	-0.00026	0	***m*+1**
***m*+2**	-0.00011	0.000225	0.000134	0.000232	0.000161	0	0	0	0.000146	-0.00016	0	-0.00015	-0.00014	***m*+2**
	n-6	*n*-5	*n*-4	*n*-3	*n*-2	*n*-1	*n*	*n*+1	*n*+2	*n*+3	*n*+4	*n*+5	*n*+6	

(a)

Imag	*n*-6	*n*-5	*n*-4	*n*-3	*n*-2	*n*-1	*n*	*n*+1	*n*+2	*n*+3	*n*+4	*n*+5	*n*+6	
***m*-2**	0	-0.00054	0	-0.00057	0	0	0	0	0	0.000527	0	0.000599	0	***m*-2**
***m*-1**	0	0.001217	-0.005	0.040012	-0.11731	0.194266	-0.22798	0.199062	-0.12396	0.044641	-0.00593	0.00135	0	***m*-1**
m	0	-0.00201	-0.00023	-0.06194	-0.00225	-0.52718	-0.22039	0.5738	0.001922	0.068056	0.000143	0.002479	0	***m***
***m*+1**	0	0.001189	0.004547	0.038649	0.118787	0.201248	0.238095	0.207048	0.126578	0.043707	0.005463	0.001342	0	***m*+1**
***m*+2**	0	-0.00053	0	-0.0006	0	0	0	0	0	0.000575	0	0.000614	0	***m*+2**
	n-6	*n*-5	*n*-4	*n*-3	*n*-2	*n*-1	*n*	*n*+1	*n*+2	*n*+3	*n*+4	*n*+5	*n*+6	

(b)

FIGURE 3 Interference to $a_{m,n}$ with time and frequency offsets of $1/L_F$ and 0.01 : **(a)** real and **(b)** imaginary components

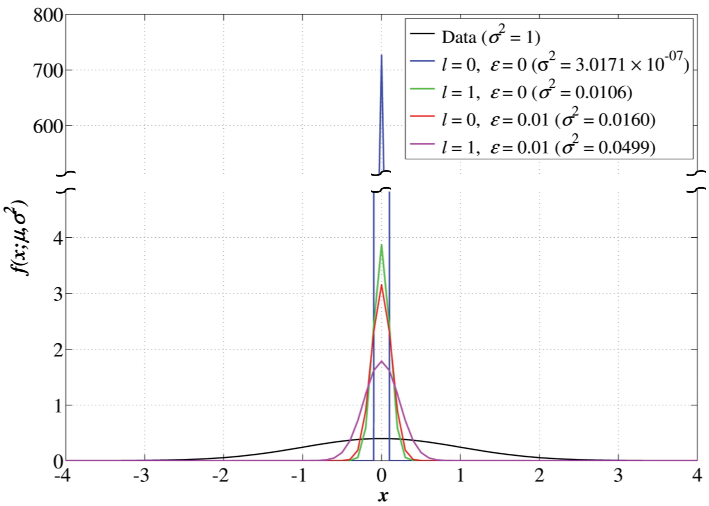

FIGURE 4 Interference by a desired symbol

3.4 Summary and discussion

Self-interferences of a basic causal asynchronous FBMC system under two categories were investigated. The analysis was customized to a particular FBMC

Real	*n*-6	*n*-5	*n*-4	*n*-3	*n*-2	*n*-1	*n*	*n*+1	*n*+2	*n*+3	*n*+4	*n*+5	*n*+6	
m-2	0.00013	0	0	0	-0.00013	0	0	0	-0.00013	0	0	0	0.00013	*m*-2
m-1	0	0	0	0	0	0	0	0	0	0	0	0	0	*m*-1
m	0.000203	0	0	0	-0.0002	0	1	0	-0.0002	0	0	0	0.000203	*m*
m+1	0	0	0	0	0	0	0	0	0	0	0	0	0	*m*+1
m+2	0.00013	0	0	0	-0.00013	0	0	0	-0.00013	0	0	0	0.00013	*m*+2
	n-6	*n*-5	*n*-4	*n*-3	*n*-2	*n*-1	*n*	*n*+1	*n*+2	*n*+3	*n*+4	*n*+5	*n*+6	

(a)

Imag	*n*-6	*n*-5	*n*-4	*n*-3	*n*-2	*n*-1	*n*	*n*+1	*n*+2	*n*+3	*n*+4	*n*+5	*n*+6	
m-2	0	-0.00059	0	-0.00059	0	0	0	0	0	0.00059	0	0.00059	0	*m*-2
m-1	0	0.001312	-0.00536	0.042882	-0.12497	0.2058	-0.23928	0.2058	-0.12497	0.042882	-0.00536	0.001312	0	*m*-1
m	0	-0.0023	0	-0.06675	0	-0.56445	0	0.564448	0	0.066755	0	0.0023	0	*m*
m+1	0	0.001312	0.005362	0.042882	0.124974	0.2058	0.239277	0.2058	0.124974	0.042882	0.005362	0.001312	0	*m*+1
m+2	0	-0.00059	0	-0.00059	0	0	0	0	0	0.00059	0	0.00059	0	*m*+2
	n-6	*n*-5	*n*-4	*n*-3	*n*-2	*n*-1	*n*	*n*+1	*n*+2	*n*+3	*n*+4	*n*+5	*n*+6	

(b)

FIGURE 5 Interference to $a_{m',n'}$ in synchronous operation : **(a)** real and **(b)** imaginary components

Real	*n*-6	*n*-5	*n*-4	*n*-3	*n*-2	*n*-1	*n*	*n*+1	*n*+2	*n*+3	*n*+4	*n*+5	*n*+6	
m-2	-0.00012	-0.00035	0	-0.00032	0.00013	0	0	0	0.000152	0.000293	0.000129	0.000245	-0.00011	*m*-2
m-1	0	0.000592	-0.00234	0.018147	-0.05087	0.08044	-0.08929	0.072726	-0.04129	0.012898	-0.00145	0.000363	0	*m*-1
m	-0.0002	-0.00074	0.000864	-0.0184	0.009803	-0.13826	-0.97473	0.111312	-0.00881	0.011203	-0.0008	0.000301	-0.00019	*m*
m+1	0	0.000208	0.00082	0.005486	0.013313	0.018279	0.017366	0.011741	0.005233	0.001147	0	0	0	*m*+1
m+2	-0.00014	0	-0.00014	0	0	0	0	0	0.000108	0	0	0	-0.00012	*m*+2
	n-6	*n*-5	*n*-4	*n*-3	*n*-2	*n*-1	*n*	*n*+1	*n*+2	*n*+3	*n*+4	*n*+5	*n*+6	

(a)

Imag	*n*-6	*n*-5	*n*-4	*n*-3	*n*-2	*n*-1	*n*	*n*+1	*n*+2	*n*+3	*n*+4	*n*+5	*n*+6	
m-2	0	0.000524	0	0.000505	0	0	0	0	0	-0.00058	0	-0.00052	0	*m*-2
m-1	0	-0.00123	0.00507	-0.04099	0.119974	-0.19832	0.230454	-0.19684	0.117402	-0.0386	0.004589	-0.00121	0	*m*-1
m	0	0.002392	0.000253	0.06662	0.002543	0.569738	-0.22039	-0.53094	-0.0017	-0.06327	-0.00013	-0.00208	0	*m*
m+1	0	-0.00134	-0.00591	-0.04466	-0.1245	-0.20073	-0.23079	-0.19744	-0.1197	-0.04099	-0.00515	-0.00126	0	*m*+1
m+2	0	0.0006	0	0.000528	0	0	0	0	0	-0.00058	0	-0.00054	0	*m*+2
	n-6	*n*-5	*n*-4	*n*-3	*n*-2	*n*-1	*n*	*n*+1	*n*+2	*n*+3	*n*+4	*n*+5	*n*+6	

(b)

FIGURE 6 Interference to $a_{m',n'}$ with time and frequency offsets of $1/L_F$ and 0.01 : **(a)** real and **(b)** imaginary components

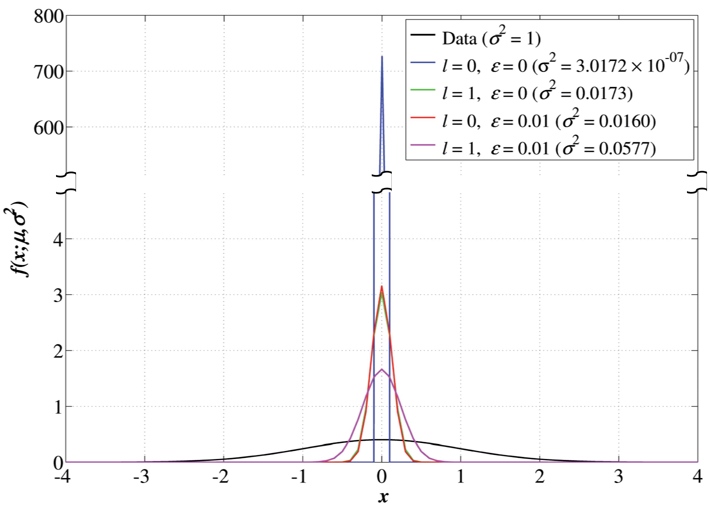

FIGURE 7 Interference to a desired symbol

setup giving detailed information without approximations or assumptions. Numerical results were presented for both synchronous and asynchronous scenarios. In accordance with the design of the filter, certain amount of interference could be observed for frequency offsets. Similarly, interference for time offsets and even higher interference for time and frequency offsets could be noted. In the same way as in [96], the variances for individual interfering components and the total interference were shown. Closed-form expressions for the probability distributions of individual and total interference were presented. Most importantly, as in [97], this analysis can provide a thorough understanding of the behavior of this particular communication technique and associated self-interference. This is immensely helpful for all the developments relating to this technique.

4 PERFORMANCE OVER CHANNELS

Performance over different channels is an essential element in the assessment of the potential of any communication technique for subsequent applications. Performance is evaluated in terms of BER for an FBMC system operated in different multipath channels under different synchronization conditions. In contrast to many available FBMC models studied, a causal multirate FBMC system without assumptions and approximations for the basic transmitter and receiver setup is used for this study. A stable receiver based on minimum Euclidean distance is introduced for the purpose of signal detection. Closed-form expressions for approximate BERs are also employed. The results are compared against that of a standard OFDM system.

4.1 Introduction

Fading effects in wireless radio channels are considered. They are somewhat different than the other forms of wireless channels encountered in ionospheric and tropospheric propagations. There are three main components which are capable of determining the characteristics of a fading model: namely, the receive signal amplitude distribution, line of sight components and the Doppler spread. Their behavior can be mathematically analyzed. There are two types of fading: large-scale fading and small-scale fading.

In large scale fading, average signal power is attenuated or the path loss is taken place due to motion over large areas. Typical causes for this phenomenon can be hills, forests, billboards, clumps of buildings and similar objects, which have the effect similar to that of terrain contours between the transmitter and the receiver. The receiver is said to be 'shadowed' by this kinds of obstacles. Many models of this kind are described in terms of mean path loss (nth-power law) and log-normally distributed variation about the mean. Small-scale fading, a characteristic of a radio propagation, is influenced by reflectors and scatterers, causing multiple versions of the transmit signal to arrive at the receiver. Those versions have distinct amplitudes, phases and angles of arrival. On the other hand small-scale fading exhibits rapid fluctuations of the receive signal strength over very short distances and short time durations. These signal fluctuations can be modeled with several statistical distributions or PDFs.

Small-scale fading is called Rayleigh fading if there are multiple reflective paths and no line-of-sight signal component. The envelope of such a receive signal is statistically described by the Rayleigh PDF. When the line-of-sight component is available, a small-scale fading envelope is described by the Rician PDF. In other words, fading statistics are said to be Rayleigh whenever no line-of-sight path is available and Rician otherwise. Based on the scenario, there is a number of fading channel models that can be used for the wireless interface. Some of the fading models are, Nakagami-m [2, Eq. 2.20], [100], Nakagami-q (Hoyt) and Weibull. All of them are special cases of $\kappa - \mu$ and $\eta - \mu$ distributions [101]. But many of them are rarely used.

In addition, many different models like vehicular-AE and vehicular-B, that are proposed or approved by the International Telecommunication Union (ITU) and by several other organizations are also available. These are related to different types of fading under numerous mobility conditions. It is important to keep in mind that none of the models may be suitable for real world scenarios and all of them are capable of giving a rough picture about a particular environment. Customized empirical models and associated evaluations based on field measurement tests are proofs for this fact. Both types of fading are possible for a mobile receiver roaming over a large area. This study, however, is narrowed down to small-scale fading.

First, a selected set of fading channels are introduced to be considered within this study. BER expressions for different channels are presented in the next section. A detection scheme and channel coding schemes for interference mitigation are also discussed. Numerical and simulation results with relevant comparisons are made available in the next section. The chapter is concluded by summarizing the contribution and outcomes of this study.

4.2 AWGN, Rayleigh, Rician and Nakagami-m Channels

Three basic channels, namely, Rayleigh, Rician and Nakagami-m with their corresponding PDFs $\left(f_{h_R}(h_R), h_R \geq 0\right)$ [2, Eq. 2.6], [100], $\left(f_{h_C}(h_C), h_C \geq 0\right)$ [2, Eq. 2.15], [100] and $\left(f_{h_N}(h_N), h_N \geq 0\right)$ [2, Eq. 2.20], [100] are considered. h_R, h_C and h_N are the relevant independent fading amplitudes. The respective average fading powers are denoted by $\overline{h}_R, \overline{h}_C$ and $\overline{h}_N$. "Rician K" and "Nakagami shape" factors are represented by $\mathcal{K}_{RK}$ $(\mathcal{K}_{RK} = \mathcal{K}_C^2)$ and m_N. All the fading channel coefficients are modeled according to these expressions. The instantaneous SNR values per symbol are represented by γ_R, γ_C and γ_N. For each fading channel model, the PDFs for γ_R, γ_C and γ_N are given by $\left(f_{\gamma_R}(\gamma_R), \gamma_R \geq 0\right)$ [2, Eq. 2.7],

$\left(f_{\gamma_C}\left(\gamma_C\right), \gamma_C \geq 0\right)$ [2, Eq. 2.16] and $\left(f_{\gamma_N}\left(\gamma_N\right), \gamma_N \geq 0\right)$ [2, Eq. 2.21]. $\overline{\gamma}_R = \mathbb{E}\left[\gamma_R\right]$, $\overline{\gamma}_C = \mathbb{E}\left[\gamma_C\right]$ and $\overline{\gamma}_N = \mathbb{E}\left[\gamma_N\right]$ are the average SNR values per symbol.

$$
\begin{aligned}
f_{h_R}\left(h_R\right) &= \frac{2h_R}{\overline{h}_R} \exp\left(-\frac{h_R^2}{\overline{h}_R}\right) && (4.1)\\
f_{\gamma_R}\left(\gamma_R\right) &= \frac{1}{\overline{\gamma}_R} \exp\left(-\frac{\gamma_R}{\overline{\gamma}_R}\right) && (4.2)\\
f_{h_C}\left(h_C\right) &= \frac{2\left(1+\mathcal{K}_C^2\right) e^{-\mathcal{K}_C^2} h_C}{\overline{h}_C} \exp\left(-\frac{\left(1+\mathcal{K}_C^2\right) h_C^2}{\overline{h}_C}\right) \\
&\quad . J_0\left(2\mathcal{K}_C h_C \sqrt{\frac{1+\mathcal{K}_C^2}{\overline{h}_C}}\right) && (4.3)\\
f_{\gamma_C}\left(\gamma_C\right) &= \frac{\left(1+\mathcal{K}_C^2\right) e^{-\mathcal{K}_C^2}}{\overline{\gamma}_C} \exp\left(-\frac{\left(1+\mathcal{K}_C^2\right) \gamma_C}{\overline{\gamma}_C}\right) \\
&\quad . J_0\left(2\mathcal{K}_C \sqrt{\frac{\left(1+\mathcal{K}_C^2\right) \gamma_C}{\overline{\gamma}_C}}\right) && (4.4)\\
f_{h_N}\left(h_N\right) &= \frac{2m_N^{m_N} h_N^{2m_N-1}}{\overline{h}_N^{m_N} \Gamma\left(m_N\right)} \exp\left(-\frac{m_N h_N^2}{\overline{h}_N}\right) && (4.5)\\
f_{\gamma_N}\left(\gamma_N\right) &= \frac{m_N^{m_N} \gamma_N^{m_N-1}}{\overline{\gamma}_N^{m_N} \Gamma\left(m_N\right)} \exp\left(-\frac{m_N \gamma_N}{\overline{\gamma}_N}\right) && (4.6)
\end{aligned}
$$

$\mathbb{E}\left[\cdot\right]$, $J_0\left(\cdot\right)$ and $\Gamma\left(\cdot\right)$ are the expectation operator, zero-order Bessel function and gamma function respectively. In the selection of channel models, attention is paid to select this set of models that are most commonly used in deriving analytical expressions. Establishment of a basis to evaluate performance of FBMC using analytical expressions is considered as one of the main aspect of this study.

4.2.1 Continuous Domain Formulation

The probabilistic properties of self-interferences are studied using continuous domain formulation with the aim of obtaining Gaussian Q-function based expressions for BERs in both asynchronous AWGN and asynchronous multipath fading channels.

Same way as (3.6) is derived, a single component of interference generated to any $a_{m',n'}$ by $a_{m'',n''}$ on path l can be presented as

$$
\begin{aligned}
v_{I''}\left(m', n', m'', n'', l, \epsilon\right) &= 2a_{m'',n''} e^{j\left(\psi_{m'',n''}-\psi_{m',n'}\right)} e^{-j2\pi F_s (m''+\epsilon)\tau_l} \\
&\quad . \int_0^{\infty} p\left(t-n'\tau_s\right) p\left(t-\tau_l-n''\tau_s\right) \\
&\quad . e^{j2\pi F_s (m''-m'+\epsilon) t}\, dt. && (4.7)
\end{aligned}
$$

The parameters are set to $(m'' \neq m, n'' \neq n, m = m')$ and $(n = n')$ to obtain self-interference in detecting $a_{m,n}$. This interference is to be canceled for effective signal recovery. Considering (4.7), and [96] it can be clearly observed that each $\{v_{I''}(m', n', m'', n'', l, \epsilon)\}$ shown by (4.7) is with a $\Re\{v_{I''}(m', n', m'', n'', l, \epsilon)\} \sim \mathcal{N}\left(0, \sigma^2_{I''}(m', n', m'', n'', l, \epsilon)\right)$. Similar to [96],

$$\begin{aligned}\sigma^2_{I''}(m', n', m'', n'', l, \epsilon) \;=\; & \left| \Re\left\{ 2e^{j\left(\psi_{m'',n''} - \psi_{m',n'}\right)} e^{-j2\pi F_s(m''+\epsilon)\tau_l} \right.\right. \\ & \cdot \int_0^\infty p(t - n'\tau_s)\, p(t - \tau_l - n''\tau_s) \\ & \left.\left. \cdot\, e^{j2\pi F_s(m''-m'+\epsilon)t}\, dt \right\} \right|^2, \end{aligned} \tag{4.8}$$

is used to show the variance $\sigma^2_{I''}(m', n', m'', n'', l, \epsilon)$ of it. It is important to note that individual variance components derived out of signals arrived through AWGN channel and single tap fading channel are the same. Therefore the total interference generated by other symbols at the receiver,

$$v_{I''}\left(m', n', l, \epsilon\right) = \sum_{\substack{m''=0 \\ m' \neq m''}}^{2M-1} \sum_{\substack{n''=0 \\ n' \neq n''}}^{\infty} v_{I''}(m', n', m'', n'', l, \epsilon), \tag{4.9}$$

is in a $\Re\{v_{I''}(m', n', l, \epsilon)\} \sim \mathcal{N}\left(0, \sigma^2_{I''}(m', n', l, \epsilon)\right)$. The individual interference components are uncorrelated. Therefore, the variances can also be summed up to get the variance of the total interference $\sigma^2_{I''}(m', n', l, \epsilon)$,

$$\sigma^2_{I''}(m', n', l, \epsilon) = \sum_{\substack{m''=0 \\ m' \neq m''}}^{2M-1} \sum_{\substack{n''=0 \\ n' \neq n''}}^{\infty} \sigma^2_{I''}(m', n', m'', n'', l, \epsilon). \tag{4.10}$$

Similarly, it can be shown that $\Im\{v_{I''}(m', n', m'', n'', l, \epsilon)\}$ and $\Im\{v_{I''}(m', n', l, \epsilon)\}$ are also in Gaussian distributions. By following the same procedure, the resultant interference from any $a_{m'',n''}$ to given $a_{m',n'}$ can be obtained for a communication in a delayed path l with a fading channel coefficient h_l as

$$\begin{aligned} y_{I''}(m', n', m'', n'', l, \epsilon) \;=\; & 2a_{m'',n''} e^{j\left(\psi_{m'',n''} - \psi_{m',n'}\right)} h_l e^{-j2\pi F_s(m''+\epsilon)\tau_l} \\ & \cdot \int_0^\infty p(t - n'\tau_s)\, p(t - \tau_l - n''\tau_s) \\ & \cdot\, e^{j2\pi F_s(m''-m'+\epsilon)t}\, dt. \end{aligned} \tag{4.11}$$

Then the total interference in a single path and the total interference in a multipath channel are shown by

$$y_{I''}\left(m',n',l,\epsilon\right) = \sum_{\substack{m''=0\\ m'\neq m''}}^{2M-1} \sum_{\substack{n''=0\\ n'\neq n''}}^{\infty} y_{I''}\left(m',n',m'',n'',l,\epsilon\right), \tag{4.12}$$

and

$$y_{I''}\left(m',n',\epsilon\right) = \sum_{l=0}^{L-1} y_{I''}\left(m',n',l,\epsilon\right), \tag{4.13}$$

accordingly. In that case, interference for a desired symbol $a_{m,n}$ can be obtained with $m'' \neq m, n'' \neq n, m = m'$ and $n = n'$.

4.3 BER Expressions

The probabilistic properties of self-interferences, particularly in an AWGN channel (or even without AWGN), are used to ensure compatibility with the Gaussian Q-function. This is followed by formulas of theoretical BERs for different fading channel models. Derivations are carried out for an asynchronous AWGN channel and extended to scenarios with asynchronous multipath fading channels. Discrete domain derivations are presented for simulations and other implementations. A detection scheme based on minimum distance is used in detecting signals in simulations.

4.3.1 BER for AWGN Channel

The probabilistic properties of self-interferences are studied using continuous domain formulation with the aim of obtaining Gaussian Q-function based expressions for BERs in both asynchronous AWGN and asynchronous multipath fading channels.

The calculation of BER over AWGN and fading channels is used as a performance measure [2, Sec. 8.1], [6, Sec. 5.2], [100]. This is defined under assumption of a single tap equalizer or a minimum Euclidean distance based receiver. The signal-to-interference-plus-noise ratio (SINR) related to $a_{m,n}$ of an FBMC system operated in an AWGN channel can be presented as

$$\mathrm{SINR}_{AWGN} = \frac{P_{a_{m,n_F}}}{\sigma^2_{I''}[m',n',l,\epsilon] + N_0}, \tag{4.14}$$

where $P_{a_{m,n_F}} = \sigma_{a_{m,n_F}}$ is the variance of the binary symmetric symbol sequence. The symbol time instance for the data symbol that has completed the full filter length is given by n_F. Noise power spectral density is given by N_0. Similar to [96], it is assumed that the performance and operating conditions of all the subcarriers are the same. Here the symbols which have completed full filter length in one of the subcarriers are considered. This can be done with proper selection of n ($n = n_F$). Considering a single tap equalizer (e.g., Zero Forcing (ZF) equalization [102]) or a minimum Euclidean distance based receiver, the total variance of the real side interference is denoted by $\sigma^2_{I''}[m', n', l, \epsilon]$ as in (3.9) (or $\sigma^2_{I''}(m', n', l, \epsilon)$ in continuous domain as in (4.10)). No multipaths are considered with $l = 0$. Since interference is in a Gaussian distribution and similar to [2, Eq. 8.4], [100] and using (4.14) BER can be expressed as

$$\mathrm{BER}_{AWGN} = Q\Big(\sqrt{2\mathrm{SINR}_{AWGN}}\Big), \tag{4.15}$$

where Gaussian Q-function is given by $Q(\cdot)$. Note that BER in form of an error function for a cellular network with approximations is available in [79]. The BER expression for OFDM is obtained when considering ICI as Gaussian in [96].

4.3.2 BER for Fading Channels

Following a similar approach as in [2, Eq. 9.9], [100], considering a system in a fading channel, a general expression for a BER can be derived in exact form. That is by statistically averaging the Gaussian Q-function over the joint PDF of the fading amplitudes. SINR expression is used for the Gaussian Q-function. In this kind of approach, power of a fading channel coefficient $|h_l|^2$, $|h_l|^2 = \gamma_l$. h_l can be h_{Rl}, h_{Cl} and h_{Nl}, which are the relevant independent fading amplitudes for the path l according to Rayleigh, Rician or Nakagami-m channel models accordingly. $|h_{Rl}|^2 = \gamma_{Rl}$, $|h_{Cl}|^2 = \gamma_{Cl}$ and $|h_{Nl}|^2 = \gamma_{Nl}$. All γ_{Rl}, γ_{Cl} and γ_{Nl} are squared variables or SNR values per symbol. PDF for the path l $f_{\gamma_l}(\gamma_l)$ is modeled with PDFs (4.2), (4.4) or (4.6) respectively. They are expressed with PDFs $f_{\gamma_{Rl}}(\gamma_{Rl})$, $f_{\gamma_{Cl}}(\gamma_{Cl})$ or $f_{\gamma_{Nl}}(\gamma_{Nl})$ accordingly. Delays are measured relative to the first path, for which no delay is given. In the case of FBMC, real side values for both signal and interference power are to be considered. But this approach is not used to get results analytically in this study due to difficulties in simplifications.

4.3.3 An Alternative form of Modeling BER for Rayleigh Channel

An alternative approach is presented to derive a closed-form expression for approximate BER. Modeling is done while considering the probabilistic properties of receive signal and interference. By further simplification of (2.24) with $(m = m')$ and $(n = n')$, it can be shown that a signal containing a desired symbol can be expressed as

$$\begin{aligned} y_a[m', n', \epsilon] &= 2a_{m,n} \sum_{l=0}^{L-1} h_l e^{-j\frac{2\pi(m+\epsilon)}{2M}l} \sum_{k=0}^{\infty} p[k - nM] \\ &\quad . \, p[k - l - nM] e^{j\frac{2\pi}{2M}(\epsilon)\left(k - \frac{L_F - 1}{2}\right)}. \end{aligned} \tag{4.16}$$

BPSK is used as the modulation scheme. Therefore, for all the transmit symbols, $\mathbb{E}\left[a_{m,n}^2\right] = \mathbb{E}\left[a_{m',n'}^2\right] = \mathbb{E}\left[a_{m'',n''}^2\right] = E_b = 1$, where energy per bit is represented by E_b. It is assumed that delays between consecutive paths are small compared to the symbol interval and multipath delays are small compared to the symbol interval in such a way that for any n or n', $p[k-nM] \approx p[k-l-nM]$ or $p[k-n'M] \approx p[k-l-n'M]$. For this scenario, a single tap subcarrier equalizer is considered. The the receive signal power of a desired symbol in a multipath channel can thus be obtained by using (4.16) with $m = m'$, $n = n'$ and [103, Eq. (5)], as in

$$P_{a_{m,n},h,\epsilon} = \left|\sum_{l=0}^{L-1} h_l e^{-j\frac{2\pi(m+\epsilon)}{2M}l}\right|^2 \left|2\sum_{k=0}^{\infty} p^2[k-nM] e^{j\frac{2\pi}{2M}(\epsilon)\left(k-\frac{L_F-1}{2}\right)}\right|^2. \quad (4.17)$$

In the case of Rayleigh channel, terms in (4.17) can be replaced with a gamma variable $\alpha_{m,\epsilon}$ and weighting factor $w_{n,\epsilon}$ as

$$\alpha_{m,\epsilon} = \left|\sum_{l=0}^{L-1} h_l e^{-j\frac{2\pi(m+\epsilon)}{2M}l}\right|^2, \quad (4.18)$$

and

$$w_{n,\epsilon} = \left|2\sum_{k=0}^{\infty} p^2[k-nM] e^{j\frac{2\pi}{2M}(\epsilon)\left(k-\frac{L_F-1}{2}\right)}\right|^2. \quad (4.19)$$

accordingly. Under the same conditions and since the individual interference components are mutually independent of each other, the total variance of the interference caused by any $a_{m',n'}$ to $a_{m,n}$ can be derived using (3.9), as

$$\sigma_{I'}^2[m,n,\epsilon] = \sum_{\substack{m'=0 \\ m'\neq m}}^{2M-1} \sum_{\substack{n'=0 \\ n'\neq n}}^{\infty} \sum_{l=0}^{L-1} \sigma_{I'}^2[m,n,m',n',l,\epsilon]. \quad (4.20)$$

Considering a single tap equalizer (e.g., ZF equalization [102]) or a minimum Euclidean distance based receiver, the total variance of the real part of interference is obtained in (4.20). The SINR can be defined as

$$\begin{aligned} \mathrm{SINR}_{mh\epsilon} &= \frac{P_{a_{m,n},h,\epsilon}}{\sigma_{I'}^2[m,n,\epsilon] + N_0} \\ &= \frac{\alpha_{m,\epsilon} w_{n,\epsilon}}{\sigma_{I'}^2[m,n,\epsilon] + N_0}. \end{aligned} \quad (4.21)$$

The squared envelope distribution of the transformed Rayleigh channel [103, Eq. (13)] can be considered as an equivalent multipath channel for this scenario as given in

$$f_{\gamma_{\Omega_{RL}}}(\alpha_{m,\epsilon}) = \frac{1}{4\Omega_{RL}} \exp\left(-\frac{\alpha_{m,\epsilon}}{4\Omega_{RL}}\right), \tag{4.22}$$

where the conversion is as [104, Eq. (5-4)]. $\Omega_{RL} = \sum_{l=0}^{L-1} \mathbb{E}\left[|h_{Rl}|^2\right] = \sum_{l=0}^{L-1} \mathbb{E}\left[\gamma_{Rl}\right]$. γ_{Rl} is a gamma variable. The numerator of (4.21) can be identified as a weighted gamma variable given by $\alpha_{w,m,\epsilon} = \alpha_{m,\epsilon} w_{n,\epsilon}$. According to [104, Eq. (5-18)], the PDF for it can be given as

$$f_{\alpha_{w,m,\epsilon}}(\alpha_{w,m,\epsilon}) = \frac{1}{4\Omega_{RL} w_{n,\epsilon}} \exp\left(-\frac{\alpha_{w,m,\epsilon}}{4\Omega_{RL} w_{n,\epsilon}}\right). \tag{4.23}$$

The average BER $P_{h_R}(E)$ is derived in the same way as in [103, Eq. (19)]. Then $P_{h_R}(E)$ is given by

$$P_{h_R}(E) = \int_0^\infty Q\left(\sqrt{2\mathrm{SINR}_{mh\epsilon}}\right) f_{\alpha_{w,m,\epsilon}}(\alpha_{w,m,\epsilon})\, d\alpha_{w,m,\epsilon}. \tag{4.24}$$

Using the Craig's formula [105] $P_{h_R}(E)$ can be further simplified to:

$$P_{h_R}(E) = \frac{1}{2}\left(1 - \sqrt{\frac{\frac{4\Omega_{RL} w_{n_F,\epsilon}}{\sigma_{I'}^2[m, n_F, \epsilon] + N_0}}{1 + \frac{4\Omega_{RL} w_{n_F,\epsilon}}{\sigma_{I'}^2[m, n_F, \epsilon] + N_0}}}\right). \tag{4.25}$$

Here also the symbols with full filter length in one of the subcarriers are considered with $n = n_F$.

4.3.4 Asymptotic BER for Nakagami-*m* Channel

Evaluation of theoretical BER for Nakagami-***m*** fading channels giving asymptotic error-rates is studied focusing to asynchronous conditions and multipath fading. As in [96], equal performance and operating conditions for all the subcarriers are assumed. Symbols of one of the subcarriers are expected to complete the full filter length in order to be considered for a calculation where it can be done with appropriate selection of n ($n = n_F$). As in [103, Eq. (19)], the average BER $P_{h_N}(E)$ is given as

$$P_{h_N}(E) = \int_0^\infty Q\left(\sqrt{2\mathrm{SINR}_{mh\epsilon}}\right) f_{\gamma_{\Omega_{NL}}}(\alpha_{m,\epsilon})\, d\alpha_{m,\epsilon}. \tag{4.26}$$

This can be expressed in a much compatible form as

$$P_{h_N}(E) = \int_0^\infty Q\left(A_{\mathrm{SINR}_{mh\epsilon}} \sqrt{\alpha_{m,\epsilon}}\right) f_{\gamma_{\Omega_{NL}}}(\alpha_{m,\epsilon})\, d\alpha_{m,\epsilon}. \tag{4.27}$$

For simplicity, let $A_{\mathrm{SINR}_{mh\epsilon}}$ be

$$A_{\mathrm{SINR}_{mh\epsilon}} = \sqrt{\frac{2w_{n_F,\epsilon}}{\sigma^2_{I'}[m,n_F,\epsilon] + N_0}}. \tag{4.28}$$

In the case of a single tap channel, it is shown that squared envelope distribution of Nakagami-$\boldsymbol{m}$ channel can be written as a Taylor series expansion [103, Eq. (24)] as

$$f_{\gamma_{\Omega_{NL}}}(\alpha_{m,\epsilon}) = \sum_{r=0}^{\infty} P_{Ar} \frac{\alpha^r_{m,\epsilon}}{r!}, \tag{4.29}$$

where r is the index used for the expansion and the derivative. In that series expansion $P_{Ar} = \left(\partial^r / \partial \alpha^r_{m,\epsilon}\right) f_{\gamma_{\Omega_{NL}}}(\alpha_{m,\epsilon})\Big|_{\alpha_{m,\epsilon}=0}$ and then,

$$\frac{1}{A_{\mathrm{SINR}_{mh\epsilon}}} f_{\gamma_{\Omega_{NL}}}\left(\frac{\alpha_{m,\epsilon}}{A_{\mathrm{SINR}_{mh\epsilon}}}\right) = \sum_{r=0}^{\infty} P_{Ar} \frac{\alpha^r_{m,\epsilon}}{r! A^{r+1}_{\mathrm{SINR}_{mh\epsilon}}}. \tag{4.30}$$

$\Omega_{NL} = \sum_{l=0}^{L-1} \mathbb{E}\left[|h_{Nl}|^2\right] = \sum_{l=0}^{L-1} \mathbb{E}\left[\gamma_{Nl}\right]$. γ_{Nl} is a gamma variable. With [103, Eq. (26)] and using two terms for a higher accuracy,

$$P_{h_N}(E)_{As} \approx P_{A1} \frac{\int_0^\infty Q(\alpha_{m,\epsilon}) \alpha_{m,\epsilon}\, d\alpha_{m,\epsilon}}{1! A^2_{\mathrm{SINR}_{mh\epsilon}}} + P_{A3} \frac{\int_0^\infty Q(\alpha_{m,\epsilon}) \alpha^3_{m,\epsilon}\, d\alpha_{m,\epsilon}}{3! A^4_{\mathrm{SINR}_{mh\epsilon}}}, \tag{4.31}$$

where $\cdot_{As}$ is used to represent a value given by an asymptotic expression. In the case of the two tap channel and when both taps are with the same m_N, approximate asymptotic error-rate can be expressed as [103, Eqs. (35)-(36)],

$$P_{h_N}(E)_{As} \approx \frac{m_N \Gamma(2m_N - 1)}{2^{2m_N - 2} \Gamma(m_N)^2} \frac{\int_0^\infty Q(\alpha_{m,\epsilon}) \alpha_{m,\epsilon}\, d\alpha_{m,\epsilon}}{A^2_{\mathrm{SINR}_{mh\epsilon}}}. \tag{4.32}$$

4.3.5 Signal Detection

Interference mitigation with channel equalization is a key area that is heavily investigated in connection to FBMC. An equalization scheme with interference cancellation is proposed in [102] to eliminate self-interference in a SISO OFDM / OQAM systems where ZF equalization is used as the primary equalization scheme. Finite impulse response per-subchannel frequency-domain equalizers are derived for the single-input multiple-output (SIMO) and the MIMO FBMC / OQAM systems in [90]. The spectral shaping capabilities of a low-complexity subchannel equalizer for filter banks are used to reduce the effects of narrow-band interferences present in adjacent subchannels of an FBMC system in [94]. A joint design of MIMO precoding and decoding matrices for FBMC systems is discussed in [106] to increase robustness against the channel frequency selectivity and support multi-stream transmission. In that case, a technique is discussed to iteratively compute precoders and equalizers by resorting to an alternating optimization method. A frequency domain receiver design for OQAM schemes is considered in [107]. It is shown that frequency-domain equalization (FDE) designed for non-offset modulations are not suitable for offset modulations due to the interference between in-phase and quadrature components. Several iterative FDE based receivers are presented for cancellation of interference between in-phase and quadrature components. A simple single tap equalization method is discussed for an FBMC implementation based on the staggered modulated multitone concept in [108], where the main objective is a complexity comparison between FBMC and OFDM.

Discrete time formulation is used for the derivations related to this section. By following the same procedure, the receive signal after filtering in a fading channel with a coefficient h_l on path l is shown as

$$\begin{aligned} y\left[m',n',l,\epsilon\right] &= 2\sum_{m=0}^{2M-1}\sum_{n=0}^{\infty} a_{m,n}e^{j\left(\psi_{m,n}-\psi_{m',n'}\right)}h_l e^{-j\frac{2\pi(m+\epsilon)}{2M}l}\sum_{k=0}^{\infty} p\left[k-n'M\right] \\ &\quad .\, p[k-l-nM]e^{j\frac{2\pi}{2M}(m-m'+\epsilon)\left(k-\frac{L_F-1}{2}\right)}+\eta\,[k], \end{aligned} \tag{4.33}$$

where $l=0$ is for a time domain synchronous scenario. h_l is to be modeled with PDFs of Rayleigh (4.1), Rician (4.3) or Nakagami-m (4.5). A complete receive signal through all paths $y[m',n',\epsilon]$ is equivalent to (2.24),

$$y\left[m',n',\epsilon\right] = \sum_{l=0}^{L-1} y\left[m',n',l,\epsilon\right]. \tag{4.34}$$

Signal detection is done under interference conditions, where a single component of interference generated to any $a_{m',n'}$ by $a_{m'',n''}$ is presented as

$$\begin{aligned} y_{I''}\left[m',n',m'',n'',l,\epsilon\right] &= 2a_{m'',n''}e^{j\left(\psi_{m'',n''}-\psi_{m',n'}\right)}h_l e^{-j\frac{2\pi\left(m''+\epsilon\right)}{2M}l}\sum_{k=0}^{\infty} p\left[k-n'M\right] \\ &\quad .\, p\left[k-l-n''M\right]e^{j\frac{2\pi}{2M}(m''-m'+\epsilon)\left(k-\frac{L_F-1}{2}\right)}. \end{aligned} \tag{4.35}$$

Delays for the consecutive paths are measured relative to the first path, and the total interference in a multipath channel is given by

$$y_{I''}\left[m',n',\epsilon\right] = \sum_{l=0}^{L-1}\sum_{\substack{m''=0\\ m'\neq m''}}^{2M-1}\sum_{\substack{n''=0\\ n'\neq n''}}^{\infty} y_{I''}\left[m',n',m'',n'',l,\epsilon\right]. \tag{4.36}$$

Parameters are set to $(m''\neq m, n''\neq n, m=m')$ and $(n=n')$ to get interference in detecting $a_{m,n}$.

A detection scheme based on the minimum distance is introduced for better symbol recovery. By observing (4.16), the receive signal containing a desired symbol can be estimated as

$$\begin{aligned} \hat{y}_{\hat{a}}\left[m',n',\hat{\epsilon}\right] &= 2\hat{a}'_{m,n}\sum_{l=0}^{L-1}\hat{h}_l e^{-j\frac{2\pi(m+\hat{\epsilon})}{2M}l}\sum_{k=0}^{\infty}p[k-nM]p[k-l-nM] \\ &\quad .\, e^{j\frac{2\pi}{2M}(\hat{\epsilon})\left(k-\frac{L_F-1}{2}\right)}. \end{aligned} \tag{4.37}$$

Possible values for $\hat{a}'_{m,n}$ are to be assigned from the symbol alphabet. $\hat{h}_l$ is the channel coefficient (estimated ideally) corresponding to the delayed path with delay l. $\hat{\epsilon}$ is the estimated CFO. The symbol is decided based on the minimum value given by the metric $\delta_{\hat{a}_{m,n}}$. Delays are determined relative to the first path with the delay for the first path as $l = 0$. For the detection, $\hat{\epsilon} = 0$ can be used for sufficiently small CFOs. Using (2.24) and (4.16) with parameters $(m = m')$ and $(n = n')$:

$$\delta_{\hat{a}_{m,n}} = \left|y\left[m',n',\epsilon\right] - \hat{y}_{\hat{a}}\left[m',n',\hat{\epsilon}\right]\right|^2. \tag{4.38}$$

This detection scheme is compared against ZF equalization [102]. Let the coefficient $\hat{H}_{\hat{a}}[m',n',\hat{\epsilon}]$ be defined as,

$$\begin{aligned} \hat{H}_{\hat{a}}\left[m',n',\hat{\epsilon}\right] &= 2\sum_{l=0}^{L-1}\hat{h}_l e^{-j\frac{2\pi(m+\hat{\epsilon})}{2M}l}\sum_{k=0}^{\infty}p[k-nM]p[k-l-nM] \\ &\quad .\, e^{j\frac{2\pi}{2M}(\hat{\epsilon})\left(k-\frac{L_F-1}{2}\right)}. \end{aligned} \tag{4.39}$$

Then the estimated data symbol is given as,

$$\hat{a}_{m,n} = \Re\left\{\frac{y\left[m',n',\epsilon\right]}{\hat{H}_{\hat{a}}[m',n',\hat{\epsilon}]}\right\}. \tag{4.40}$$

It could be noted that, with the assumption of zero CFO estimate, performance of this detection principle is equivalent to the commonly used subcarrier-wise single-tap equalizer.

4.3.6 Interference Mitigation

The performance can be enhanced through application of a proper channel coding scheme. A convolutional code [6, Sec. 8.2.5, p. 492] is selected for this study and a Viterbi decoder [6, Sec. 8.2.2] is used for decoding at the receiver.

4.4 Numerical and Simulation Results

A causal multirate FBMC system containing 64 subcarriers is considered to obtain relevant numerical results and for corroborative system simulations. The setup is operated under various synchronization and fading conditions. An OFDM system having the same number of subcarriers operated under same conditions is used for the purpose of comparisons.

4.4.1 AWGN Channel

Results from the simulations and the closed-form expression for the AWGN channel are shown in Figure 8 as a comparison. Minimum distance based receiver with symbol alphabet $\hat{a}'_{m,n} \in \{-1, 1\}$ is used for the signal detection. The synchronous mode of operation is considered. For the theoretical plot, 3.0171×10^{-07} is taken as the variance of total self-interference which can be calculated when considering a single direct path with (3.9).

4.4.2 Fading Channels

In estimating $\hat{y}_{\hat{a}}[m', n', \hat{\epsilon}]$, $\hat{a}'_{m,n} \in \{-1, 1\}$ is used as the symbol alphabet with $\hat{\epsilon} = 0$. For all three scenarios, the results are compared with OFDM systems [96]. Both synchronous and asynchronous cases are considered. Only one propagation path with no CFO is taken as the synchronous scenario. Four path channels are used for the asynchronous scenarios. All path delays are assumed to be in equal steps and CFO is set to 0.04. Perfect channel state information is used at the receiver.

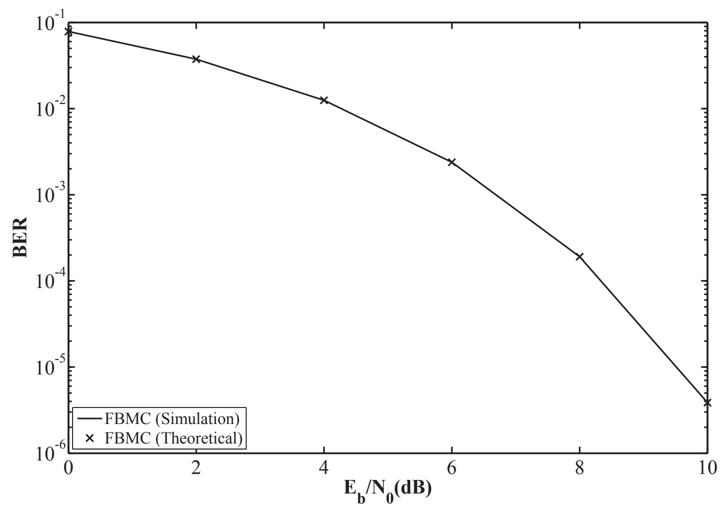

FIGURE 8 Performance of an FBMC system in a AWGN channel

The detection scheme based on minimum distance is compared against simple ZF equalization scheme under Rayleigh fading conditions as in Figure 9. FBMC system is operated under synchronous, asynchronous and multipath fading conditions. It could be noted that, performance of both schemes are the same. In that case, closed-form expressions for the performance measures should also be the same for the both schemes. In otheer words, according to this proof, ZF can be identified as an compatible equalization scheme for the minmum distance based receiver provided that no extesions are used for cancellation of self-interference in both mechanisms.

The performance of an FBMC system over Rayleigh, Rician and Nakagami-m quasi-static fading channels is presented in Figure 10, Figure 11 (a), (b) and Figure 12, respectively. In all these figures, the performance is similar to the OFDM technique in the synchronous mode of operation. But it can be seen that the FBMC technique is highly sensitive to both time and frequency offsets. A considerable drop in performance can be observed with time and / or frequency offsets. In the case of asynchronous OFDM, the performance is severely affected with the increase of number of subcarriers. However, in an FBMC system supported by a PHYDYAS type of filter, it is limited to a certain extent.

When considering performance over Rician and Nakagami-m channels values for the parameters $\mathcal{K}_{RK} = 0, 10$ and $m_N = 2, 3$ are used. In all these cases specific shapes of those BER curves can clearly be observed under the synchronous mode of operation. However, deteriorations are observed in asynchronous mode of operation with CFOs and multipaths. Importantly, the performance of FBMC is better than that of OFDM in all three channels under asynchronous conditions in lower SNR values.

For the Rayleigh channel, theoretical and simulation plots are compared in Figure 13. The variances calculated using (4.20) for the four scenarios (tap 1, $\epsilon =$

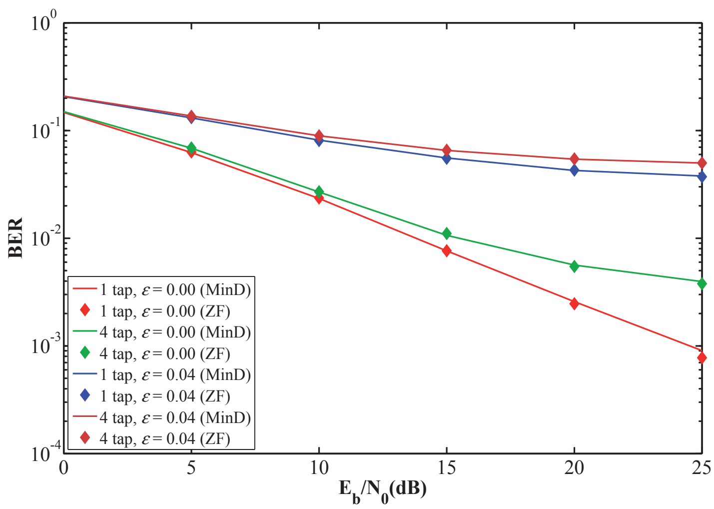

FIGURE 9 Performance of detectors : Rayleigh channel

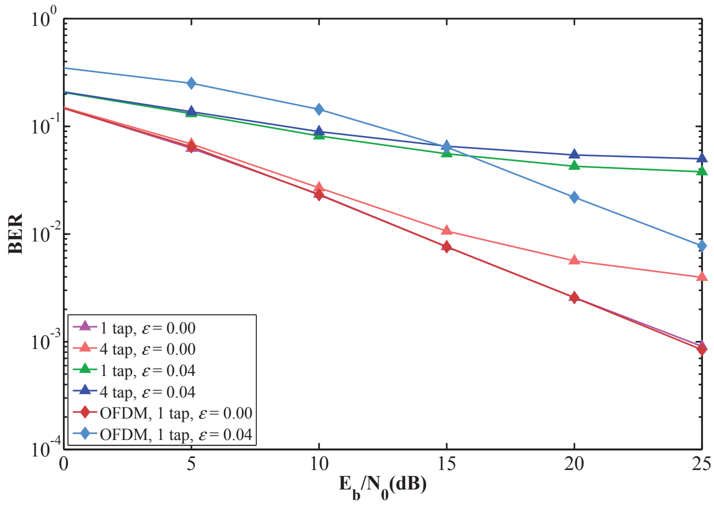

FIGURE 10 Performance in fading channel model : Rayleigh

0.0), (tap 1, $\epsilon = 0.04$), (tap 4, $\epsilon = 0.0$) and (tap 4, $\epsilon = 0.04$) are 3.01713×10^{-7}, 2.35731×10^{-1}, 1.40229×10^{-1} and 5.43365×10^{-1}, respectively. Both results are the same in the case of the one tap synchronous operation. The curves are in parallel and closer to each other in other scenarios.

When considering free distance properties [6, Sec. 8.2.5, p. 492], a half-rate convolutional code with the maximum free distance and constraint length of 9 with generator polynomials [561, 753] (octal) [6, Table 8.2.1, p. 493] is selected for the purpose of simulations. As shown in Figure 14, some improvement can be achieved in all the scenarios. In them, significant performance enhancements could be achieved for the cases with frequency offsets. Subsequently, another maximum free distance, rate half, constraint length 6 convolutional code (code 2) with generator polynomials [53, 75] (octal) [6, Table 8.2.1, p. 493] is used for a comparison against the previous code (code 1). Lower performance for the code with smaller constraint length is depicted in Figure 15.

Performance of an FBMC system over single tap, quasi-static Nakagami-$\boldsymbol{m}$ fading channel with $m_N = 1$ and 2 is presented in Figure 16 - (**a**). A significant drop in performance can be seen with time and / or frequency offsets. $P_{A1} = 2$ and $P_{A3} = 12$ used for $m_N = 1$ [103, Table 1]. Similarly $P_{A1} = 0$ and $P_{A3} = 48$ used for $m_N = 2$ [103, Table 1] (These values can be computed the procedure given in [103]). The variances calculated using (4.20) for $A_{\mathrm{SINR}_{mh\epsilon}}$ in four scenarios ($m_N = 1$, $\epsilon = 0.0$), ($m_N = 1$, $\epsilon = 0.04$), ($m_N = 2$, $\epsilon = 0.0$) and ($m_N = 2$, $\epsilon = 0.04$) are 3.01713×10^{-7}, 2.35731×10^{-1}, 3.01713×10^{-7} and 2.35731×10^{-1} respectively. In most of the cases, both curves of theoretical and simulation results are closer or coincide with each other. The performance of an FBMC system over Nakagami-$\boldsymbol{m}$ two-tap quasi-static fading channel with $m_N = 1$ and 2 is shown in Figure 16 - (**b**). The variances for $A_{\mathrm{SINR}_{mh\epsilon}}$ in four scenarios ($m_N = 1$, $\epsilon = 0.0$), ($m_N = 1$, $\epsilon = 0.04$), ($m_N = 2$, $\epsilon = 0.0$) and ($m_N = 2$, $\epsilon = 0.04$) are 1.72710×10^{-2}, 3.34903×10^{-1}, 1.72710×10^{-2} and 3.34903×10^{-1}, accordingly. Here the curves

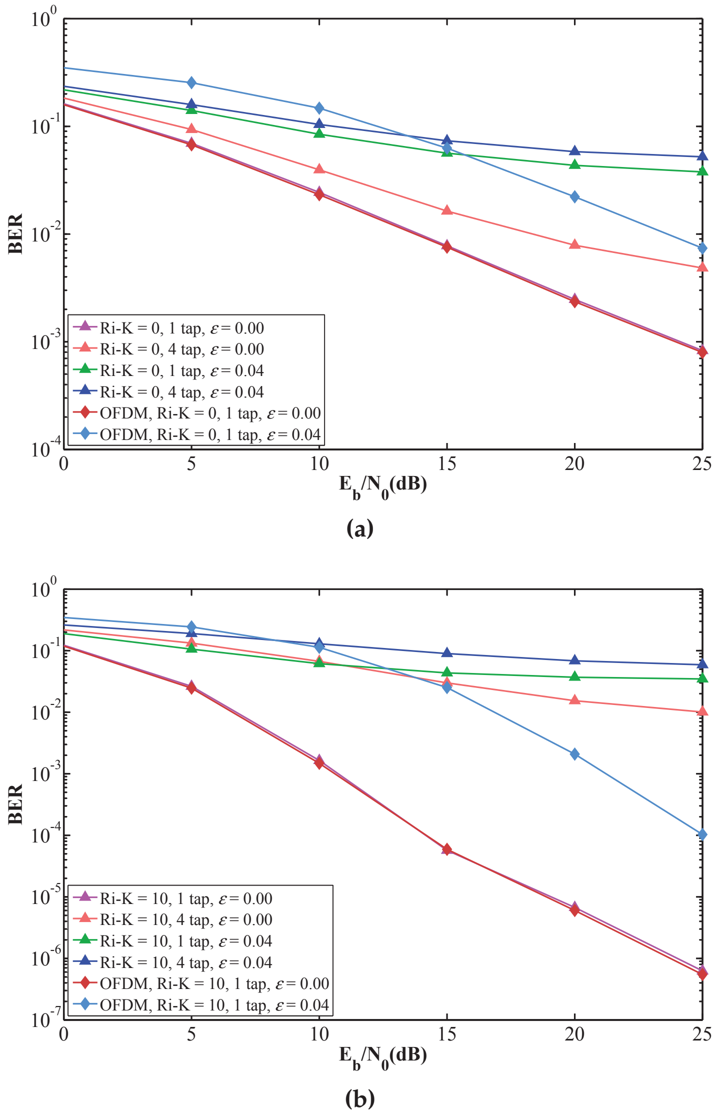

FIGURE 11 Performance in fading channel models : **(a)** Rician $\mathcal{K}_{RK} = 0$ and **(b)** Rician $\mathcal{K}_{RK} = 10$

of the theoretical and simulation results are closer and parallel to each other in respective cases. Note that the asymptotic error-rate curves for both m_N are on top of each other for particular synchronization cases.

A constraint length 9 convolutional code designed to have maximum free distance and rate half with generator polynomials [561, 753] (octal) [6, Table 8.2.1, p. 493] is employed to evaluate a set of scenarios with frequency offset of 0.04. As shown in Figure 17, a significant improvement in performance can be accomplished in all the circumstances. Then another maximum free distance, rate half,

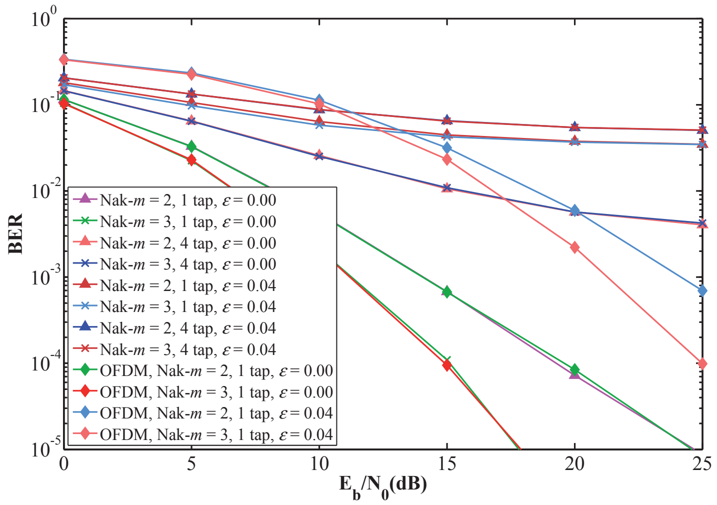

FIGURE 12 Performance in fading channel model : Nakagami-m

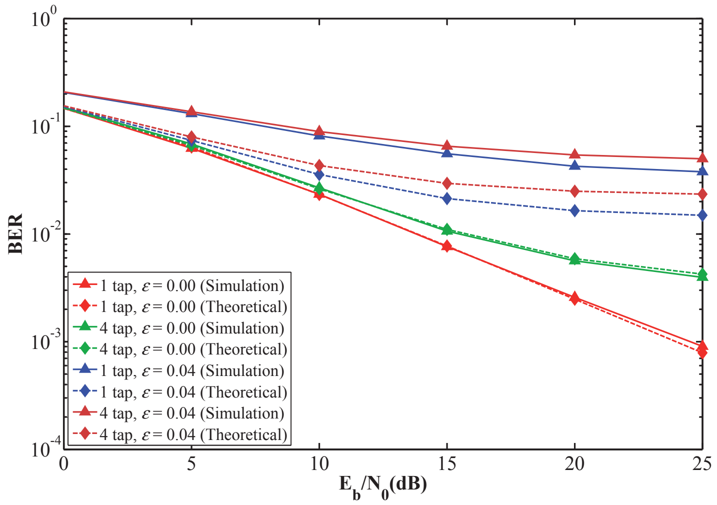

FIGURE 13 Performance of an FBMC system vs theoretical formulation

constraint length 6 convolutional code (code 2) having lower decoder complexity with generator polynomials [53, 75] (octal) [6, Table 8.2.1, p. 493] is used for a comparison against previous code (code 1). The results are shown in Figure 18. Sensitivity to the constraint length and generator polynomials could be observed where lesser performance for the code with smaller constraint length could be seen.

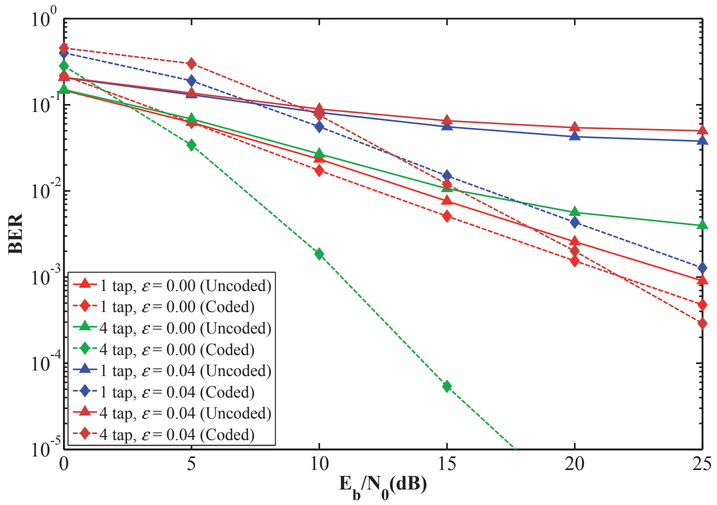

FIGURE 14 Performance of a coded FBMC system - Rayleigh Channel

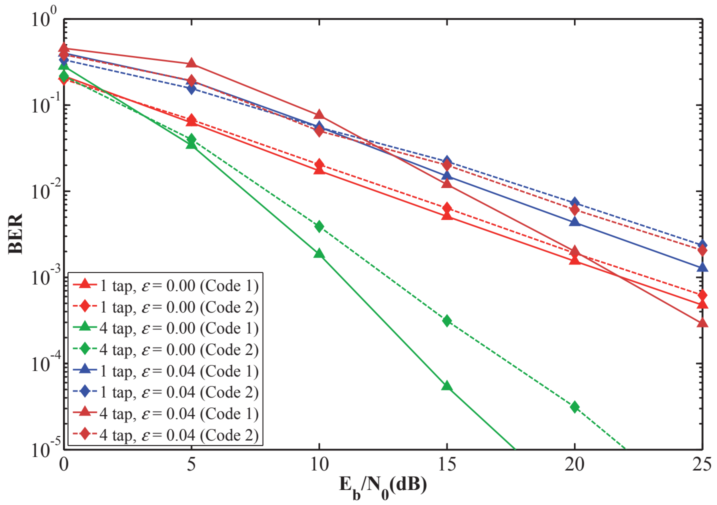

FIGURE 15 Performance of two coded FBMC systems - Rayleigh Channel

4.5 Summary and Discussion

BER performance of a causal asynchronous multirate FBMC system under different channel and synchronization conditions were discussed. Expressions for BERs in general were presented followed by a closed-form BER expression for the Rayleigh channel and asymptotic BER for the Nakagami-m fading channel. A symbol recovery mechanism based on minimum distance was used at the receiver. It was proved that performance of minimum distance based detector with-

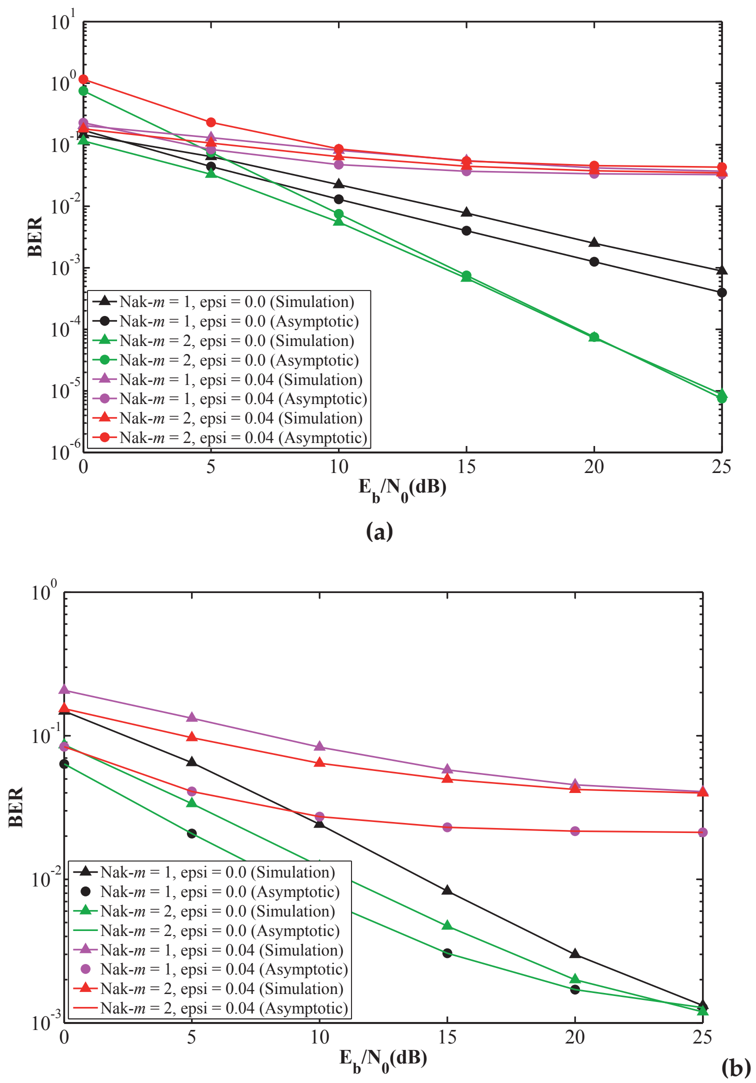

FIGURE 16 Performance of an FBMC system : **(a)** one tap channel and **(b)** two tap Nakagami channel

out self-interference cancellation is same as that of ZF equalizer. Quasi-static multipath fading channels in both synchronous and asynchronous conditions were used for simulations. It was shown that with the use of suitable channel codes, a significant improvement in the performance can be achieved. As in [97], this analysis can be used to get a thorough understanding about the behavior of this particular communication technique and associated self-interference, which can be helpful for the developments related to it.

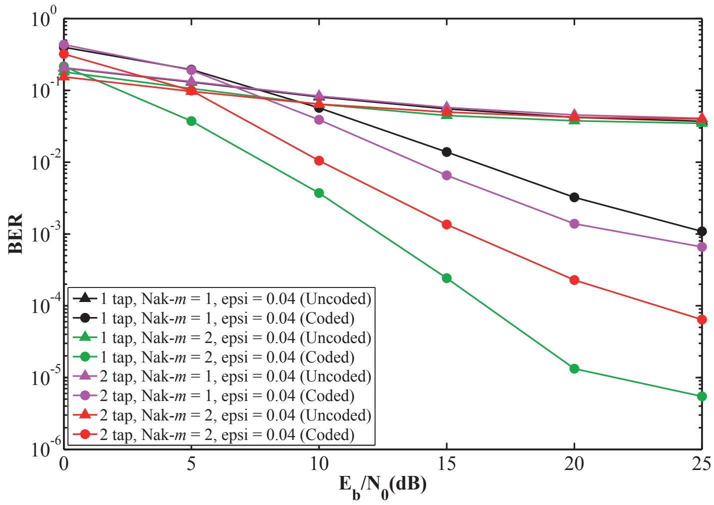

FIGURE 17 Performance of a coded FBMC system - Nakagami Channel

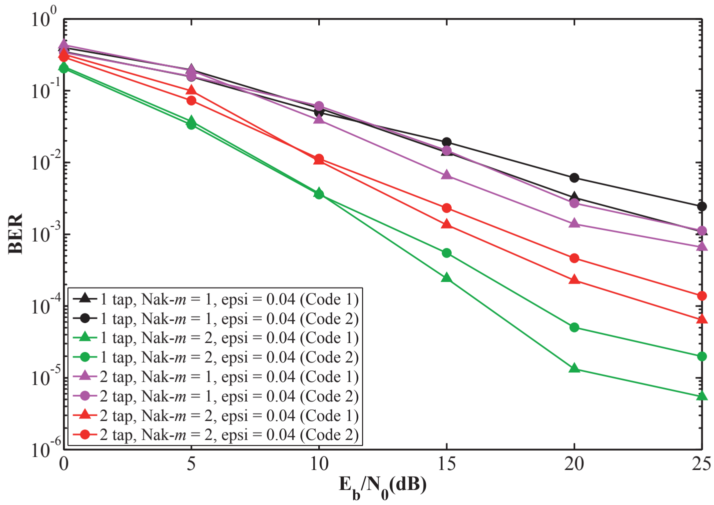

FIGURE 18 Performance comparison of two coded FBMC systems - Nakagami Channel

5 BASIC RELAYS WITH FBMC

Cooperative wireless network communication schemes, also known as wireless relay networks, are primarily proposed to maintain a successful link from source to destination when direct transmission is not possible and to improve the reliability of end-to-end transmission. Even though there are some wider application areas where the relay concepts are used, this study is narrowed down to the relays which are used for mobile wireless communications. In most of the cases, the origins of applications related to other areas go much further back than the origins of mobile wireless communications.

5.1 Introduction

In data communication, relay networks can be built up with fixed or mobile terminals under different channel and fading conditions including widely used Rayleigh, Nakagami-m and Rician [109] - [112] channels. These terminals can be user nodes and / or relay stations. A source to destination link can be created with two or more hops, with or without a direct source to the destination link. One receiver may be able to receive from one relay node or from many relay nodes. Different types of supportive techniques and algorithms, which include combining techniques, access techniques (e.g., time division multiple access), resource allocation algorithms, scheduling schemes and interference management techniques are widely used to handle complicated scenarios. Principles of DF, amplify-and-forward (AF), code-and-forward or adaptive schemes [113] are used as the bases for these schemes. Code-and-forward is a category of relays that can be considered as an extension of DF relays or a separate category of relays. Different types of relay network techniques including hybrid categories and techniques with advanced processing algorithms [114] are widely studied, due to their attractive features and performance, in connection with broadband and other multicarrier communication techniques. Advantages of cooperative diversity also can be gained by certain configurations enriched with multiple relays that receive the same source signal. In those occasions, the receive signal is forwarded to destination by all the relays through parallel transmissions. Orthogonal (non-interfering) channels are used for the all the transmissions. Finally, source and relayed signals are combined at the destination achieving a better signal reception. Most of the relay network scenarios are compatible with almost all the transmission techniques and associated concepts. Thus, a greater potential for further developments and enhancements is shown by them.

A relay network can be supported by nodes with different types of transmitters, for example with the CDMA or direct sequence-code division multiple access (DS-CDMA) transmitter. A multihop medium access control (mMAC) scheme for time division duplexing-code division multiple access (TDD-CDMA) cellular networks with two-hop relay architecture for packet data transmissions is suggested in [115]. The scheme is included with code selection, power control and multihop relaying. It is shown that, in terms of performance and coverage, two-hop networks are substantially better than single-hop TDD-CDMA cellular networks. Alternatively, there can be OFDM transmitters. A multi-subcarrier DF relay strategy to accomplish a larger rate region using the cross-subcarrier channel coding is given in [116]. An optimal resource allocation algorithm to characterize the achievable rate region of the proposed strategy is also presented. Even the transmitters may be MC-CDMA. An analysis on the spectral efficiency of MC-CDMA two-hop relay systems is done in [117], either with global CSI only at the relay or with local CSI only at every node. That is followed by an asymptotic performance analysis with random-matrix theory deriving the average spectral efficiency of DF and AF two-hop relay systems. Impacts of spreading sequences, fading channel statistics and low-complexity transceivers are also analyzed.

A relay can be a mobile or stationary device capable of capturing signals transmitted from a source and retransmitting to a device at the destination. The source and the destination equipments can be stationary or mobile devices. But mobility-related issues are not addressed in this formulation. However, the basic formulation presented earlier can be used for those types of scenarios as well.

Most of the times, relays are categorized based on the associated processing functionality. They can be AF [113], [118], DF or compress-and-forward (CF) [119]. There are other categorizations as well, with schemes like detect-and-forward and code-and-forward [120]. Sometimes the latter two categories can be considered as alternative names, subcategories or derivations of the original basic categorization. In that case, if any processing functionality is done other than the operation of AF, it may be categorized as DF or CF. The coded performance of a cooperative system with multiple parallel relays is analyzed in [121] using detect-and-forward principle, where the overheard signal is modulated at each relay and the detected binary words are forwarded. The proposed method is based on a probabilistic characterization of the reliability metrics. Thus the mechanism is more likely to be considered as a DF scheme. According to certain categorizations, there are only two categories: regenerative relays (also known as digital relays), containing both DF and CF relays, and non-regenerative relays, containing AF relays (also known as analog relays) [122].

5.1.1 AF Relays

When a processing functionality is considered, this is the simplest form of cooperative wireless network diversity scheme. In it, a relay is only capable of acquiring signals from source and retransmitting it to the destination or destinations. There are some advantages and disadvantages associated with it. Low implementation complexity or simplicity, low power consumption and comparatively shorter delay for end-to-end transmission can be considered as the main advantages [123]. Noise amplification and error propagation are the main disadvantages associated with it [124]. In addition, if there is any background interference it is also amplified and transferred in the same way as noise. An AF cooperative strategy for interference-limited networks is considered and the effect of multiuser interference in AF schemes is analyzed in [125]. They are recommended as more suitable schemes for operation under low noise and interference environments. There are two prominent subcategories of AF relays: fixed gain relays and variable gain relays.

Fixed Gain Relays

This is also referred to as blind or semi-blind relay. No instantaneous CSI of incoming signals is used [122], [126] in order to determine the amplifier gain for the transmission. Long-term statistics are used for that. Lesser processing requirements lead to a lesser system complexity while the performance remains comparatively poor.

Variable Gain Relays

Alternatively this is introduces as CSI assisted relay where instantaneous CSI of incoming signals is used to determine the amplifier gain for the transmission [122], [127]. The gain is updated or changed periodically. This category is capable of outperform fixed gain relays in the expense of processing power and system complexity.

5.1.2 DF Relays

The receive signal is demodulated and decoded at the receiver. Then the signal is, most of the times, encoded, modulated and transmitted to the destination [128]. The main disadvantage of AF relays, noise, including interference amplification and retransmission, is eliminated. Even an intermediate interference reduction scheme can be easily employed. Considerable performance enhancements can be achieved using supportive schemes like proper relay selection algorithms, resource management mechanisms and scheduling algorithms or combined schemes of them. Joint relay selection and power allocation algorithms that can perform robustly in imperfect CSI for a DF cellular relay networks are proposed in [128]. The proposal aims to minimize the uplink transmit power of a network that takes the target data rate of each user as a quality of service constraint. Fairly good performance can be achieved even in worst case scenarios, and evidence for the success of this mechanism is there. Relatively higher power consumption at the intermediate relay nodes and overall end-to-end system delay compared to those of AF relays, can be considered as the two major demerits associated with this category of relays.

5.1.3 CF Relays

Under this scheme, the receive signal is quantized and retransmitted at the relay [129]. The CF relay strategy is used when the relay is incapable or not willing to decode the message sent by the source but still capable of compressing and forwarding the observation to the destination. In conventional CF relay schemes, the decoding process is operated in a successive manner at the destination, where the compression of the relay is decoded first and then the original message. A number of modified CF relay schemes have been proposed. In many of them, the destination jointly decodes the compression and the message instead of successive decoding that is easier. Here the important thing to note is that the original message can be decoded even without completely decoding the compression. This provides more freedom to the relay in selecting the compression. Most importantly, any successive decoding cannot be supported by any compression where loss of rate can be a resistant of an inappropriate selection. On the other hand, complete successive decoding or joint decoding cannot be supported by any compression. The observed improvement is not a result of repetitive encoding but the benefit of delayed decoding after all the blocks have been finished.

There are number of advantages associated with DF and other relay networks. The main advantages or some of the key features of relay networks are briefly considered below.

I. Relay networks can be used to provide solutions for signal fading and shadowing.
II. They can be used to increase throughputs resulting from better signal quality [130].
III. Aerial network coverage can be increased.
IV. They can be used to increase capacity.
V. System-wide power saving leading to a better energy efficiency can be achieved [130].
VI. In the case of DF relays, an intermediate processing stage can be used for signal reconstruction and retransmission in targeting reduction of interference and noise.
VII. In general, overall performance and stability of the network can be significantly improved with the employment of power and resource allocation schemes.

Specially by considering the properties of inherent self-interference it is decided to use a DF relay concept to develop a relay network for FBMC instead of using an AF relay for this study. The typical reason behind that is, the effect of accumulated self-interference can be eliminated to a certain extend without being amplified and forwarded to the next stage. Even in a single hop basic FBMC communication system, particularly in the case of asynchronous operation in a multipath channel and in the absence of an interference cancellation or management scheme, this can be considered as a inherent limiting factor. This phenomenon is quite important because if the self-interference of hop one is amplified, that may contribute to generate more interference than usual at the second hop other than the external interference arisen from different sources.

5.1.4 Applications and Recent Developments

Some of the associated enhancements related to relay concepts that can be considered as most recent, upcoming or likely to be further developed are identified in this section. But many of the already well established applications are not discussed. In connection to wireless relay networks, recent notable achievements are to be found in the areas of vehicular communication, cognitive radio, interference alignment, communication systems for unmanned aerial vehicles (UAVs), intelligent schemes, CoMP, green energy and physical layer security.

- Vehicular communication is considered in [131], which presents an analytical model with a generic radio channel model to fully characterize access probability and connectivity probability performance in a vehicular relay network, considering both one-hop and two-hop communications between a vehicle and the infrastructure. Closed-form expressions for them are also presented. An asynchronous cooperative communication protocol exploiting polarization diversity for vehicle-to-vehicle communication where synchronization is not required at the relay node is given in [132]. Dual-polarized antennas are employed at the relay node to achieve full-duplex AF communication. The transmission duration is reduced due to that leading to an increase in throughput. A lesser amount of transmission energy is consumed by this scheme compared to the conventional AF and non-cooperative scheme. Therefore this network is pronounced as an energy efficient high data rate scheme relay enabled communication network.

- In the case of CoMP, beamformer designs are only allowed to use the CSI feedbacks of the wireless links inside a network. That is led to a challenging optimization problem when attempting to maintain the SINR under the estimation and quantization errors in CSI. A conservative criterion and a solution method are proposed for this robust design problem in [133]. Applications of cooperative relaying schemes in Long Term Evolution-Advanced (LTE-Advanced) systems is considered in [134] where special attention is paid to two intra-cell CoMP schemes in LTE-Advanced systems and the performance of those schemes is evaluated. It is shown that cooperative relaying leads to both network coverage extension and capacity expansion in LTE-Advanced systems.

- Cognitive radio networks and cognitive transmissions with multiple relays are investigated in [135]. The two phases over Rayleigh fading channels namely the spectrum sensing phase and data transmission phase are jointly considered for that. In the spectrum sensing phase, only the initial spectrum sensing results are selected and used for fusion. Spectrum sensing results are the signals, which are received from the cognitive relays and decoded correctly at a cognitive source. In the data transmission phase, only the best relay is utilized to assist the cognitive source for data transmissions. A selective fusion spectrum sensing and best relay data transmission scheme for multiple-relay cognitive radio networks is also discussed. Similarly, a selective relay spectrum sensing and best relay data transmission scheme for multiple-relay cognitive radio networks is presented in [136]. In the spectrum sensing phase, only a set of selected cognitive relays are utilized to transmit or forward their initial detection results to a cognitive source for fusion. In the data transmission phase, only the relay that is with the best performance is selected to assist the cognitive source.

- In the case of interference alignment, three cooperative algorithms are proposed in [137] to find suboptimal solutions for the end-to-end sum rate maximization problem in a multiple antenna AF relay with an interference channel. Minimization of the sum power of enhanced noise from the relays and interference at the receivers is aimed by the first algorithm. Minimization of matrix-weighted sum mean square errors with either equality or inequality power constraints to utilize a connection between mean square error and mutual information is targeted by the second and third algorithms. A scheme called Pair-Aware Interference Alignment is proposed in [138], in order to cancel self-interference. The transmit precoding matrices and the relay processing matrix are chosen in such a way that at any given receiver all the interfering signals except the self-interference are within the interference subspace and the useful signal is in a subspace linearly independent of the interference subspace.

- A communication system in which UAVs are used as relays between ground-based terminals and a network base station is presented in [139]. An algorithm for optimizing the performance of the ground-to-relay links through control of the UAV heading angle is also discussed. An ergodic normalized transmission rate for the links between the ground nodes and the relay is defined. Then a closed-form expression for it in terms of the eigenvalues of the channel correlation matrix also presented. Results on the investigations of communication-aware steering algorithms for cooperative micro UAVs swarms is made available in [140]. The mission objective is to achieve a maximum spatial exploration efficiency with the simultaneous ability to self-optimize the air-to-ground communication links by exploiting controlled mobility. Algorithms are investigated for static as well as dynamically changing environments.

- Intelligent schemes in connection with relay networks have come under discussion as well. In [141], it is shown that optimal selection and transmission of a single relay among a set of multiple AF candidates minimizes the outage probability and is capable of outperforming any other strategy that involves simultaneous transmissions from more than one AF relay under an aggregate power constraint. Maximization of cooperation benefits with intelligent scheduling among AF relays is demonstrated by this outage optimality. An achievable rate region and its instantaneous interference relay channel boundary are presented in [142] for the scenario of (a) uninformed non-cooperative source-destination nodes (the source and destination nodes are not aware of the existence of the relay and are non-cooperative) and (b) informed and cooperative source-destination nodes. In the latter scenario, relay networks with intelligent relays and dump relays are considered.

- Use of green energy is one aspect related to green communication. The network resource management issues in next generation wireless networks with sustainable energy supply are discussed in [143]. The objectives are to deploy a minimal number of relay nodes powered by green energy and optimize resource allocation to ensure full network connectivity and quality of service requirements that can be satisfied with the harvested energy based on the cost threshold. The problem of joint power and subcarrier allocation is solved in the context of maximizing the energy efficiency of a multiuser, OFDMA cellular network, where the objective function is formulated as the ratio of the spectral efficiency over the total power dissipation [144]. It is proved that the fractional programming problem considered is quasi-concave where the Dinkelbach's method can be employed to find the optimal solution at a low complexity. The impact of various system parameters on the attainable energy efficiency and spectral efficiency of the system employing both energy efficiency maximization and spectral efficiency maximization algorithms is characterized. In particular, it is observed that increasing the number of relays for a range of cell sizes, although marginally increases the attainable spectral efficiency, reduces the energy efficiency significantly.

- Considering the security aspects, an achievable secrecy rate for the general untrusted relay channel is given in [145]. Two types of relay models are considered: the first one is with an orthogonal link from the source to the relay and the second one with an orthogonal link from the relay to the destination. For a special class of the second model where the relay is not interfering itself, an upper bound for the secrecy rate is found by using an argument whose net effect is to separate the eavesdropper from the relay. In [146], consider an untrusted relay network, with passive security attacks, where the message of the source can be decoded. Two ways to transmit confidential information of the source to the destination are discussed: non-cooperative secure beamforming and cooperative secure beamforming.

Cooperative network communication and rely strategies are not confined only to wireless mobile technologies. They are being used in many other areas as well. The important aspect is that they can be empowered with FBMC transmitters while incorporating all the inherent properties. Some of the large application areas like optical communication and satellite systems, including aerospace communication and underwater acoustic communication, also be benefited. Optical relaying techniques are proposed to improve the performance and overall distance coverage of free space optical communication systems. Laser communication systems are suggested to provide a low power, low cost and lightweight means for data relay between ground and space and for deep space communications in interplanetary probes [147]. A precision pointing strategy that can be used for the purpose are developed, as discussed in [147]. Relay concepts are widely used for satellite communications as well. An interference relay network with a satellite as a relay is presented in [148]. Using that basic setup, a cooperative strategy based on physical layer network coding and superposition modulation decoding for unidirectional communications among users is proposed. In the case of underwater acoustic communication, a multihop underwater acoustic line network, which consists of a series of equal-distance hops connected by relay transceivers in tandem, is considered in [149]. Many of the underlying properties of acoustic channels like frequency-dependent signal attenuation and noise, interhop interference, half-duplex modem constraint and large propagation delay are taken into account in this analysis.

Concepts of FBMC transmission and DF relaying are combined within this presentation, with the intention of integration of the inherent advantages associated with either of these technologies. It is essential to have insight knowledge on the end-to-end performance of the proposed network under different synchronization and channel conditions to suggest further enhancements. Fulfillment of that requirement is aimed in this study by employing three key performance measures [2, Sec. 1.1]: BER, outage probability and ergodic capacity. In contrast to [21], [150], [151] and other available literature, here transmission between two nodes is modeled with a complete causal asynchronous basic FBMC communication system in its exact form without any major assumptions or approximations and customized to a subcarrier filter.

5.2 Asymmetric and Asynchronous DF Relay System

End-to-end link performance of an asymmetric and asynchronous dual-hop DF relay system built up using a causal multirate FBMC technique operated under Rayleigh fading is considered here for further investigation [152]. Three main performance measures namely BER, outage probability and channel capacity are used for this evaluation and approximate closed-form expressions for them are also made available. An FBMC setup is modeled in its exact form without any approximations and customized to one of the most efficient subcarrier filter. Simulations are carried out in quasi-static multipath fading channels under symmetric, asymmetric, synchronous and asynchronous conditions and a receiver based on minimum distance is employed for symbol recovery. Performance characteristics are identified under different noise, interference, channel and synchronization conditions.

The system model that is used for this study is described in this section. In the same way as in [11], discrete time formulations for a complete causal asynchronous SISO basic multirate FBMC communication system operated in one of the hops are presented. The model is designed to transmit real-valued symbols. The characteristics of self-interferences of an asynchronous FBMC system are also considered. The relay network is limited to a primary dual-hop system with no interference from source S to destination D, where transmission takes place from source to relay R and then from relay to destination. It is assumed that both hops are with Rayleigh fading and there is no interference from the source node to the destination node. The configurations for the two transmitters are considered to be identical. The same settings are used for the two receivers. The properties of the hops are considered to be independent from each other, making them asymmetric. At the relay node R, no additional processing algorithms are employed other than those for basic signal detection and retransmission. The configuration of the dual-hop DF relay network is given in Figure 19.

Note **:** $\hbar$, $\hbar \in \{1,2\}$ is the index for a hop. When $\hbar$ or the hop number at the place of $\hbar$ is given on the left hand side of a equation, all the parameters on the right hand side are for that particular hop (e.g., although channel coefficient h_l is not separately indexed, but it is not common for both hops.). This method is employed in order to avoid excessive complexity of notations. Hop one is for source-to-relay and hop two is for relay-to-destination.

Asynchronous receive signal after filtering $v_\hbar[m', n', l, \epsilon]$ for the hop $\hbar$ is given same way as in (2.19) or [86, Eq. (8)],

$$\begin{aligned} v_\hbar\left[m', n', l, \epsilon\right] &= 2\sum_{m=0}^{2M-1}\sum_{n=0}^{\infty} a_{m,n} e^{j\left(\psi_{m,n}-\psi_{m',n'}\right)} e^{-j\frac{2\pi(m+\epsilon)}{2M}l} \sum_{k=0}^{\infty} p\left[k-n'M\right] \\ &\quad .\ p[k-l-nM] e^{j\frac{2\pi}{2M}(m-m'+\epsilon)\left(k-\frac{L_F-1}{2}\right)}. \end{aligned} \tag{5.1}$$

For the same hop, the receive signal after filtering with a channel coefficient h_l on path l and AWGN $\eta\,[k]$ is shown as

$$\begin{aligned} y_\hbar\left[m', n', l, \epsilon\right] &= 2\sum_{m=0}^{2M-1}\sum_{n=0}^{\infty} a_{m,n} e^{j\left(\psi_{m,n}-\psi_{m',n'}\right)} h_l e^{-j\frac{2\pi(m+\epsilon)}{2M}l} \sum_{k=0}^{\infty} p\left[k-n'M\right] \\ &\quad .\ p[k-l-nM] e^{j\frac{2\pi}{2M}(m-m'+\epsilon)\left(k-\frac{L_F-1}{2}\right)} + \eta\,[k]. \end{aligned} \tag{5.2}$$

Complete receive signal through all paths $y_\hbar[m', n', L_\hbar, \epsilon]$ in a $L_\hbar$ path channel is equivalent to

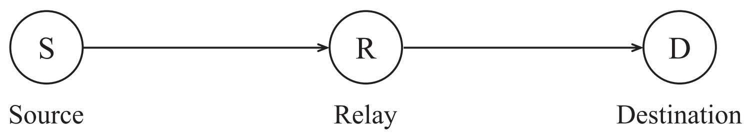

FIGURE 19 Basic DF relay configuration

$$y_{\hbar}\left[m',n',L_{\hbar},\epsilon\right] = \sum_{l=0}^{L_{\hbar}-1} y_{\hbar}\left[m',n',l,\epsilon\right]. \quad (5.3)$$

The filtered receive signal is known as a composition of a signal with the desired information symbol, interferences generated to other symbols and noise. By further simplification of (5.3) with $m = m'$ and $n = n'$, the signal containing the intended symbol can be expressed as

$$\begin{aligned} y_{a,\hbar}[m,n,L_{\hbar},\epsilon] &= 2a_{m,n}\sum_{l=0}^{L_{\hbar}-1} h_l e^{-j\frac{2\pi(m+\epsilon)}{2M}l} \sum_{k=0}^{\infty} p[k-nM]p[k-l-nM] \\ &\quad . \, e^{j\frac{2\pi}{2M}(\epsilon)\left(k-\frac{L_F-1}{2}\right)}. \end{aligned} \quad (5.4)$$

$y_{a,\hbar}[m,n,L_{\hbar},\epsilon]$ is a component of $y_{\hbar}[m',n',L_{\hbar},\epsilon]$. With $l = 0$ and $\epsilon = 0$,

$$\hat{a}_{m,n} = \Re\left\{\frac{y_{a,\hbar}[m,n,1,0]}{\hat{h}_0}\right\} = a_{m,n}. \quad (5.5)$$

It is assumed that perfect channel state information (PCSI) is available at the receiver. Here the symbols that have completed the full filter length can be correctly recovered. By following the approach of [86, Eq. (16)], a single component of interference generated to $a_{m,n}$ by any other symbol $a_{m'',n''}$ is presented in (5.6).

$$\begin{aligned} y_{\hbar,I''}\left[m,n,m'',n'',l,\epsilon\right] &= 2a_{m'',n''}e^{j\left(\psi_{m'',n''}-\psi_{m,n}\right)}h_l e^{-j\frac{2\pi(m''+\epsilon)}{2M}l}\sum_{k=0}^{\infty} p[k-nM] \\ &\quad . \, p\left[k-l-n''M\right]e^{j\frac{2\pi}{2M}(m''-m+\epsilon)\left(k-\frac{L_F-1}{2}\right)} \end{aligned} \quad (5.6)$$

Delays for the consecutive paths are measured relative to the first path, and the total interference to $a_{m,n}$ in a multipath channel is given by

$$y_{\hbar,I''}\left[m,n,L_{\hbar},\epsilon\right] = \sum_{l=0}^{L_{\hbar}-1} \sum_{\substack{m''=0 \\ m\neq m''}}^{2M-1} \sum_{\substack{n''=0 \\ n\neq n''}}^{\infty} y_{\hbar,I''}\left[m,n,m'',n'',l,\epsilon\right]. \quad (5.7)$$

Parameters are set to $m'' \neq m$ and $n'' \neq n$ to get the total self-interference in detecting $a_{m,n}$ (two cases, $m'' \neq m$ with $n'' = n$ and $m'' = m$ with $n'' \neq n$, are also included). Considering the probabilistic properties of

$$\begin{aligned} v_{\hbar,I''}\left[m,n,m'',n'',l,\epsilon\right] &= 2a_{m'',n''}e^{j\left(\psi_{m'',n''}-\psi_{m,n}\right)}e^{-j\frac{2\pi\left(m''+\epsilon\right)}{2M}l}\sum_{k=0}^{\infty}p[k-nM] \\ &\quad .\, p\left[k-l-n''M\right]e^{j\frac{2\pi}{2M}\left(m''-m+\epsilon\right)\left(k-\frac{L_F-1}{2}\right)}, \end{aligned} \tag{5.8}$$

and those of [86] and [96], it can be observed that $\Re\{v_{\hbar,I''}[m,n,m'',n'',l,\epsilon]\} \sim \mathcal{N}\left(0,\sigma^2_{\hbar,I''}[m,n,m'',n'',l,\epsilon]\right)$. Similar to [86, Eq. (18)] and [96],

$$\begin{aligned} \sigma^2_{\hbar,I''}\left[m,n,m'',n'',l,\epsilon\right] &= \Bigg|\Re\Bigg\{2e^{j\left(\psi_{m'',n''}-\psi_{m,n}\right)}e^{-j\frac{2\pi\left(m''+\epsilon\right)}{2M}l}\sum_{k=0}^{\infty}p[k-nM] \\ &\quad .\, p\left[k-l-n''M\right]e^{j\frac{2\pi}{2M}\left(m''-m+\epsilon\right)\left(k-\frac{L_F-1}{2}\right)}\Bigg\}\Bigg|^2, \end{aligned} \tag{5.9}$$

is used to show the variance. The individual interference components are uncorrelated. Therefore, as in [86, Eq. (19)], for the multipath channel also individual variances can be summed up to get the variance of the total interference $\sigma^2_{\hbar,I''}[m',n',L_\hbar,\epsilon]$,

$$\sigma^2_{\hbar,I''}[m,n,L_\hbar,\epsilon] = \sum_{\substack{m''=0 \\ m''\neq m}}^{2M-1}\sum_{\substack{n''=0 \\ n''\neq n}}^{\infty}\sum_{l=0}^{L_\hbar-1}\sigma^2_{\hbar,I''}\left[m,n,m'',n'',l,\epsilon\right]. \tag{5.10}$$

Then the total interference at the receiver generated by other symbols in (5.7) is in a $\Re\{y_{\hbar,I''}\left[m,n,L_\hbar,\epsilon\right]\} \sim \mathcal{N}\left(0,\sigma^2_{\hbar,I''}[m,n,L_\hbar,\epsilon]\right)$.

5.3 Performance Analysis

Performance is evaluated using three main performance measures viz. BER, outage probability and channel capacity [152]. There are some important features associated this process. Firstly, the basic FBMC system is modeled in its exact form without approximations for this purpose. Secondly, the deteriorative influence of self-interference, which is endemic to FBMC is specifically taken into account. The modeling is done by considering the probabilistic properties of receive signal and interferences.

SINR expression for each hop and PDF for the channel are derived as common formulas for all three performance measures. $\mathbb{E}\left[a^2_{m,n}\right] = \mathbb{E}\left[a^2_{m',n'}\right] =$

$\mathbb{E}\left[a^2_{m'',n''}\right] = E_b = 1$. It is assumed that delays between consecutive paths are small compared to the symbol interval and multipath delays are small compared to the symbol interval in such a way that for any n or n', $p[k-nM] \approx p[k-l-nM]$ or $p[k-n'M] \approx p[k-l-n'M]$. Symbols with full filter length in one of the subcarriers are taken into account with $n = n_F$ for these derivations. In this case a single tap equalizer (e.g., ZF equalization [102]) or a minimum distance based receier is considered. Then the receive signal power of a desired symbol in a multipath channel can be obtained using (5.4) and [103, Eq. (5)], as

$$P_{\hbar,a_{m,n_F},h,\epsilon} = \left|\sum_{l=0}^{L_\hbar-1} h_l e^{-j\frac{2\pi(m+\epsilon)}{2M}l}\right|^2 \left|2\sum_{k=0}^{\infty} p^2[k-n_F M] e^{j\frac{2\pi}{2M}(\epsilon)\left(k-\frac{L_F-1}{2}\right)}\right|^2. \quad (5.11)$$

Considering properties, the terms in (5.11) can be replaced with a gamma variable $\alpha_{\hbar,m,\epsilon}$ and a weighting factor $w_{\hbar,n_F,\epsilon}$ as

$$\alpha_{\hbar,m,\epsilon} = \left|\sum_{l=0}^{L_\hbar-1} h_l e^{-j\frac{2\pi(m+\epsilon)}{2M}l}\right|^2, \quad (5.12)$$

and

$$w_{\hbar,n_F,\epsilon} = \left|2\sum_{k=0}^{\infty} p^2[k-n_F M] e^{j\frac{2\pi}{2M}(\epsilon)\left(k-\frac{L_F-1}{2}\right)}\right|^2, \quad (5.13)$$

accordingly. Total power of the interference to a_{m,n_F} in a multipath channel is given by,

$$P_{\hbar,I''}[m,n_F,L_\hbar,\epsilon] = \sum_{l=0}^{L_\hbar-1} \sum_{\substack{m''=0 \\ m\neq m''}}^{2M-1} \sum_{\substack{n''=0 \\ n_F\neq n''}}^{\infty} \left|\Re\{y_{\hbar,I''}[m,n_F,m'',n'',l,\epsilon]\}\right|^2. \quad (5.14)$$

Since the total interference is in the form of Gaussian distribution, here also it can be taken as $P_{\hbar,I''}[m,n,L_\hbar,\epsilon] = \sigma^2_{\hbar,I''}[m,n_F,L_\hbar,\epsilon]$. Considering a single tap equalizer (e.g., ZF equalization [102]) or a minimum distance based receiver, the total variance of the real side interference is taken. The SINR can be defined as

$$\begin{aligned} \mathrm{SINR}_{\hbar m h \epsilon} &= \frac{P_{\hbar,a_{m,n_F},h,\epsilon}}{P_{\hbar,I''}[m,n_F,L_\hbar,\epsilon] + N_0} \\ &= \frac{\alpha_{\hbar,m,\epsilon} w_{\hbar,n_F,\epsilon}}{\sigma^2_{\hbar,I''}[m,n_F,L_\hbar,\epsilon] + N_0}. \end{aligned} \quad (5.15)$$

Same way as in (4.22), the squared envelope distribution of the transformed Rayleigh channel [103, Eq. (13)] is considered as an equivalent multipath channel for this scenario as given by,

$$f_{\gamma_{\Omega_{RL}}}\left(\alpha_{\hbar,m,\epsilon}\right) = \frac{1}{4\Omega_{RL}} \exp\left(-\frac{\alpha_{\hbar,m,\epsilon}}{4\Omega_{RL}}\right). \tag{5.16}$$

Conversion is as in [104, Eq. (5-4)]. $\Omega_{RL} = \sum_{l=0}^{L_{\hbar}-1} \mathbb{E}\left[\left|h_{Rl}\right|^2\right] = \sum_{l=0}^{L_{\hbar}-1} \mathbb{E}\left[\gamma_{Rl}\right]$. The numerator of the expression (5.15) can be identified as a weighted gamma variable $\alpha_{\hbar,w,m,\epsilon} = \alpha_{\hbar,m,\epsilon} w_{\hbar,n_F,\epsilon}$. According to [6, Eq. (5-18)] the PDF for it can be given as,

$$f_{\alpha_{\hbar,w,m,\epsilon}}\left(\alpha_{\hbar,w,m,\epsilon}\right) = \frac{1}{4\Omega_{RL} w_{\hbar,n_F,\epsilon}} \exp\left(-\frac{\alpha_{\hbar,w,m,\epsilon}}{4\Omega_{RL} w_{\hbar,n_F,\epsilon}}\right). \tag{5.17}$$

5.3.1 BER

Using (4.25) average BER $P_{\hbar,h}\left(E\right)$ for the hop $\hbar$ is derived as

$$P_{\hbar,h}\left(E\right) = \frac{1}{2}\left(1 - \sqrt{\frac{\frac{4\Omega_{RL} w_{\hbar,n_F,\epsilon}}{\sigma^2_{\hbar,I''}[m,n_F,L_{\hbar},\epsilon] + N_0}}{1 + \frac{4\Omega_{RL} w_{\hbar,n_F,\epsilon}}{\sigma^2_{\hbar,I''}[m,n_F,L_{\hbar},\epsilon] + N_0}}}\right). \tag{5.18}$$

Therefore, average BER from source to destination $P_h\left(E\right)$ with asymmetric and asynchronous channel hops is expressed as

$$P_h\left(E\right) = 1 - \prod_{\hbar=1}^{2}\left(1 - P_{\hbar,h}\left(E\right)\right). \tag{5.19}$$

5.3.2 Outage Probability

For this purpose, derivation (5.15) can be identified as a weighted gamma variable,

$$\mathrm{SINR}_{\hbar m h \epsilon} = \alpha_{\hbar,m,\epsilon} \mathcal{W}_{\hbar,m,h,\epsilon}. \tag{5.20}$$

For simplicity let $\mathcal{W}_{\hbar,m,h,\epsilon}$ be the weight of the gamma variable $\alpha_{\hbar,m,\epsilon}$,

$$\mathcal{W}_{\hbar,m,h,\epsilon} = \frac{w_{\hbar,n_F,\epsilon}}{\sigma^2_{\hbar,I''}[m,n_F,L_{\hbar},\epsilon] + N_0}. \tag{5.21}$$

Then PDF $f_{\mathrm{SINR}_{\hbar m h \epsilon}}\left(\mathrm{SINR}_{\hbar m h \epsilon}\right)$ can be expressed as a function of the weighted gamma variable [6, Eq. (5-18)]. Using (5.16),

$$f_{\text{SINR}_{\hbar mh\epsilon}}\left(\text{SINR}_{\hbar mh\epsilon}\right) = \frac{1}{\mathcal{W}_{\hbar,m,h,\epsilon}} f_{\gamma_{\Omega_{RL}}}\left(\frac{\text{SINR}_{\hbar mh\epsilon}}{\mathcal{W}_{\hbar,m,h,\epsilon}}\right). \tag{5.22}$$

The outage probability [7, Eq. (6.46)], [153] for the hop $\hbar$ with the threshold SINR, $\text{SINR}_{\hbar,th}$ is defined as

$$\begin{aligned} P_{\hbar,out} &= \Pr\left(\text{SINR}_{\hbar mh\epsilon} < \text{SINR}_{\hbar,th}\right) \\ &= \int_0^{\text{SINR}_{\hbar,th}} f_{\text{SINR}_{\hbar mh\epsilon}}\left(\text{SINR}_{\hbar mh\epsilon}\right) d\text{SINR}_{\hbar mh\epsilon} \\ &= 1 - \exp\left(-\frac{\text{SINR}_{\hbar,th}}{4\Omega_{RL}\mathcal{W}_{\hbar,m,h,\epsilon}}\right). \end{aligned} \tag{5.23}$$

$\Pr(\cdot)$ is the probability of the event. The outage probability from source to destination P_{out} with asymmetric and asynchronous channel hops can be given as

$$P_{out} = 1 - \prod_{\hbar=1}^{2}\left(1 - P_{\hbar,out}\right). \tag{5.24}$$

5.3.3 Channel Capacity

Instantaneous capacity for a single hop of an FBMC system can be expressed as in [154] with normalized subcarrier bandwidth while considering the symbols on the real side,

$$C_{\hbar,I} = \log_2\left(1 - \text{SINR}_{\hbar mh\epsilon}\right). \tag{5.25}$$

Then ergodic capacity is given by [7, Eq. (4.4)], [153],

$$\begin{aligned} C_{\hbar,E} &= \int_0^{\infty} \log_2\left(1 - \text{SINR}_{\hbar mh\epsilon}\right) f_{\alpha_{\hbar,w,m,\epsilon}}\left(\alpha_{\hbar,w,m,\epsilon}\right) d\alpha_{\hbar,w,m,\epsilon} \\ &= \frac{1}{\log(2)} \exp\left(\frac{\sigma^2_{\hbar,I''}[m, n_F, L_\hbar, \epsilon] + N_0}{4\Omega_{RL} w_{\hbar,n_F,\epsilon}}\right) \\ &\quad . \,\text{Ei}\left(\frac{\sigma^2_{\hbar,I''}[m, n_F, L_\hbar, \epsilon] + N_0}{4\Omega_{RL} w_{\hbar,n_F,\epsilon}}\right). \end{aligned} \tag{5.26}$$

$\text{Ei}(\cdot)$ is the exponential integral function. End-to-end ergodic capacity C_E can be given as

$$C_E = \min\left\{C_{1,E}, C_{2,E}\right\}, \tag{5.27}$$

where it is limited by the hop that is with the minimum capacity. The minimum of elements is given by $\min\{\cdot\}$.

5.3.4 Basic Signal Detection

A detection scheme based on the minimum distance is introduced for better symbol recovery. By observing (5.4), the receive signal containing desired symbol with parameters $m = m'$ and $n_F = n'$ can be estimated as (5.28) [152]

$$\begin{aligned}\hat{y}_{\hat{a},\hbar}[m, n_F, L_\hbar, \hat{\epsilon}] &= 2\hat{a}'_{m,n_F} \sum_{l=0}^{L_\hbar-1} \hat{h}_l e^{-j\frac{2\pi(m+\hat{\epsilon})}{2M}l} \sum_{k=0}^{\infty} p[k - n_F M] p[k - l - n_F M] \\ &\quad . e^{j\frac{2\pi}{2M}(\hat{\epsilon})\left(k - \frac{L_F - 1}{2}\right)}. \end{aligned} \tag{5.28}$$

Possible values for $\hat{a}'_{m,n_F}$ are to be assigned from the symbol alphabet. Symbol is decided based on the minimum value given by the metric $\delta_{\hat{a}_{m,n_F}}$. Delays are determined relative to the first path with the delay for the first path as $l = 0$. Using (5.3) and (5.28) it can be expressed as

$$\delta_{\hbar,\hat{a}_{m,n_F}} = \left| y_\hbar[m', n', L_\hbar, \epsilon] - \hat{y}_{\hat{a},\hbar}[m, n_F, L_\hbar, \hat{\epsilon}] \right|^2. \tag{5.29}$$

Same as in (4.38), it could be noted that, with the assumption of zero CFO estimate, performance of this detection principle is equivalent to the commonly used subcarrier-wise single-tap equalizer.

5.4 Numerical and Simulation Results

Discrete time equations developed for an asymmetric and asynchronous decode-and-forward basic causal FBMC relay system are used for simulations. The same normalized PHYDYAS filter [24]-[26], [86] is used as both the transmit and the receive subcarrier filters with the parameter settings as in [86]. The number of subcarriers is set to 64. In estimation of $\hat{y}_{\hat{a},\hbar}[m, n_F, L_\hbar, \hat{\epsilon}]$, $\hat{a}'_{m,n_F} \in \{-1, 1\}$ is used as the symbol alphabet with $\hat{\epsilon} = 0$ considering sufficiently small CFOs. Combinations of synchronous, asynchronous, symmetric and asymmetric cases are considered for both hops. If the conditions for both hops are equal, it is considered a symmetric case. If the link is with one propagation path with no CFO, the scenario is considered synchronous. In source-to-destination asynchronous scenarios, there is at least one hop with a multipath channel and / or CFO. In this presentation, all path delays are assumed to be in equal steps and CFO is set to 0.02 or 0.035. The variances calculated using (5.10) for the four senoras (1 tap, ϵ = 0.0), (2 taps, ϵ = 0.0), (1 tap, ϵ = 0.02) and (2 taps, ϵ = 0.035) are $3.01713 \times 10^{-7}, 1.72710 \times 10^{-2}, 6.211025 \times 10^{-2}$ and 2.76619×10^{-1} respectively. FBMC and OFDM systems are operated over Rayleigh quasi-static fading channel and PCSI is employed for symbol detection. Respective configurations for the two hops are given in the legends of the figures as (configuration for the hop one),(configuration for the hop two) (e.g., (1 tap, ϵ = 0.000), (1 tap, ϵ = 0.020)).

Initial results of an FBMC system setup are compared against the results of an OFDM system setup [96] in Figure 20 - (**a**). Both systems are with same number of subcarriers and operated under the same channel conditions. In the synchronous mode of operation, it may be noticed that the performance of the FBMC relay setup is similar to that of the OFDM setup. In the case of FBMC, a higher sensitivity for both time and frequency offsets can be observed. Importantly, the performance of FBMC is better than OFDM under asynchronous conditions in lower SNR values (bellow 15 - 20 dB). But in the case of FBMC with time and / or frequency offsets, comparatively there is no considerable improvement in the performance, especially in the higher SNR region (above 15 - 20 dB). Theoretical and simulation BER plots of the FBMC relay system are compared in Figure 20 - (**b**). Both results are the same in the case of one-tap, symmetric, synchronous operation. But the pair sets of results are in parallel and closer to each other for other scenarios.

Theoretical and simulation results for the outage probability are shown in Figure 21. Outage threshold is set to 0 dB. Both results are same in the case of one tap, symmetric and synchronous scenario. But the pair sets of results are in parallel and closer to each other for other cases.

The curves for the ergodic capacity for the system are shown by Figure 22. Here the system is operated under combinations of asymmetric, symmetric, asynchronous and synchronous conditions. The overall end-to-end capacity is limited by the capacity of the hop which is with the minimum capacity. Due to that, coincidence of many of the curves can be observed. It is important to note that capacity is not mainly limited by the number of hops, but it is severely affected by the synchronization conditions and other parameters. Since there is no linear relationship between capacity and SNR, when the system is not properly synchronized, the contribution made with the increase of SNR is not that attractive. It is apparent that there is a rapid decrease in the rate of increase of capacity with the increase of SNR. In this particular system setup, this can be observed particularly when the SNR is below 15 dB. So it is important to operate the system under near-synchronized conditions.

5.5 Summary and Discussion

The background and the importance of using relay networks were discussed at the beginning. End-to-end performance of an asymmetric and asynchronous DF dual-hop relay system which was developed using a causal multirate FBMC technique was investigated. The system was operated over a quasi-static multipath Rayleigh fading channel. Approximate closed-form expressions for three main performance measures, viz. BER, outage probability and ergodic capacity, were also presented. Using a symbol estimation mechanism based on minimum distance, simulation results were obtained for symmetric, asymmetric, synchronous and asynchronous scenarios. A better system performance over OFDM could be

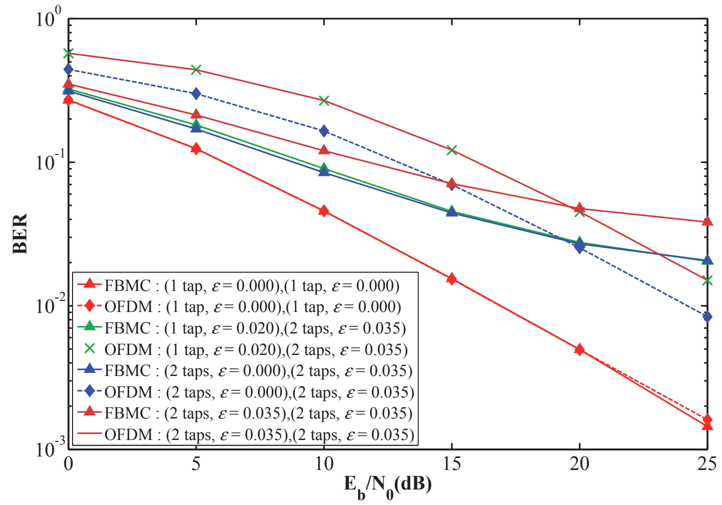

(a)

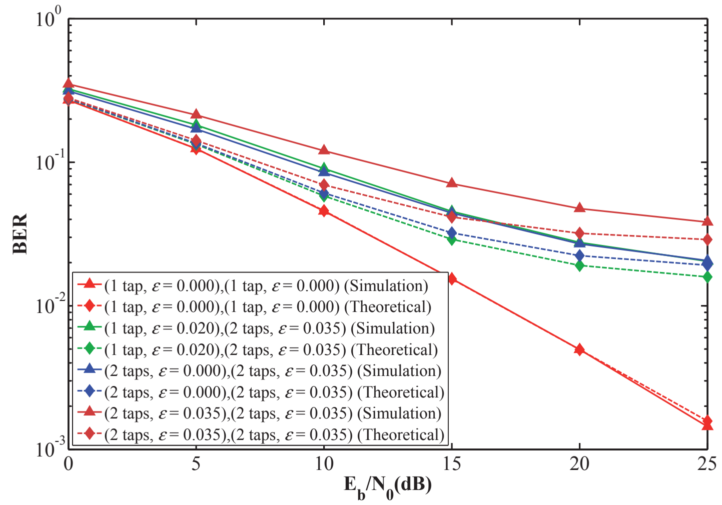

(b)

FIGURE 20 BER performance under asymmetric and symmetric conditions : **(a)** vs OFDM System and **(b)** vs Theoretical formulation

observed for lower SNR values. It is emphasized that the discussion in this chapter is the starting point and that there is tremendous potential with relay and associated concepts in many of the aspects for which they are being used at this moment.

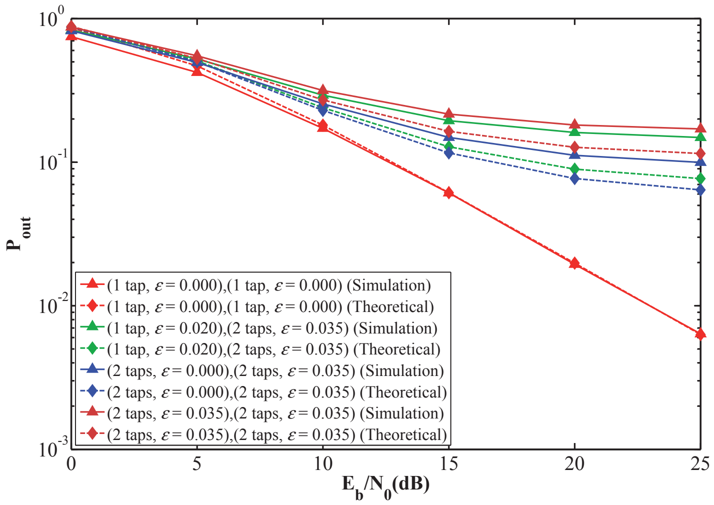

FIGURE 21 Outage probability under asymmetric and symmetric conditions

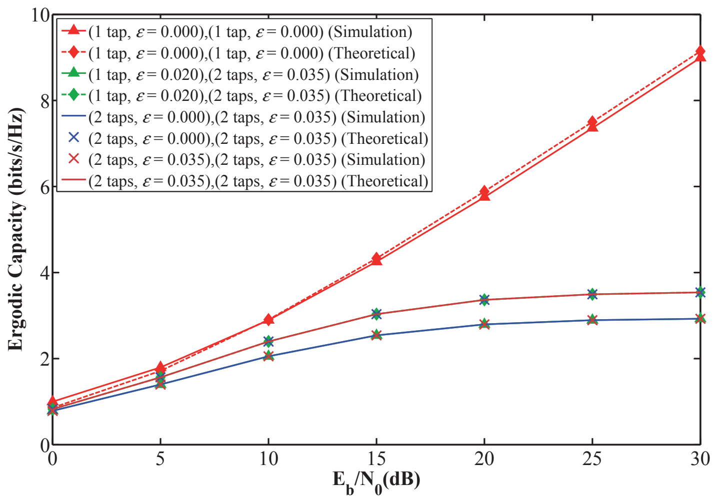

FIGURE 22 Ergodic capacity under asymmetric and symmetric conditions

6 FBMC RELAYS WITH DIVERSITY RECEPTION AND ANTENNA CORRELATION

Coverage and transmission quality of most of the wireless networks can be drastically improved by using antenna arrays while reducing interference and fading. The capacity of wireless channels can also be significantly increased by that. An antenna array can be defined as a spatio-temporal filter, which takes advantage of both time-domain and space-domain signal characteristics [155]. Sophisticated space-time coding and space-time signal processing techniques are developed for joint use of time-domain and space-domain data in multi-element antenna systems. That is led to developments in space-time channel models as well. However, this study is confined to the relays used for mobile wireless communications. The model can be extended to other areas of communications where relay concepts are used. A careful investigation is always recommended before such a extension, to find the best transmission technique for a given environment.

6.1 Introduction

Performance of corporative wireless network communication schemes or relay networks can be effectively further improved or boosted by integrating associated technological concepts. That can be achieved through analyzing the properties of a particular relay network concept and the transmission technique. Usually no adverse effects due to those supportive schemes are expected. However, a proper analysis before an amalgamation of a supportive scheme is recommended. The FBMC transmission technique itself can be considered as a typical example. After a careful analysis, for this particular scenario also, the DF relay technique is selected as a compatible relay model for FBMC. Other types of relay techniques are considered less suitable, due to self-interference associated with FBMC.

A set of basic concepts, namely FBMC transmission technique, DF relaying and diversity reception are combined in this study to make use of the numerous advantages associated with them. End-to-end performance is evaluated using the same key performance measures viz. BER, outage probability and ergodic capacity [2, Sec. 1.1]. All the receivers are modeled to employ diversity reception with two receive antennas. This is made more realistic by considering antenna correlation properties. In contrast to [21], [150], [151] and other available literature, transmission between two nodes is modeled with a complete causal basic FBMC communication system in its exact form and asymmetric channel conditions are used. The relay network is limited to a primary dual-hop system with no interference from source to destination.

In this study, source, relay and destination nodes can be stationary or mobile devices, even though mobility-related scenarios are not specifically considered here. However, the basic formulation presented in this study can be extended to address those kinds of scenarios as well. Functionalities of the relay node are limited to capturing, detecting and retransmitting the source signal to the destination node, making the entire system a conventional DF relay system.

Apart from the previous categorization, relay nodes can be divided into two main groups: dedicated relays and peer nodes acting as relays. Dedicated relays are types of relays which are designed to support or facilitate information exchange between the source node and the destination node. They are incapable of acting as source or destination nodes. But there can be certain intermediate processing functionalities. The peer nodes, acting as relays, are not primarily designed to act as relays. They may be mobile handsets, sensor nodes or similar devices mainly designed to send and receive information. Depending on the situation, their role can be changed to make them act as relays forwarding information to destination nodes. Each method has its merits and demerits. The second category, especially, is very easy to deploy and operate without much additional cost. But all the resources allocated to a particular device are to be shared to deal with information arriving from anonymous users, which is an clear disadvantage. On the other hand, there is a higher possibility that the structure and the configuration of the network will be more dynamic. In that case, even the main objectives associated with relay networks can be met occasionally.

Diversity combining, in which two or more copies of the same receive signal are merged yielding a better overall SNR or SNIR, is recognized as one of the most efficient and simplest approaches to improve the radio link performance.

6.1.1 Receiver Combining Techniques

Basically two categories of combining techniques viz. pure combining techniques and hybrid combining techniques can be identified. In addition, a number of variants of them can also be found. The main types, that are also known as the pure combining techniques [2, Sec. 9], are briefly introduced. In selection combining, the strongest signal is selected at the receiver from a number of receive-signal branches. Since the coherent sum of the individual branch signals and the knowledge of the signal phases on each branch are not required, this scheme can be used in conjunction with differentially coherent and noncoherent modulation techniques. In switch combining, the branch with the highest instantaneous SNR is selected. A SNR or SINR threshold is used to maintain the stability of the selected branch. If the selected branch is below the threshold, scanning is done to search for a new diversity branch that is higher than the threshold. In maximal-ratio combining (MRC), signals from all the branches are weighted, according to their individual SNR or SINR ratios, and summed up. From some angle, in the absence of interference, this is considered as the optimum technique. Because the weighted sum is taken from all the branches, the final SNR value of the MRC receiver is the sum of the SNR values of individual branches. This scheme has the advantage of producing an acceptable final SNR value regardless of very poor SNR values in some of the individual branches. Therefore, MRC is highly recommended for severely or deeply fading environments. Since knowledge of channel fading amplitudes is needed, this scheme can be used in conjunction with unequal energy signals as well. However MRC is not practical for differentially coherent and noncoherent detection. Equal-gain combing (EGC) is a method where all the receive branch weights are set to unity and signals from each branch are co-phased and combined. Since estimation of the fading amplitudes is not required, this combining technique with coherent detection is often an attractive solution. This combination can be considered as a reduced complexity scheme relative to the optimum MRC scheme. However, EGC is often limited in practice to coherent modulations with equal energy symbols. A simple detection technique for a receiver with a single antenna that is similar to EGC is presented (See APPENDIX 2), where that can be extended to a receivers with more than one antenna.

6.1.2 Antenna Correlation

When evaluating the suitability of a multiple receiving antenna system for diversity or MIMO applications, correlation coefficients between antennas are calculated. Correlation coefficient is an indicator of the amount of correlation between the antenna responses in a multipath-rich environment. One of the design goals is to ensure that the transfer functions of a given pair of antennas are uncorrelated and independent of each other. The desired transfer function is measured from the transmitter through the multipath channel and to the output terminals of each antenna. However, in a multipath-rich environment, usually the priority is to mitigate multipath fades. The value of the antenna or received waveform correlation coefficient may be less important than ensuring that if one antenna is in a multi path fade, while the other one is not. The specific nature of the multipath environment and the choice of diversity scheme or MIMO implementation may be more important in this situation than the value of the antenna correlation coefficient. But, in real world, this phenomenon must be accounted in order to achieve a much more realistic design.

All the advantages associated with DF relays can be incorporated in this setup as well. The main features only with diversity reception, over some of the other receiver techniques can be summarized as below. Alternatively, for this type of receiver these properties can be considered as the key merits in which this particular technique excels in the field of wireless communications.

I. Several observations of the same transmit signal can be used to ameliorate the effect of multipaths.
II. Deep fades of one antenna can easily be avoided.
III. Simple combining techniques can be used with minimum of processing power consumption for the basic signal detection while complex, power-consuming algorithms may be used to improve the quality of the receive signal associated with single antenna systems.
IV. The spatial need to accommodate antennas has diminished due to the increase in carrier frequency. Because of this and lower power consumption, these types of solutions can easily be used for handsets as well.
V. If only receive diversity is used, no additional modifications are needed at the transmitter.
VI. Since diversity concepts are identified as well-established and mature techniques, they can be directly incorporated to any transmission technique after a basic study like this.

However the concept of diversity reception always invokes the phenomenon of antenna correlation where it can be considered as a demerit.

6.1.3 Applications and Recent Developments

In many of the recent developments related to different types of receivers, more than one receive antenna is employed. However, there are also numerous accomplishments with diversity transmitters and receivers. They are already being incorporated into well-established systems containing transmission techniques such as OFDM. A set of associated enhancements related to diversity reception in relay networks can now be considered. These consist of a set of concepts which are recent, upcoming or likely to be further developed. Many of the already well-established applications will not be discussed here, however. Some of the relevant achievements in relation to the proposed relay network are in the areas of diversity relays, cognitive radio with combining techniques, interference alignment and precoding.

- Antenna diversity rather than relay diversity is discussed and analyzed in [156]. For a DF relaying system with MRC at the destination, spatial diversity is lost, except when the source-relay link is reliable. To find how to avoid that loss, an adaptive transmission scheme, which is referred to as smart relaying, is considered and analyzed. If properly designed, relaying can achieve diversity order up to the number of diversity paths, which can be referred to as the maximal diversity order. In [157], the performance of a multiple-relay system with fixed-gain AF relaying in Nakagami-*m* fading is studied. A tight upper bound on the average symbol error probability is obtained for a system with multiple relays when the MRC is used at the destination. Based on the obtained bound, a maximum diversity order also is shown. Moreover, the problem of power allocation to minimize the symbol error probability upper bound is investigated.

- A cognitive radio network consisting of a primary-transmitter / primary-receiver pair, and a secondary-base-station / secondary-receiver pair is considered in [158]. To improve the performance of both the primary and secondary pair, an overlay spectrum-sharing scheme is also proposed. For half of the time, the primary user's slots are leased to the secondary user in exchange for the secondary user cooperatively relaying the primary user's data using the AF scheme. To analyze the performance of the proposed scheme, closed-form expressions for the rate and bit-error rate for arbitrary SNR are derived. In [159], a general framework for a comprehensive performance analysis of cooperative spectrum sensing in cognitive radio networks is discussed. Exact and approximated closed-form expressions for the average detection probability and the average false alarm probability employing two diversity combining techniques, namely, the MRC scheme and the selection combining scheme are also derived.

- In [160], a secrecy relaying communication scenario where all nodes are equipped with multiple antennas is proposed. The concept of interference alignment is combined with cooperative jamming to ensure that artificial noise from transmitters can be aligned at the destination but not at the eavesdropper due to the randomness of wireless channels. Analytical results related to multiplexing and diversity gains are developed. In [161], a general precoding design scheme for multiple two-way relaying scenarios is proposed. There are several schemes which can be viewed as its special cases. The diversity order achieved by such transmission protocol is also analyzed.

- Energy-efficient secure communication in wireless networks in the presence of eavesdroppers is considered in [162]. For a secure transmission to the destination, a set of intermediate jammer nodes are chosen to generate artificial noise that confuses the eavesdropper. Two jamming strategies, beamforming and cooperative diversity, are considered. In [163], the outage performance of an information-theoretically secure secrecy communication system is considered. It is an important criterion to measure whether users' predefined quality of service can be met. By introducing cooperative transmission into secrecy communication systems, it can be shown that outage probability approaching zero can be achieved. In particular, scenarios with single-antenna nodes and multiple-antenna nodes will both be addressed, and the optimal design of beamforming / precoding will also be investigated. Explicit expressions of the achievable outage probability and diversity-multiplexing tradeoff are developed to demonstrate the performance of the proposed cooperative secure transmission schemes.

Relay networks associated with diversity reception can be used in other areas, including optical communication, satellite communication and underwater acoustic communication. All the merits and benefits associated with them can be integrated to those systems without much effort.

6.2 Asymmetric FBMC Relay System with Receive Antenna Diversity

An asymmetric dual-hop DF FBMC relay system operated under quasi-static Rayleigh multipath fading is considered here for the development of a relay network. The same three main performance measures, namely, BER, outage probability and channel capacity, are used to evaluate end-to-end link performance. Approximate closed-form expressions for them are also made available. Here also FBMC setup is modeled in its exact form without any approximations and customized to one of the most efficient subcarrier filter. Simulations are carried out under symmetric and asymmetric conditions where an MRC based receiver is used for symbol recovery. Performance characteristics are identified under different noise, interference, channel and synchronization conditions.

The system model used for this study is described in this section. It is an extension to the system model in Section 5. Discrete time formulations for a complete causal SIMO basic multirate FBMC communication system operated in one of the hops are discussed. But this is for a two receive antenna diversity scenario. The characteristics of self-interferences associated with the FBMC system and effects of antenna correlation are taken into account. The relay network is with two hops with a relay node where transmission takes place from source node S to a selected relay node $\mathrm{R}_{\mathcal{L}}$ $(\mathrm{S} \rightarrow \mathrm{R}_{\mathcal{L}})$ and then relay to destination node $\mathrm{D}_{\mathcal{L}}$ $(\mathrm{R}_{\mathcal{L}} \rightarrow \mathrm{D}_{\mathcal{L}})$, as in Figure 23. $\cdot_{\mathcal{L}}$ is used to denote any node that is with a $\mathcal{L}$ diversity receive antennas. Only one $\mathrm{S} \rightarrow \mathrm{D}_{\mathcal{L}}$ link is active with two hops after relay selection and they are given by the straight lines. It is assumed that both hops are under Rayleigh fading and there is no interference or signal reception through $\mathrm{S} \rightarrow \mathrm{D}_{\mathcal{L}}$ link. The configurations of all transmitters are considered to be identical. Similarly the settings of all the receivers are considered to be equal. Properties of the hops are considered to be mutually independent of each other, where they are made asymmetric. No additional processing algorithms are employed at the relay node other than the basic signal detection and retransmission. This type of setup is highly recommended for a downlink of a mobile wireless network.

Note **:** $\hbar$, $\hbar \in \{1, 2\}$ is the index for a hop. Here the hop 1 is for the link from source to any selected relay node and it is denoted by $(\mathrm{S} \rightarrow \mathrm{R}_{\mathcal{L}})$. Hop 2 is for the link from that node to the destination node and it is denoted by $(\mathrm{R}_{\mathcal{L}} \rightarrow \mathrm{D}_{\mathcal{L}})$. When $\hbar$ or the hop number at the place of $\hbar$ is given on the left hand side of an equation, all the parameters on the right hand side are for that particular hop (e.g., Channel coefficient transmit antenna to receive antenna ℓ, $h_{\ell,l}, \ell \in \{1, 2, \ldots, \mathcal{L}\}, \mathcal{L} = 2$ is not separately indexed, but it is not common for both hops.). This method is followed in order to avoid excessive complexity in the notations.

A wireless link from a transmit antenna to one of the two receive antennas of a basic FBMC communication system with $2M$ subcarriers is considered. Using

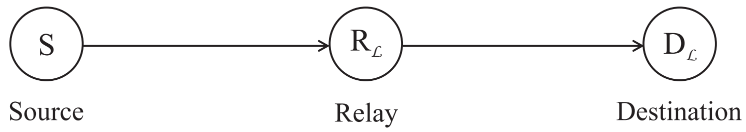

FIGURE 23 Basic DF relay configuration with diversity reception

[86, Eq. (8)], (2.19), FBMC receive signal after filtering, containing real-valued data symbol $a_{m,n}$ at transmit time instance k with the channel coefficient $h_{\ell,l}$, path delay index l and AWGN without subcarrier frequency offset is shown by

$$\begin{aligned} y_{\ell,\hbar}[m',n',l] &= 2\sum_{m=0}^{2M-1}\sum_{n=0}^{\infty} a_{m,n} e^{j\left(\psi_{m,n}-\psi_{m',n'}\right)} h_{\ell,l} e^{-j\frac{2\pi m}{2M}l} \sum_{k=0}^{\infty} p\left[k-n'M\right] \\ &\quad .\ p[k-l-nM] e^{j\frac{2\pi}{2M}(m-m')\left(k-\frac{L_F-1}{2}\right)} + \eta\,[k]. \end{aligned} \tag{6.1}$$

Delays are determined relative to the first path, the first path having the values $l = 0$. This is for the hop $\hbar$ and $l = 0$ is for the time domain synchronous scenario. Complete receive signal through all paths in a $L_\hbar$ path channel is equivalent to,

$$y_{\ell,\hbar}[m',n',L_\hbar] = \sum_{l=0}^{L_\hbar-1} y_{\ell,\hbar}[m',n',l]. \tag{6.2}$$

By simplification of (6.2) with $m = m'$ and $n = n'$, a signal containing the intended data symbol $a_{m,n}$ can be expressed as

$$y_{a,\ell,\hbar}[m,n,L_\hbar] = 2a_{m,n}\sum_{l=0}^{L_\hbar-1} h_{\ell,l} e^{-j\frac{2\pi m}{2M}l} \sum_{k=0}^{\infty} p[k-nM]p[k-l-nM]. \tag{6.3}$$

The symbols which have completed a full filter length or near full filter length can be recovered correctly. By following the same approach as for [86, Eq. (16)], a single component of interference generated to $a_{m,n}$ by any other symbol $a_{m'',n''}$ is presented as in

$$\begin{aligned} y_{\ell,\hbar,I''}[m,n,m'',n'',l] &= 2a_{m'',n''} e^{j\left(\psi_{m'',n''}-\psi_{m,n}\right)} h_{\ell,l} e^{-j\frac{2\pi m''}{2M}l} \sum_{k=0}^{\infty} p[k-nM] \\ &\quad .\ p\left[k-l-n''M\right] e^{j\frac{2\pi}{2M}(m''-m)\left(k-\frac{L_F-1}{2}\right)}. \end{aligned} \tag{6.4}$$

The total interference to $a_{m,n}$ in a multipath channel is given by

$$y_{\ell,\hbar,I''}[m,n,L_\hbar] = \sum_{l=0}^{L_\hbar-1} \sum_{\substack{m''=0\\ m\neq m''}}^{2M-1} \sum_{\substack{n''=0\\ n\neq n''}}^{\infty} y_{\ell,\hbar,I''}[m,n,m'',n'',l]. \tag{6.5}$$

Parameters are set to $m'' \neq m$ and $n'' \neq n$ to get the total self-interference in detecting $a_{m,n}$ (two cases $m'' \neq m$ with $n'' = n$ and $m'' = m$ with $n'' \neq n$ are also included). Considering probabilistic properties of

$$\begin{aligned} y_{\hbar,I''}[m,n,m'',n'',l] &= 2a_{m'',n''}e^{j\left(\psi_{m'',n''}-\psi_{m,n}\right)}e^{-j\frac{2\pi m''}{2M}l}\sum_{k=0}^{\infty}p[k-nM] \\ &\quad .\, p[k-l-n''M]e^{j\frac{2\pi}{2M}(m''-m)\left(k-\frac{L_F-1}{2}\right)}, \end{aligned} \tag{6.6}$$

with [86] and [96], it is an apparent basic fact that $\Re\{y_{\hbar,I''}[m,n,m'',n'',l]\} \sim \mathcal{N}\left(0,\sigma^2_{\hbar,I''}[m,n,m'',n'',l]\right)$. Similar to [86, Eq. (18)] and [96],

$$\begin{aligned} \sigma^2_{\hbar,I''}[m,n,m'',n'',l] &= \left|\Re\left\{2e^{j\left(\psi_{m'',n''}-\psi_{m,n}\right)}e^{-j\frac{2\pi m''}{2M}l}\sum_{k=0}^{\infty}p[k-nM]\right.\right. \\ &\quad \left.\left. .\;\, p[k-l-n''M]e^{j\frac{2\pi}{2M}(m''-m)\left(k-\frac{L_F-1}{2}\right)}\right\}\right|^2, \end{aligned} \tag{6.7}$$

is used to show the variance. Individual interference components are uncorrelated. Therefore, as in [86, Eq. (19)], in the case of multipath channel also individual variances can be summed to get the variance of the total interference $\sigma^2_{\hbar,I''}[m,n,L_\hbar]$,

$$\sigma^2_{\hbar,I''}[m,n,L_\hbar] = \sum_{\substack{m''=0\\ m''\neq m}}^{2M-1}\sum_{\substack{n''=0\\ n''\neq n}}^{\infty}\sum_{l=0}^{L_\hbar-1}\sigma^2_{\hbar,I''}[m,n,m'',n'',l]. \tag{6.8}$$

The total interference generated by other symbols that is presented in (6.5) is in a $\Re\{y_{\ell,\hbar,I''}[m,n,L_\hbar]\} \sim \mathcal{N}\left(0,\sigma^2_{\hbar,I''}[m,n,L_\hbar]\right)$.

Here the transmit diversity is not considered. The receive antenna correlation matrix can now be defined as $\mathbf{R}$ [164] with entry (p_x,q_x),

$$\mathcal{R}_{p_x,q_x} = e^{-j2\pi(q_x-p_x)d_{rx}\cos(\theta_{rx})}e^{-\frac{1}{2}(2\pi(q_x-p_x)d_{rx}\sin(\theta_{rx})\sigma_{rx})^2}. \tag{6.9}$$

$\mathbf{R}^{\frac{1}{2}}$ is with the element (p_x,q_x) given as $\mathcal{R}_{p_x,q_x}$. Relative antenna spacing between two adjacent antennas in number of wavelengths, destination angle spread and mean angle of arrival are given by d_{r_x}, $\sigma^2_{r_x}$ and θ_{r_x} respectively. Here the system is configured to a dual-antenna ($\ell \in \{1,2\}$) reception case with properties $|\mathcal{R}_{1,2}|^2 = |\mathcal{R}_{2,1}|^2$, $|\mathcal{R}_{1,1}|^2 = |\mathcal{R}_{2,2}|^2$ and $|\mathcal{R}_{1,1}|^2 + |\mathcal{R}_{1,2}|^2 = \mathcal{R}$. For simplicity, they can be taken as:

$$\mathcal{R}_1 \triangleq |\mathcal{R}_{1,1}|^2 = |\mathcal{R}_{2,2}|^2. \tag{6.10}$$

$$\mathcal{R}_2 \triangleq |\mathcal{R}_{1,2}|^2 = |\mathcal{R}_{2,1}|^2. \tag{6.11}$$

Two antennas are close enough to each other to be assumed that number of delayed paths and delay lengths are the same for them. According to [164, Eq. (3)] and the associated principles, using (6.2) and antenna correlation properties, receive signals for two antennas on a multipath channel can be expressed as:

$$\begin{aligned} y_{1,\hbar,AC}\left[m',n',L_{\hbar}\right] &= 2\sum_{m=0}^{2M-1}\sum_{n=0}^{\infty} a_{m,n}e^{j\left(\psi_{m,n}-\psi_{m',n'}\right)}\sum_{l=0}^{L_{\hbar}-1}\left(\mathcal{R}_{1,1}h_{1,l}+\mathcal{R}_{1,2}h_{2,l}\right)e^{-j\frac{2\pi m}{2M}l} \\ &\quad .\sum_{k=0}^{\infty} p\left[k-n'M\right]p[k-l-nM] \\ &\quad .\, e^{j\frac{2\pi}{2M}(m-m')\left(k-\frac{L_F-1}{2}\right)}+\eta\,[k]. \end{aligned} \tag{6.12}$$

$$\begin{aligned} y_{2,\hbar,AC}\left[m',n',L_{\hbar}\right] &= 2\sum_{m=0}^{2M-1}\sum_{n=0}^{\infty} a_{m,n}e^{j\left(\psi_{m,n}-\psi_{m',n'}\right)}\sum_{l=0}^{L_{\hbar}-1}\left(\mathcal{R}_{2,1}h_{1,l}+\mathcal{R}_{2,2}h_{2,l}\right)e^{-j\frac{2\pi m}{2M}l} \\ &\quad .\sum_{k=0}^{\infty} p\left[k-n'M\right]p[k-l-nM] \\ &\quad .\, e^{j\frac{2\pi}{2M}(m-m')\left(k-\frac{L_F-1}{2}\right)}+\eta\,[k]. \end{aligned} \tag{6.13}$$

respectively. $\cdot_{AC}$ is used to denote a signal or a value after filtering with antenna correlation. Then using (6.3) the receive signal containing a desired symbol on the receive antennas can be expressed as:

$$\begin{aligned} y_{a,1,\hbar,AC}[m,n,L_{\hbar}] &= 2a_{m,n}\sum_{l=0}^{L_{\hbar}-1}\left(\mathcal{R}_{1,1}h_{1,l}+\mathcal{R}_{1,2}h_{2,l}\right)e^{-j\frac{2\pi m}{2M}l} \\ &\quad .\sum_{k=0}^{\infty} p[k-nM]p[k-l-nM]. \end{aligned} \tag{6.14}$$

$$\begin{aligned} y_{a,2,\hbar,AC}[m,n,L_{\hbar}] &= 2a_{m,n}\sum_{l=0}^{L_{\hbar}-1}\left(\mathcal{R}_{2,1}h_{1,l}+\mathcal{R}_{2,2}h_{2,l}\right)e^{-j\frac{2\pi m}{2M}l} \\ &\quad .\sum_{k=0}^{\infty} p[k-nM]p[k-l-nM]. \end{aligned} \tag{6.15}$$

With the estimated channel parameters and antenna correlation coefficients, two terms $\hat{H}_{1,\hbar}[m,n,L_{\hbar}]$ and $\hat{H}_{2,\hbar}[m,n,L_{\hbar}]$ are defined as:

$$\begin{aligned} \hat{H}_{1,\hbar,}[m,n,L_{\hbar}] &= 2\sum_{l=0}^{L_{\hbar}-1}\left(\hat{\mathcal{R}}_{1,1}\hat{h}_{1,l}+\hat{\mathcal{R}}_{1,2}\hat{h}_{2,l}\right)e^{-j\frac{2\pi m}{2M}l}\sum_{k=0}^{\infty} p[k-nM] \\ &\quad .\, p[k-l-nM]. \end{aligned} \tag{6.16}$$

$$\hat{H}_{2,\hbar}[m,n,L_\hbar] \;=\; 2\sum_{l=0}^{L_\hbar-1}\left(\hat{\mathcal{R}}_{2,1}\hat{h}_{1,l}+\hat{\mathcal{R}}_{2,2}\hat{h}_{2,l}\right)e^{-j\frac{2\pi m}{2M}l}\sum_{k=0}^{\infty}p[k-nM] \\ .\,p[k-l-nM]. \tag{6.17}$$

Using (6.5), [164, Eq. (3)] and the associated principles, the total of all the interference components at each antenna can be given as:

$$y_{1,\hbar,I'',AC}[m,n,L_\hbar] \;=\; \mathcal{R}_{1,1}y_{1,\hbar,I''}[m,n,L_\hbar]+\mathcal{R}_{1,2}y_{2,\hbar,I''}[m,n,L_\hbar]. \tag{6.18}$$

$$y_{2,\hbar,I'',AC}[m,n,L_\hbar] \;=\; \mathcal{R}_{2,1}y_{1,\hbar,I''}[m,n,L_\hbar]+\mathcal{R}_{2,2}y_{2,\hbar,I''}[m,n,L_\hbar]. \tag{6.19}$$

Using (6.7), (6.8), (6.10), (6.11) and their properties, the total variance of all the interference components at each antenna can be given as:

$$\begin{aligned}\sigma^2_{1,\hbar,I'',AC}[m,n,L_\hbar] &= \sum_{\substack{m''=0\\ m''\neq m}}^{2M-1}\sum_{\substack{n''=0\\ n''\neq n}}^{\infty}\sum_{l=0}^{L_\hbar-1}(\mathcal{R}_1+\mathcal{R}_2)\sigma^2_{\hbar,I''}[m,n,m'',n'',l] \\ &= (\mathcal{R}_1+\mathcal{R}_2)\,\sigma^2_{\hbar,I''}[m,n,L_\hbar].\end{aligned} \tag{6.20}$$

$$\begin{aligned}\sigma^2_{2,\hbar,I'',AC}[m,n,L_\hbar] &= \sum_{\substack{m''=0\\ m''\neq m}}^{2M-1}\sum_{\substack{n''=0\\ n''\neq n}}^{\infty}\sum_{l=0}^{L_\hbar-1}(\mathcal{R}_2+\mathcal{R}_1)\sigma^2_{\hbar,I''}[m,n,m'',n'',l] \\ &= (\mathcal{R}_2+\mathcal{R}_1)\,\sigma^2_{\hbar,I''}[m,n,L_\hbar].\end{aligned} \tag{6.21}$$

Real side interference of single tap equalization based receivers are considered for them. By considering the properties of (6.20) and (6.21), it can be noted that they are the same. In that case,

$$\sigma^2_{\hbar,I'',AC}[m,n,L_\hbar] \;\triangleq\; \sigma^2_{\ell,\hbar,I'',AC}[m,n,L_\hbar]. \tag{6.22}$$

By careful observation of (6.5) and (6.8) with the derivation procedure of (6.18) and (6.19), it can be noted that total interferences generated to the signal received to the first and second antennas $y_{\ell,\hbar,I'',AC}[m,n,L_\hbar]$ are in $\Re\{y_{\ell,\hbar,I'',AC}[m,n,L_\hbar]\}$ $\sim\mathcal{N}\left(0,\sigma^2_{\hbar,I'',AC}[m,n,L_\hbar]\right)$.

6.3 Performance Analysis

Performance is evaluated using three main performance measures viz. BER, outage probability and channel capacity. Due to two main reasons, the approaches for them are with clear differences when compared to the existing expressions in literature. Firstly, the basic FBMC system is modeled in its exact form without approximations. Secondly, the deteriorative influence of self-interference, which is endemic to FBMC is specifically taken into account. Modeling is done considering the probabilistic properties of receive signal and interferences.

SINR expression for each hop and PDF for the channel are derived as common formulas for all the three performance measures. In this scenario also it is assumed that delays between consecutive paths are small compared to the symbol interval and multipath delays are small compared to the symbol interval in such a way that for any n or n', $p[k-nM] \approx p[k-l-nM]$ or $p[k-n'M] \approx p[k-l-n'M]$. Symbols with full filter length in one of the subcarriers are taken into account with $n = n_F$ for these derivations. Then the approximate receive signal power of a desired symbol in a multipath channel through the first antenna can be obtained using (6.10), (6.11), (6.14) and [103, Eq. (5)], as

$$\begin{aligned} P_{1,\hbar,a_{m,n_F},AC} &= \left| \sum_{l=0}^{L_\hbar-1} \left(\mathcal{R}_{1,1} h_{1,l} + \mathcal{R}_{1,2} h_{2,l}\right) e^{-j\frac{2\pi m}{2M}l} \right|^2 \left| 2 \sum_{k=0}^{\infty} p^2[k-n_F M] \right|^2 \\ &\approx \mathcal{R}_1 \left| \sum_{l=0}^{L_\hbar-1} h_{1,l} e^{-j\frac{2\pi m}{2M}l} \right|^2 + \mathcal{R}_2 \left| \sum_{l=0}^{L_\hbar-1} h_{2,l} e^{-j\frac{2\pi m}{2M}l} \right|^2 . \end{aligned} \tag{6.23}$$

Since the power of the filter is normalized to $1/2$ [86, Eq. (3)], the effect of the filter can be completely removed. By considering properties, the terms in (6.23) can be replaced with gamma variables $\alpha_{1,\hbar,m}$ and $\alpha_{2,\hbar,m}$ as $\alpha_{1,\hbar,m} = \left| \sum_{l=0}^{L_\hbar-1} h_{1,l} e^{-j\frac{2\pi m}{2M}l} \right|^2$ and $\alpha_{2,\hbar,m} = \left| \sum_{l=0}^{L_\hbar-1} h_{2,l} e^{-j\frac{2\pi m}{2M}l} \right|^2$. Here the receive signal power can be modeled as

$$P_{1,\hbar,a_{m,n_F},AC} \approx \mathcal{R}_1 \alpha_{1,\hbar,m} + \mathcal{R}_2 \alpha_{2,\hbar,m}. \tag{6.24}$$

The same procedure can be applied to (6.15) yielding the receive signal power associated with the second antenna,

$$P_{2,\hbar,a_{m,n_F},AC} \approx \mathcal{R}_2 \alpha_{1,\hbar,m} + \mathcal{R}_1 \alpha_{2,\hbar,m}. \tag{6.25}$$

Then with (6.22), (6.24) and (6.25), an approximate SINR for each antenna can be defined as:

$$\begin{aligned} \mathrm{SINR}_{1,\hbar,m} &= \frac{P_{1,\hbar,a_{m,n_F},AC}}{\sigma^2_{1,\hbar,I'',AC}[m, n_F, L_\hbar] + N_0} \\ &= \frac{\mathcal{R}_1 \alpha_{1,\hbar,m} + \mathcal{R}_2 \alpha_{2,\hbar,m}}{\sigma^2_{\hbar,I'',AC}[m, n_F, L_\hbar] + N_0}. \end{aligned} \tag{6.26}$$

$$\begin{aligned}\mathrm{SINR}_{2,\hbar,m} &= \frac{P_{2,\hbar,a_{m,n_F},AC}}{\sigma^2_{2,\hbar,I'',AC}[m,n_F,L_\hbar]+N_0}\\ &= \frac{\mathcal{R}_2\alpha_{1,\hbar,m}+\mathcal{R}_1\alpha_{2,\hbar,m}}{\sigma^2_{\hbar,I'',AC}[m,n_F,L_\hbar]+N_0}. \end{aligned} \tag{6.27}$$

MRC is used at the receiver. With the use of (6.26) and (6.27) total SINR at the receiver can alternatively be expressed as

$$\begin{aligned}\mathrm{SINR}_{\hbar,m} &= \mathrm{SINR}_{1,\hbar,m}+\mathrm{SINR}_{2,\hbar,m}\\ &= \frac{(\mathcal{R}_1+\mathcal{R}_2)\,\alpha_{1,\hbar,m}}{\sigma^2_{\hbar,I'',AC}[m,n_F,L_\hbar]+N_0}+\frac{(\mathcal{R}_1+\mathcal{R}_2)\,\alpha_{2,\hbar,m}}{\sigma^2_{\hbar,I'',AC}[m,n_F,L_\hbar]+N_0}\\ &= w_{\hbar,n_F}\alpha_{1,\hbar,m}+w_{\hbar,n_F}\alpha_{2,\hbar,m}. \end{aligned} \tag{6.28}$$

Total SINR can be considered as a summation of two weighted gamma variables with the weight,

$$w_{\hbar,n_F}=\frac{(\mathcal{R}_1+\mathcal{R}_2)}{\sigma^2_{\hbar,I'',AC}[m,n_F,L_\hbar]+N_0}. \tag{6.29}$$

Then the squared envelope distribution of the transformed Rayleigh channel [103, Eq. (13)], (4.22) is considered as an equivalent multipath channel for this scenario as given by

$$f_{\gamma_{\Omega_{RL}}}\left(\alpha_{\ell,\hbar,m}\right) = \frac{1}{4\Omega_{RL}}\exp\left(-\frac{\alpha_{\ell,\hbar,m}}{4\Omega_{RL}}\right). \tag{6.30}$$

Conversion is as in [104, Eq. (5-4)]. For any selected receive antenna $\left|h_{\ell,l}\right|^2=\gamma_{\ell,l}$ and $\Omega_{RL}=\sum_{l=0}^{L_\hbar-1}\mathbb{E}\left[\left|h_{\ell,l}\right|^2\right]=\sum_{l=0}^{L_\hbar-1}\mathbb{E}\left[\gamma_{\ell,l}\right]$. According to [104, Eq. (5-18)] the PDF for $w_{\hbar,n_F}\alpha_{\ell,\hbar,m}$ or $\mathrm{SINR}_{\ell,\hbar,m}$ can be given as

$$f_{\mathrm{SINR}_{\ell,\hbar,m}}\left(\mathrm{SINR}_{\ell,\hbar,m}\right) = \frac{1}{4\Omega_{RL}w_{\hbar,n_F}}\exp\left(-\frac{\mathrm{SINR}_{\ell,\hbar,m}}{4\Omega_{RL}w_{\hbar,n_F}}\right). \tag{6.31}$$

Using [104, Eq. (6-45)], which is similar to [2, Eq. (9.5)] the PDF of $\mathrm{SINR}_{\hbar,m}$ is given as

$$f_{\mathrm{SINR}_{\hbar,m}}\left(\mathrm{SINR}_{\hbar,m}\right) = \frac{\mathrm{SINR}_{\hbar,m}}{\left(4\Omega_{RL}w_{\hbar,n_F}\right)^2}\exp\left(-\frac{\mathrm{SINR}_{\hbar,m}}{4\Omega_{RL}w_{\hbar,n_F}}\right). \tag{6.32}$$

6.3.1 BER

Here, two weighted gamma variables in (6.28) with the relevant PDF (6.32) are used to derive the BER. Expression for the BER is derived as [2, Eq. (9.6)]

$$P_{\hbar}\left(E\right) = \int_{0}^{\infty} Q\left(\sqrt{2\mathrm{SINR}_{\hbar,m}}\right) f_{\mathrm{SINR}_{\hbar,m}}\left(\mathrm{SINR}_{\hbar,m}\right) d\mathrm{SINR}_{\hbar,m}. \tag{6.33}$$

$P_{\hbar}\left(E\right)$ can be further simplified using Craig's formula [105] as in

$$P_{\hbar}\left(E\right) = \frac{1}{2} - \frac{3}{4}\left(\frac{4\Omega_{RL} w_{\hbar,n_F}}{1+4\Omega_{RL} w_{\hbar,n_F}}\right)^{\frac{1}{2}} + \frac{1}{4}\left(\frac{4\Omega_{RL} w_{\hbar,n_F}}{1+4\Omega_{RL} w_{\hbar,n_F}}\right)^{\frac{3}{2}}. \tag{6.34}$$

Now the average BER form source to destination $P\left(E\right)$ for symmetric and asymmetric channel hops can be expressed as

$$P\left(E\right) = 1 - \prod_{\hbar=1}^{2}\left(1 - P_{\hbar}\left(E\right)\right). \tag{6.35}$$

6.3.2 Outage Probability

Outage probability [7, Eq. (6.46)], [153] for the hop $\hbar$ with the SINR threshold $\mathrm{SINR}_{\hbar,th}$ is defined by using (6.32),

$$\begin{aligned} P_{\hbar,out} &= \Pr\left(\mathrm{SINR}_{\hbar,m} < \mathrm{SINR}_{\hbar,th}\right) \\ &= \int_{0}^{\mathrm{SINR}_{\hbar,th}} f_{\mathrm{SINR}_{\hbar,m}}\left(\mathrm{SINR}_{\hbar,m}\right) d\mathrm{SINR}_{\hbar,m} \\ &= 1 - \left(1 + \frac{\mathrm{SINR}_{\hbar,th}}{4\Omega_{RL} w_{\hbar,n_F}}\right) \exp\left(-\frac{\mathrm{SINR}_{\hbar,th}}{4\Omega_{RL} w_{\hbar,n_F}}\right). \end{aligned} \tag{6.36}$$

The outage probability from source to destination P_{out} with symmetric and asymmetric channel hops can be given as

$$P_{out} = 1 - \prod_{\hbar=1}^{2}\left(1 - P_{\hbar,out}\right). \tag{6.37}$$

6.3.3 Channel Capacity

Instantaneous capacity for a single hop in an FBMC system can be expressed as in [154] with normalized subcarrier bandwidth,

$$C_{\hbar,I} = \log_2\left(1 + \mathrm{SINR}_{\hbar,m}\right). \tag{6.38}$$

The ergodic capacity is given by [7, Eq. (4.4)], [153],

$$\begin{aligned} C_{\hbar,E} &= \int_0^\infty \log_2\left(1+\mathrm{SINR}_{\hbar,m}\right) f_{\mathrm{SINR}_{\hbar,m}}\left(\mathrm{SINR}_{\hbar,m}\right) d\mathrm{SINR}_{\hbar,m} \\ &= \frac{1}{\log(2)} \exp\left(\frac{1}{4\Omega_{RL} w_{\hbar,n_F}}\right) \\ &\cdot \left(\mathrm{Ei}\left(\frac{1}{4\Omega_{RL} w_{\hbar,n_F}}\right) + \frac{\Gamma\left(-1, \frac{1}{4\Omega_{RL} w_{\hbar,n_F}}\right)}{4\Omega_{RL} w_{\hbar,n_F}}\right). \end{aligned} \tag{6.39}$$

$\Gamma(\cdot,\cdot)$ is the incomplete gamma function. End-to-end ergodic capacity C_E can be given as in

$$C_E = \min\left\{C_{1,E}, C_{2,E}\right\}, \tag{6.40}$$

where it is limited by the hop that is with the minimum capacity.

6.3.4 MRC Based Signal Detection

Maximal-ratio combining is used for signal detection at the receiver using (6.14), (6.15), (6.16) and (6.17). The receive signal containing a desired symbol with parameters $m = m'$ and $n = n_F = n'$ can be estimated as

$$\hat{a}_{m,n} = \Re\left\{ \frac{\sum_{\ell=1}^{2} \hat{H}_{\ell,\hbar}[m,n,L_\hbar]^* y_{\ell,\hbar,AC}\left[m',n',L_\hbar\right]}{\sum_{\ell=1}^{2} \left|\hat{H}_{\ell,\hbar}[m,n,L_\hbar]\right|^2} \right\}. \tag{6.41}$$

6.4 Numerical and Simulation Results

Discrete time equations developed for an asymmetric DF basic causal FBMC relay system are used for simulations. The same normalized PHYDYAS filter [86], [24]-[26] is used as both the transmit and the receive subcarrier filters with the parameter settings as in [86]. The number of subcarriers is set to 64. Combinations of non-multipath, multipath, symmetric and asymmetric cases are considered for both hops. If the conditions for both of them are equal, it is considered a symmetric case. In a case of a source-to-destination multipath scenario, there is at least one hop with a multipath channel. All the path delays are assumed to be in equal steps in this presentation. Variances calculated without antenna correlation, the main path when there is an antenna correlation and variance from the correlated component (using (6.8), (6.10) and (6.11)), for a single link, scenarios with 1, 2, 3, 4 and 5 taps are used to get the analytical plots. Antenna correlation parameters are set to $d_{r_x} = 1/2$, $\theta_{r_x} = \pi/2$ and $\sigma^2_{r_x} = \pi/20$. The FBMC system is operated over a quasi-static Rayleigh fading channel while using PCSI and perfect antenna correlation parameters for symbol detection. Respective configurations for the two hops are given in the legends of the figures as (Taps = number of paths for S $\rightarrow$ $R_{\mathcal{L}}$ $\times$ number of paths for $R_{\mathcal{L}}$ $\rightarrow$ $D_{\mathcal{L}}$) (e.g., (Taps = 3 $\times$ 4)).

Analytical and simulation BER plots for a dual-hop basic DF FBMC relay system are compared in Figure 24. Pair sets of results are in parallel and closer to each other for all the scenarios. Performance sensitivity to self-interference and the delayed paths can also be seen.

The results for the outage probability are made available in Figure 25. The outage threshold is set to 0 dB. Comparisons are done for analytical and simulation results where both of them are the same in the case of one-tap symmetric scenario. It can also be observed that pair sets of results are in parallel and closer to each other for the other cases. As indicated for BER results, sensitivity to self-interference and the signal components arriving in delayed paths can also be seen.

The curves for the ergodic capacity for the system are shown in Figure 26. Here the system is operated under combinations of asymmetric and symmetric channel conditions. The overall end-to-end capacity is limited by the capacity of the hop that is with the minimum capacity. Subsequently, coincidence of many curves (simulation and analytical pair sets for Taps 2 $\times$ 4 and Taps 3 $\times$ 4 scenarios) can be observed. It is important to note that capacity is not limited by the number of hops, but it is severely affected by the effects due to multipaths, other conditions and parameters. There is no apparent linear relationship between ca-

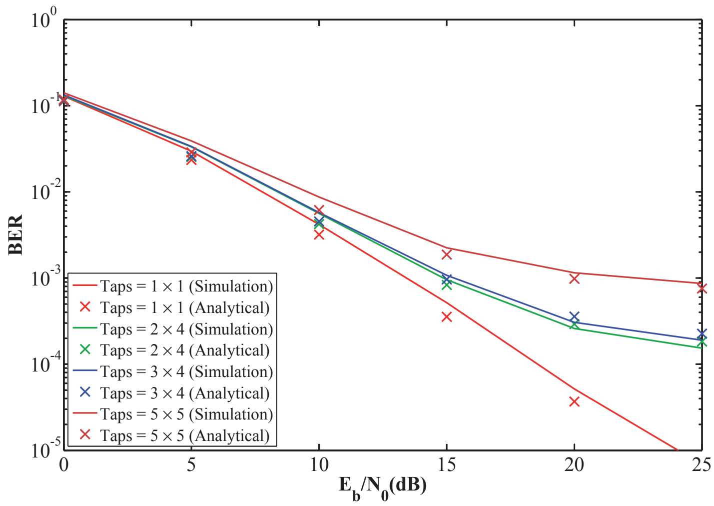

FIGURE 24 BER performance under asymmetric and symmetric conditions with diversity reception

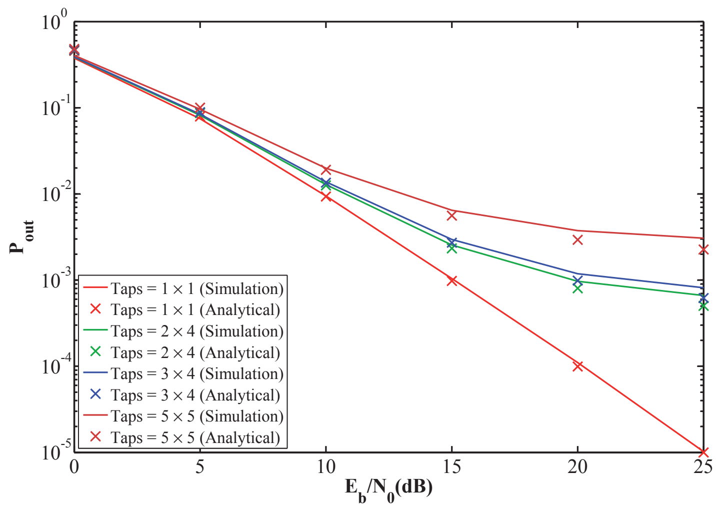

FIGURE 25 Outage probability under asymmetric and symmetric conditions with diversity reception

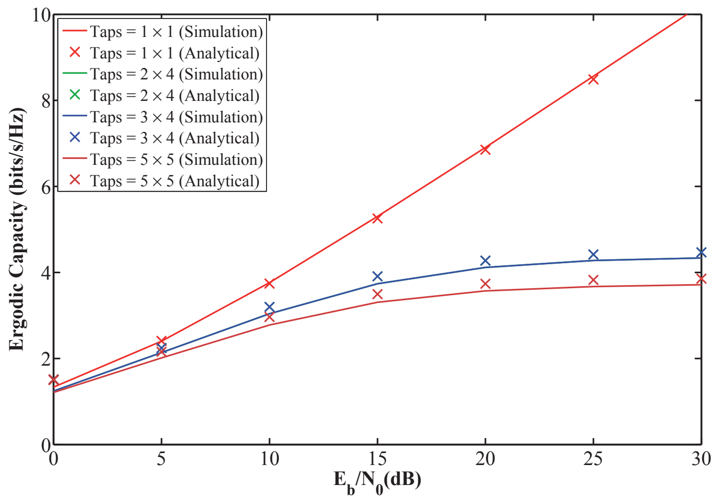

FIGURE 26 Ergodic capacity under asymmetric and symmetric conditions with diversity reception

pacity and SNR. If the system is not properly synchronized and if the links are effected with delayed paths, the contribution due to increase of SNR is not that attractive. There is a clear tendency towards of having a rapid decrease in the rate of capacity increase with the increase of SNR for any given scenario other than the 1×1 taps case. In this particular system setup, it can be particularly observed when SNR is below 20 dB.

In relation to the outage probability and the ergodic capacity, no difference could be seen between the cases of without antenna correlation and with antenna correlation. That is due to the property of $|\mathcal{R}_{1,1}|^2 + |\mathcal{R}_{1,2}|^2 = \mathcal{R} = 1$ of this antenna correlation model and this particular MRC based detection strategy used for dual-antenna diversity receivers.

6.5 Summary and Discussion

End-to-end performance of an asymmetric dual-hop relay DF system which was developed using the causal multirate FBMC transmission technique was investigated. The system was operated under quasi-static multipath Rayleigh fading channel conditions, using diversity receivers. Correlation properties of receive antennas were also considered. Approximate closed-form expressions for three main performance measures, viz. BER, outage probability and ergodic capacity, were presented. The simulation results for symmetric and asymmetric scenarios were obtained using an MRC signal detection mechanism.

7 CONCLUSIONS AND FUTURE WORK

Studies were carried out to analyze and evaluate performance of FBMC and some of the associated concepts. Results from both simulations and analytical expressions were used for the study. Finally FBMC-based investigations were extended to relay systems, including diversity reception.

7.1 Conclusions

Detail substance of this presentation containing background information, information on previous work, literature survey, formulations and results on different aspects can be summarized as follows.

- The background to this study was presented in Chapter 1. There was a brief discussion on the current status of wireless communication technologies and on upcoming trends. Out of them FBMC was identified for the further study. OFDM technique was recognized as the closest well-established multicarrier transmission technique for comparisons. Some of the characteristics of the operational environment, main reasons to initiate this study and the basic limitations were also discussed.

- Both OFDM and FBMC techniques covering some of the variants and characteristics were introduced in detail. There was a discussion on a number of major trends prioritizing possible future applications and related developments. Some potential candidates for future wireless communication applications were highlighted in the process. FBMC was identified as being still in the early stage of its life cycle and some inherent technical barriers for its rapid development were pointed out. The basic conventional formulation used with the study relating to OFDM was also made available. Both continuous and discrete time formulations for a basic causal multirate asynchronous FBMC system that can be operated under different fading conditions in a multipath channel were presented.

- Chapter 3 was used to analyze the properties of self-interference, distinguishing two main categories in it: interference caused by a particular symbol and interference caused to a desired symbol. That detailed study was customized to a particular FBMC setup supported by the PHYDYAS filter [86] in its exact form without approximations and assumptions. Due to the design of the filter and as a generic feature, smaller frequency offsets experienced less interference. Numerical results were tabled for both synchronous and asynchronous scenarios where higher interference for time offsets and even higher interference for time and frequency offsets could be observed. Variances for individual interfering components and total interference were shown and the expressions for the probability distributions of individual and total interference were presented. This analysis can be used to obtain detailed information on the behavior of the communication technique customized to a particular filter and associated self-interference.

- The performance of a causal asynchronous multirate FBMC system under various channel and synchronization conditions was considered in Chapter 4. A general approach for BER that can be used with any channel modeled with a PDF and considering an uniform delay profile was briefly introduced. That was followed by a closed-form BER expression for the Rayleigh and asymptotic BER for the Nakagami-m channels. For the simulations, a symbol detection mechanism based on minimum Euclidean distance was used at the receiver. A performance comparison between ZF equalizer and the minimum distance based receiver was also done identifying the fact that performance of minimum distance based receiver can be further enhanced by addressing interference terms with the expense of processing power. Quasi-static multipath fading channels in both synchronous and asynchronous conditions were considered for the simulations. A remarkable performance enhancement was achieved with the use of channel coding. Convolutional codes with maximum free distance were used for that. A thorough understanding on the behavior of this communication technique that can be used for later developments was provided by the results of those investigations.

- A DF dual-hop relay system was developed with the help of FBMC transmitters and receivers in Chapter 5. End-to-end performance under asymmetric and asynchronous multipath channel conditions was investigated. A quasi-static Rayleigh fading channel was used for the purpose. Three main performance measures, viz. BER, outage probability and ergodic capacity, were considered for the performance evaluation. Approximate closed-form expressions for them were also presented. The results for symmetric, asymmetric, synchronous and asynchronous scenarios were obtained from simulations and analytical expressions. A symbol estimation mechanism based on minimum distance was used for signal detection. It could be observed that the results for FBMC were better than those for OFDM for lower SNR values.

- The concept of FBMC relay networks was further developed in Chapter 6. The same DF dual-hop relay system was used as the basis. All the receivers were converted to dual-antenna diversity receivers and MRC was used to combine and detect the signals. End-to-end performance under asymmetric multipath channel conditions was investigated in quasi-static Rayleigh fading environments. Three main performance measures, namely, BER, outage probability and ergodic capacity, were considered for the performance evaluation. Approximate closed-form expressions for all three performance measures were also derived. Simulation and analytical results for symmetric and asymmetric scenarios where an MRC-based receiver was used were discussed. The results for FBMC were better than those for the single antenna reception scenarios.

7.2 Future Work

This study is on a particular technology at its basic level. Many other well-established associated or supportive techniques and concepts are not dealt with this. The main idea is to lay down a sound foundation for the projection or extrapolation which is to be initialized from that level. Some of the suggestions for future studies related to FBMC can be briefed as follows.

- Descriptions of various approaches and formulations related to systems and their subsequent developments are available in literature. Most of them are with modeling approximations or assumptions. Due to this, they are confined to individual presentations only. They cannot be considered as general cases or scenarios. If it is possible, those kinds of presentations must be reformulated and derived again, either without assumptions or with proper assumptions of the general kind. They must be reimplemented to observe their actual performance and to get a true and accurate picture on the real situation. It is a vital to have accurate insight and precise information on them.

- Before going into complex advance systems and configurations, more grass root level work should be done to create a more uniform and concrete foundation. Currently, there are many subcategories of FBMC, but only few of them are strong enough for further developments. They are needed to be transparent and backed by both theoretical proofs and corroborative simulation results. That kind of information is imperative for subsequent developments and studies. As it is identified, FBMC is a mixture of several other concepts and techniques. In that case, careful study of a gradual development of that kind of transmission technique like MC-CDMA or OFDM-CDMA can be recommended to see, how the natural technical evolution of a particular transmission technique takes place. Both of them can be considered as resultants of mixing different concepts and techniques.

- Some of the existing presentations are confined to simulation based approaches. Many of their parameters, conditions and even theoretical presentations are not clear enough for duplication or reconstruction them again in order to come up with new developments on top of them. Those unclear and ambiguous topics and details should be cleared by subsequent presentations. Proper theoretical proofing and approaches are needed for later developments. Need of such a work is a significant factor in this area of studies. Because many unsuccessful attempts to duplicate systems could be seen where start is with the same formulation, but the end results are not the same. Usually that should not be the case.

- It might be possible to develop a reduced complexity receiver where the process can be originated from a receiver similar to the one presented here. There is a tradeoff between the performance of the current multicarrier communication techniques and FBMC. That tradeoff should be properly balanced. Alternatively, even a transmitter-receiver pair could be developed.

- Even though there are some high-quality subcarrier filters that can be used for FBMC, filter designs and a simpler method of polyphase integration are always in demand. A study can be commence to design a set of filters where the performance is better than existing filters when the system is operated in multipath channel environment under asynchronous conditions. Even dissimilar transmit and receive filters can be considered for this purpose concentrating on to overall performance of the system rather than individual components.

- After laying a strong foundation for the basic systems and techniques, problems and developments related to FBMC can be viewed from different angles and new avenues for them should be opened. Solutions provided in this presentation may be regarded as resulting from multivariate probabilistic problem formulation, a practice quite common in studies related to telecommunication. In this connection, it is important to note that the analysis of self-interference that is customized to a particular FBMC transmitter and receiver setup is to be done before attempting to give solutions for other problems. The properties and causes of self-interference should be included in that analysis.

- Anyone attempting to handle receiver development or self-interference cancellation must pay more attention to the asynchronous modes of operations where there is a severe performance degradation with CFO due to self-interference rather than multipaths. At some point, system performance is interference-limited rather than noise-limited. The range of performance should be compared against existing multicarrier communication techniques. It is not expected that an optimum receiver would be produced initially. But the solution produced should be accurate and feasible.

- Investigation of possibilities of designing a pilot sequence aided detection technique can be introduced as an another type of approach. That is to be followed by an appropriate design of a pilot sequence. Same sequence can be used to estimate other parameters like CFO and channel coefficients. Same way as for many of the other mulicarrier techniques, this approach is recognized as one of the main stream of studies related to FBMC as well. Probabilistic approaches are highly recommended for scenarios limited by severe interference. Encoders and decoders implemented here and the receiver based on minimum Euclidean distance are not confined to just another simple application of coding and to a particular detection technique. A set of concrete evidences for the success of probability-based receiver development is provided by them.

- There are certain merits and demerits associated with both OFDM and FBMC. There is room for a precise study for automatic transmission scheme selection, which could be implemented by a handover algorithm facilitating the selection of the best transmission technique for a given scenario in order to maintain the essential factors like connectivity and quality of service.

- Not only the receiver development, but associated concepts also must be taken into account as much as possible where there is a great potential for those concepts. More work addressing both theoretical and practical challenges is needed at least in the areas that were presented under Sections 2.2.3, 2.3.3, 5.1.4 and 6.1.3 while exploring more avenues.

By observing both the theoretical formulation and simulation results it could be seen that both OFDM and FBMC systems are highly susceptible or sensitive to CFO related problems. Here the CFO can be divided into two parts. Fractional CFO refers to a CFO part the value of witch less than one subcarrier spacing, while integer CFO represents a CFO with an integer multiple of the subcarrier spacing. The former destroys orthogonality among subcarriers and gives rise to a reduction in performance, whereas the latter causes a cyclic shift of subcarriers and results in detection errors. Here the results for fractional CFO are presented. Specially in the case of uplink, it is led to much worse scenarios with the presence of multiuser interference [165]. To guarantee reliable communication, the CFO should be estimated correctly. The difference between the true CFO and the estimated CFO, which is defined as the residual CFO, should not exceed a certain level. Determination of an outlier, in the case where the residual CFO is greater than a certain threshold should also be taken into account. CFO estimation and correction is still be considered as an important area to study [166].

SUMMARY

Concept of FBMC was selected to be analyzed and to evaluate performance. Selection was done based on the competitive advantages over existing other prominent multicarrier communication techniques like OFDM. Other main objective was to present an accurate and complete information on a causal FBMC scheme that can be used for all the latter developments related to the technique.

Study was initialized with continuous and discrete domain formulations for a basic causal multirate FBMC system. Analysis of self-interference was done identifying them under two categories namely, interference generated from a desired symbol to other symbols and interference generated from any symbol to a particular symbol. Investigation was done under different synchronization conditions and probabilistic properties of self-interference were also discussed. Then the study was broadened to an analysis when the asynchronous FBMC system was operated under multipath environments. A general analytical expression for BER that can be used with any channel model was presented. Closed-form expressions for approximate BERs in AWGN and Rayleigh channels followed by an asymptotic error rate analysis for the Nakagami-*m* channel were presented. A receiver based on minimum Euclidean distance was used for the signal detection. It was shown that performanc of the minimum Euclidean distance based ditector without cancellation of self-nterference is same as that of the ZF equilizer. Results from corroborative simulations and numerical expressions were used for this study. It was shown that a remarkable improvement in performance could be achieved with the approaches based on the probability theories like some of the channel coding schemes. Convolutional codes with maximum free distance were used as illustrative scenarios or to demonstrate it.

Then study was extended to a simple FBMC relay network equipped with identical transmitter and receiver pairs. A DF relay network operated under symmetric and asynchronous conditions in a quasi-static Rayleigh channel was considered. Three main performance measures namely, BER, outage probability and ergodic capacity, were used to evaluate the performance of the network. In that scenario also closed-form expressions were presented and both simulation and analytical results were made available. Then, the same relay network was further enhanced with diversity reception at all the receivers under asymmetric and synchronous channel conditions. Correlation properties among receive antennas were also taken into account making the system more realistic. The same three performance measures were used to evaluate performance using closed-form expressions and simulation results. All transmitters and receivers were made identical separately. A MRC based receivers were used for signal reception. It could be noted that, both analytical and simulation pair sets of results were closer to each other. A clear avenue to derive many of the closed-form expressions that can be used to evaluate performance and an attractive set of results to originate studies on the direction of FBMC relays were presented by this study.

YHTEENVETO (FINNISH SUMMARY)

Tässä väitöskirjassa on analysoitu ja evaluoitu FBMC-konseptin suorituskykyä. Valinta perustui kilpailullisiin etuihin muihin olemassa oleviin monikantoaaltoon perustuviin kommunikaatiotekniikoihin, kuten OFDM:iin, nähden. Toinen päätavoite oli esitellä tarkka ja täydellinen kuvaus kausaalisesta FBMC - järjestelmästä, jota voidaan käyttää tutkimuksen myöhemmissä vaiheissa.

Tämän väitöskirja, jonka nimi on FBMC teknologian analyysi ja suorituskyky välitysverkoissa (Analysis and Performance of FBMC Techniques with Application to Relay Networks), alkaa yksinkertaisen kausaalisen moninopeus-FBMC-järjestelmän jatkuvan ja diskreetin määrittelyjoukon muodostamisella. Itsehäiriöanalyysi suoritettiin jakamalla se kahteen kategoriaan: häiriö, jonka symboli tuottaa muille symboleille ja jonkin symbolin häiriöntuotto toiseen tiettyyn symboliin. Tutkimus suoritettiin vaihtelevilla synkronointitilanteilla, käsitellen myös itsehäiriön todennäköisyysominaisuuksia. Työ laajennettiin analyysiin, jossa asynkroninen FBMC-järjestelmä toimi monitieympäristössä. Työssä esiteltiin analyyttinen malli bittivirhesuhteen laskemiseen, jota voi soveltaa mihin tahansa kanavamalliin. Työssä esiteltiin bittivirhesuhteen arviointiin AWGN-ja Rayleigh-kanavissa käytettävät lausekkeet suljetussa muodossa ja asymptoottinen virhesuhdeanalyysi Nakagami-*m*-kanavalle. Signaalin havaitsemiseen käytettiin yksinkertaista Euklidiseen etäisyyteen perustuvaa vastaanotinta. Tähän asiaan liittyen osoitettiin, että pienimpään Euklidiseen etäisyyteen perustuvan vaastanotimen suorituskyky ilman itsehäiriöanalyysin poistoa on sama kuin ZF - taajuuskorjaimella. Tutkimuksessa käytettiin tuloksia vahvistavia simulaatioita ja numeerisia osoituksia. Tutkimuksessa osoitettiin, että huomattavia suorituskykyparannuksia voidaan saavuttaa todennäköisyysteorioihin perustuvilla menettelytavoilla, kuten osa kanavakoodausmenetelmistä. Havainnollistamiseen tai kyseisen osoituksen demonstroimiseen käytettiin konvoluutiokoodeja vapaalla etäisyydellä.

Tutkimusta laajennettiin yksinkertaiseen FBMC-relay-verkkoon identtisillä lähetinvastaanotin-pareilla. Työssä tarkasteltiin DF-relay-verkkoa symmetrisissä ja asynkronisissa olosuhteissa kvasi-staattisessa Rayleigh-kanavassa. Verkon suorituskyvyn arviointiin käytettiin kolmea menetelmää: bittivirhesuhdetta, katkostodennäköisyyttä ja ergodista kapasiteettia. Myös tässä skenaariossa esiteltiin lausekkeet suljetussa muodossa ja tulokset tuotettiin sekä simulaatioilla että analyyttisesti. Samaa relay-verkkoa parannettiin tukemaan diversiteettiä vastaanottoa jokaisessa vastaanottimessa asymmetrisissä ja synkronisissa kanavaolosuhteissa. Vastaanotinantennien korrelaatio-ominaisuudet otettiin myös huomioon, jolla parannettiin järjestelmän realismia. Edellä mainittuja kolmea mittaria käytettiin arvioimaan suorituskykyä käyttämällä suljetun muodon lausekkeita ja simulaatiotuloksia. Jokainen lähetin ja vastaanotin tehtiin erikseen identtisiksi. MRC-vastaanottimia käytettiin signaalin vastaanottoon. Voidaan huomioida, että sekä analyyttiset ja simulaatiolla tuotetut tulokset olivat lähellä toisiaan. Työssä on esitelty selkeä tie useiden suljetussa muodossa olevien lausekkeiden johtamiseen, joita voidaan käyttää suorituskyvyn ja tulosten arviointiin ja tutkimusten ohjaamiseen FBMC-relay-verkkojen suuntaan.

REFERENCES

[1] J. B. Anderson, F. Rusek, and V. Owall, "Faster-Than-Nyquist Signaling," *Proceedings of IEEE*, vol. 101, no. 8, pp. 1817-1830, August 2013.

[2] M. K. Simon, and M. -S. Alouini, *Digital Communication over Fading Channels*, John Wiley & Sons, Inc., 2nd Edition, 2005.

[3] R. V. L. Hartley, "Transmission of Information," *Bell System Technical Journal*, vol. 3, pp. 535-564, July 1928.

[4] C. E. Shannon, "Communication in the Presence of Noise," *Proceedings Institute of Radio Engineers*, vol. 37, no. 1, pp. 10-21, January 1949.

[5] C. E. Shannon, "Capacity of Multi-antenna Gaussian Channels," *European Transactions on Telecommunications*, vol. 10, pp. 585-595, November 1999.

[6] J. G. Proakis, *Digital Communications*, McGraw-Hill Inc., 4th Edition, 2001.

[7] A. Goldsmith, *Wireless Communications*, Cambridge University Press, 1st Edition, 2005.

[8] D. Tse, and P. Viswanath, *Fundamentals of Wireless Communication*, Cambridge University Press, 2005.

[9] G. L. Stüber, *Principles of Mobile Communication*, Kluwer Academic Publishers, 2nd Edition, 2001.

[10] T. Rappaport, *Wireless Communications Principles and Practice*, Prentice Hall, 2nd Edition, 2001.

[11] P. Siohan, C. Siclet, and N. Lacaille, "Analysis and Design of OFDM / OQAM Systems Based on Filterbank Theory," *IEEE Transactions on Signal Processing*, vol. 50, no. 5, pp. 1170-1183, August 2002.

[12] J. G. Proakis, and M. Salehi, *Digital Communications*, McGraw-Hill Inc., 5th Edition, 2007.

[13] E. Biglieri, J. Proakis, and S. Shamai, "Fading Channels: Information-Theoretic and Communications Aspects," *IEEE Transactions on Information Theory*, vol. 44, no. 6, pp. 2619-2692, October 1998.

[14] J. Armstrong, "Analysis of New and Existing Methods of Reducing Intercarrier Interference Due to Carrier Frequency Offset in OFDM," *IEEE Transactions on Communications*, vol. 47, no. 3, pp. 365-369, March 1999.

[15] P. Tan, and N. C. Beaulieu, "Reduced ICI in OFDM Systems Using the "Better Than" Raised-cosine Pulse," *IEEE Communications Letters*, vol. 8, no. 3, pp. 135-137, March 2004.

[16] X. Cai, and G. B. Giannakis, "Bounding Performance and Suppressing Intercarrier Interference in Wireless Mobile OFDM," *IEEE Transactions on Communications*, vol. 51, no. 12, pp. 2047-2056, December 2003.

[17] L. Hanzo, M. Münster, B. J. Choi, and T. Keller, *OFDM and MC-CDMA for Broadband Multi-user Communications, WLANs and Broadcasting*. John Wiley-IEEE Press. 2002.

[18] L. Hanzo, C. H. Wong, and M. S. Yee, *Adaptive Wireless Transceivers: Turbo-Coded, Turbo-Equalised and Space-Time Coded TDMA, CDMA, MC-CDMA and OFDM Systems*. John Wiley-IEEE Press. 2002.

[19] P. Siohan, and N. Lacaille, "Analysis of OFDM / OQAM Systems Based on the Filterbank Theory," *IEEE Global Telecommunications Conference*, Rio de Janeiro, Brazil, December 1999.

[20] B. Farhang-Boroujeny, "OFDM Versus Filter Bank Multicarrier," *IEEE Signal Processing Magazine*, vol. 28, no. 3, pp. 92-112, May 2011.

[21] R. Zakaria, and D. Le Ruyet, "A Novel Filter-Bank Multicarrier Scheme to Mitigate the Intrinsic Interference: Application to MIMO Systems," *IEEE Transactions on Wireless Communications*, vol. 11, no. 3, pp. 1112-1123, March 2012.

[22] P. P. Vaidyanathan, *Multirate Systems and Filter Banks*. Prentice-Hall, 1993.

[23] N. J. Fliege, *Multirate Digital Signal Processing*. John Wiley & Sons, Ltd., 1993.

[24] M. Bellanger, "Efficiency of Filter Bank Multicarrier Techniques in Burst Radio Transmission," *IEEE Global Telecommunications Conference*, Miami, Florida, USA, December 2010.

[25] M. Bellanger, "Physical Layer for Future Broadband Radio Systems," *IEEE Radio and Wireless Symposium*, New Orleans, Los Angelis, USA, January 2010.

[26] M. Bellanger, "Specification and Design of a Prototype Filter for Filter Bank Based Multicarrier Transmission," *IEEE International Conference on Acoustics, Speech, and Signal Processing*, Utah, USA, May 2001.

[27] B. Le Floch, M. Alard, and C. Berrou, "Coded orthogonal frequency division multiplex [TV broadcasting]," *Proceedings of the IEEE*, vol. 83, no. 6, pp. 982-9110, June 1995.

[28] P. Siohan, and C. Roche, "Cosine-modulated Filterbanks Based on Extended Gaussian Functions," *IEEE Transactions on Signal Processing*, vol. 48, no. 11, pp. 3052-3061, November 2000.

[29] S. B. Weinstein, "The history of orthogonal frequency-division multiplexing [History of Communications]," *IEEE Communications Magazine*, vol. 47, no. 11, pp. 26-35, Novembe 2009.

[30] R. W. Chang, "Synthesis of band-limited orthogonal signals for multichannel data transmission," *Bell System Technical Journal*, vol. 46, pp. 1775-1796, December 1966.

[31] P. Banelli, and S. Cacopardi, "Theoretical analysis and performance of OFDM signals in nonlinear AWGN channels," *IEEE Transactions on Communications*, vol. 48, no. 3, pp. 430-411, August 2002.

[32] W. Shieh, X. Yi, Y. Ma, and Q. Yang, "Coherent Optical OFDM: Has Its Time Come? [Invited]," *Journal of Optical Networking*, vol. 7, no. 3, pp. 234-255, 2008.

[33] J. Armstrong, "OFDM for Optical Communications," *Journal of Lightwave Technology*, vol. 27, no. 3, pp. 189-204, February 2009.

[34] W. Shieh, "OFDM for Flexible High-Speed Optical Networks," *Journal of Lightwave Technology*, vol. 29, no. 10, pp. 1560-1577, May 2011.

[35] S. Weinstein, and P. Ebert, "Data Transmission by Frequency-Division Multiplexing Using the Discrete Fourier Transform," *IEEE Transactions on Communication Technology*, vol. 19, no. 5, pp. 628-634, October 1971.

[36] M. L. Dolez, E. T. Heald, and D. L. Martin, "Binary Data Transmission Techniques for Linear Systems," *Proceedings of Institute of Radio Engineers*, vol. 45, pp. 656-661, May 1957.

[37] G. A. Franco, and G. Lachs, "An Orthogonal Coding Technique for Communications," *Institute of Radio Engineers International Convention record*, vol. 8, pp. 126-133, 1961.

[38] H. K. Markey, and G. Antheil, "Secret communication system," US Patent 2,292,387, issued August 11, 1942.

[39] A. Peled, and A. Ruiz, "Frequency domain data transmission using reduced computational complexity algorithms," *IEEE International Conference on Acoustics, Speech, and Signal Processing*, Denver, Colorado USA, April 1980.

[40] L. Hanzo, M. Münster, B. J. Choi, and T. Keller, *OFDM and MC-CDMA for Broadcasting Multi-User Communications, WLANs and Broadcasting*. John Willey & Sons Ltd., West Sussex, England, 2003.

[41] S. Hara, and R. Prasad, "Design and performance of multicarrier CDMA system in frequency-selective Rayleigh fading channels," *IEEE Transaction on Vehicular Technology*, vol. 48, no. 5, pp. 1584-1595, September 1999.

[42] A. Nasri, R. Schober, and L. Lampe, "Performance of BICM-OFDM systems in UWB interference," *IEEE Transaction on Wireless Communications*, vol. 8, no. 9, pp. 4389-4392, September 2009.

[43] S. Kaiser, "On the performance of different detection techniques for OFDM-CDMA in fading channels," *IEEE Global Telecommunications Conference*, Singapore, November 1995.

[44] P. Cheng, M. Tao, Y. Xiao, and W. Zhang, "V-OFDM: On Performance Limits over Multi-Path Rayleigh Fading Channels," *IEEE Transaction on Communications*, vol. 59, no. 7, pp. 1878-1892, July 2011.

[45] A. Batra, J. Balakrishnan, G. R. Aiello, J. R. Foerster, and A. Dabak, "Design of a multiband OFDM system for realistic UWB channel environments," *IEEE Transaction on Microwave Theory and Techniques*, vol. 52, no. 9, pp. 2123-2138, September 2004.

[46] W. Zhiqiang, and C. R. Nassar, "Narrowband interference rejection in OFDM via carrier interferometry spreading codes," *IEEE Transaction on Wireless Communications*, vol. 4, no. 4, pp. 1491-1505, July 2005.

[47] L. Luo, J. Zhang, and Z. Shi, "BER Analysis for Asymmetric OFDM Systems," *IEEE Global Telecommunications Conference*, New Orleans, Louisiana USA, December 2008.

[48] S. F. A. Shah, and A. H. Tewfik, "Design and analysis of post-coded OFDM systems," *IEEE Transaction on Wireless Communications*, vol. 7, no. 12, pp. 4907-4918, December 2008.

[49] B. LeFloch, M. Alard, and C. Berrou, "Coded Orthogonal Frequency Division Multiplex [TV broadcasting]," *Proceedings of IEEE*, vol. 83, no. 6, pp. 982-996, June 1995.

[50] T. Zemen, L. Bernado, N. Czink, and A. F. Molisch, "Iterative Time-Variant Channel Estimation for 802.11p Using Generalized Discrete Prolate Spheroidal Sequences," *IEEE Transactions on Vehicular Technology*, vol. 61, no. 3, pp. 1222-1233, March 2012.

[51] J. A. Fernandez, K. Borries, L. Cheng, B. V. K. V. Kumar, D. D. Stancil, and F. Bai, "Performance of the 802.11p Physical Layer in Vehicle-to-Vehicle Environments," *IEEE Transactions on Vehicular Technology*, vol. 61, no. 1, pp. 3-14, January 2012.

[52] Y. Tachwali, B. F. Lo, I. F. Akyildiz, and R. Agusti, "Multiuser Resource Allocation Optimization Using Bandwidth-Power Product in Cognitive Radio Networks," *IEEE Journal on Selected Areas in Communications*, vol. 31, no. 3, pp. 451-463, March 2013.

[53] R. Wang, V. R. N. Lau, L. Lv, and B. Chen, “Joint cross-layer scheduling and spectrum sensing for OFDMA cognitive radio systems,” *IEEE Transactions on Wireless Communications*, vol. 8, no. 5, pp. 2410-2416, May 2009.

[54] C. Studer, and E. G. Larsson, “PAR-Aware Large-Scale Multi-User MIMO-OFDM Downlink,” *IEEE Journal on Selected Areas in Communications*, vol. 31, no. 2, pp. 303-313, February 2013.

[55] L. Dai, Z. Wang, and Z. Yang, “Spectrally Efficient Time-Frequency Training OFDM for Mobile Large-Scale MIMO Systems,” *IEEE Journal on Selected Areas in Communications*, vol. 31, no. 2, pp. 251-263, February 2013.

[56] O. E. Ayach, S. W. Peters, and R. W. Heath, “The Feasibility of Interference Alignment Over Measured MIMO-OFDM Channels,” *IEEE Transactions on Vehicular Technology*, vol. 59, no. 9, pp. 4309-4321, November 2010.

[57] N. Lertwiram, P. Popovski, and K. Sakaguchi, “A Study of Trade-Off Between Opportunistic Resource Allocation and Interference Alignment in Femtocell Scenarios,” *IEEE Wireless Communications Letters*, vol. 1, no. 4, pp. 356-359, August 2012.

[58] V. K. N. Lau, and C. H. Koh “Tradeoff Analysis of Delay-Power-CSIT Quality of Dynamic Backpressure Algorithm for Energy Efficient OFDM Systems,” *IEEE Transactions on Signal Processing*, vol. 60, no. 8, pp. 4254-4263, August 2012.

[59] T-S. Chang, K-T. Feng, J-S. Lin, and L-C. Wang, “Green Resource Allocation Schemes for Relay-Enhanced MIMO-OFDM Networks,” *IEEE Transactions on Vehicular Technology*, vol. 62, no. 9, pp. 4539-4554, November 2013.

[60] Y. Tsai, H. Huang, Y. Chen, and K. Yang, “Simultaneous Multiple Carrier Frequency Offsets Estimation for Coordinated Multi-Point Transmission in OFDM Systems,” *IEEE Transactions on Wireless Communications*, vol. 12, no. 9, pp. 4558-4568, September 2013.

[61] D. Choi, D. Lee, and J. H. Lee, “Resource Allocation for CoMP With Multiuser MIMO-OFDMA,” *IEEE Transactions on Vehicular Technology*, vol. 60, no. 9, pp. 4626-4632, November 2011.

[62] F. F Bernardo, R. R. Agusti, J. J. Perez-Romero, and O. Sallent, “Inter cell Interference Management in OFDMA Networks: A Decentralized Approach Based on Reinforcement Learning,” *IEEE Transactions on Systems, Man, and Cybernetics, Part C: Applications and Reviews*, vol. 41, no. 6, pp. 968-976, November 2011.

[63] V. Krishnamurthy, C. R. N. Athaudage, and D. Huang, “Adaptive OFDM synchronization algorithms based on discrete stochastic approximation,” *IEEE Transactions on Signal Processing*, vol. 53, no. 4, pp. 1561-1574, April 2005.

[64] Z. Li, and X-G. Xia, "A distributed differentially encoded OFDM scheme for asynchronous cooperative systems with low probability of interception," *IEEE Transactions on Wireless Communications*, vol. 8, no. 7, pp. 1536-1276, July 2009.

[65] D. W. K. Ng, E. S. Lo, and R. Schober, "Energy-Efficient Resource Allocation for Secure OFDMA Systems," *IEEE Transactions on Vehicular Technology*, vol. 61, no. 6, pp. 2572-2585, July 2012.

[66] Z. Wang, S. Zhou, J. Catipovic, and P. Willett, "Asynchronous Multiuser Reception for OFDM in Underwater Acoustic Communications," *IEEE Transactions on Wireless Communications*, vol. 12, no. 3, pp. 1050-1061, March 2013.

[67] G. Ren, S. Qiao, H. Zhao, C. Li, and Y. Hei, "Mitigation of Periodic Impulsive Noise in OFDM-Based Power-Line Communication," *IEEE Transactions on Power Delivery*, vol. 28, no. 2, pp. 825-834, April 2013.

[68] L. Xia J. Vucic, V. Jungnickel, and J. Armstrong, "On the Capacity of Intensity-Modulated Direct-Detection Systems and the Information Rate of ACO-OFDM for Indoor Optical Wireless Applications," *IEEE Transactions on Communications*, vol. 60, no. 2, pp. 799-809, March 2012.

[69] J. R. G. D. Arroyo, and J. A. Jackson, "WiMAX OFDM for Passive SAR Ground Imaging," *IEEE Microwave and Wireless Components Letters*, vol. 23, no. 8, pp. 433-435, August 2013.

[70] L. Hanzo, L -L. Yang, E -L. Kuan, and K. Yen, *Single- and Multi-Carrier DSCDMA: Multi-User Detection, Space-Time Spreading, Synchronisation, Networking and Standards*. John Wiley & Sons, Inc. 2003.

[71] C. K. Sung, and I. Lee, "Multiuser Bit-Interleaved Coded OFDM with Limited Feedback Information," *IEEE Vehicular Technology Conference*, Dallas, Texas, USA, September 2005.

[72] P. Ciblat, and E. Serpedin, "A fine blind frequency offset estimator for OFDM / OQAM systems," *IEEE Transaction on Signal Processing*, vol. 52, no. 1, pp. 291-296, January 2004.

[73] M. Caus, A. I. Perez-Neira, and A. Garcia-Armada, "A Discrete Bit Loading Algorithm for FBMC / OQAM," *IEEE Signal Processing Letters*, vol. 19, no. 6, pp. 324-327, June 2012.

[74] B. Farhang-Boroujeny, and L. Lin, "Analysis of post-combiner equalizers in cosine-modulated filterbank-based transmultiplexer systems," *IEEE Transaction on Signal Processing*, vol. 51, no. 12, pp. 3249-3262, December 2003.

[75] B. G. Negash, and H. Nikookar, "Wavelet based OFDM for wireless channels," *IEEE 53rd Vehicular Technology Conference*, Rhodes, Greece, May 2001.

[76] K-H. Chen, and T-D. Chiueh, “A Cognitive Radio System Using Discrete Wavelet Multitone Modulation,” *IEEE Transaction on Circuits and Systems I: Regular Papers*, vol. 56, no. 10, pp. 3246-3258, November 2008.

[77] A. M. Tonello, “Performance limits for filtered multitone modulation in fading channels,” *IEEE Transaction on Wireless Communications*, vol. 4, no. 5, pp. 2121-2135, September 2005.

[78] L. Youhong, and J. M. Morris, “A novel design technique for biorthogonal filterbank systems,” *IEEE Transaction on Signal Processing*, vol. 48, no. 2, pp. 563-566, February 2000.

[79] Y. Medjahdi, M. Terré, D. Le Ruyet, D. Roviras, and A. Dziri, “Performance Analysis in the Downlink of Asynchronous OFDM / FBMC Based Multi-Cellular Networks,” *IEEE Transactions on Wireless Communications*, vol. 10, no. 8, pp. 2630-2639, August 2011.

[80] T. Ihalainen, A. Viholainen, T. H. Stitz, and M. Renfors, “Generation of Filter Bank-Based Multicarrier Waveform Using Partial Synthesis and Time Domain Interpolation,” *IEEE Transactions on Circuits and Systems*, vol. 57, no. 7, pp. 1767-1778, July 2010.

[81] H. Zhang, D. L. Ruyet, D. Roviras, and H. Sun, “Noncooperative Multi-cell Resource Allocation of FBMC-Based Cognitive Radio Systems,” *IEEE Transactions on Vehicular Technology*, vol. 61, no. 2, pp. 799-811, February 2012.

[82] D. L. Wasden, H. Moradi, and B. Farhang-Boroujeny, “Design and Implementation of an Underlay Control Channel for Cognitive Radios,” *IEEE Transactions on Selected Areas in Communications*, vol. 30, no. 10, pp. 1875-1889, November 2012.

[83] S. Premnath, D. Wasden, S. K. Kasera, N. Patwari, and S. Farhang-Boroujeny, “Beyond OFDM: Best-Effort Dynamic Spectrum Access Using Filterbank Multicarrier,” *IEEE / ACM Transactions on Networking*, vol. 21, no. 3, pp. 869-882, June 2013.

[84] H. Lin, and P. Siohan, “Capacity Analysis for Indoor PLC Using Different Multi-Carrier Modulation Schemes,” *IEEE Transactions on Power Delivery*, vol. 25, no. 1, pp. 113-124, January 2010.

[85] P. Achaichia, M. L. Bot, and P. Siohan, “OFDM / OQAM: A Solution to Efficiently Increase the Capacity of Future PLC Networks,” *IEEE Transactions on Power Delivery*, vol. 26, no. 4, pp. 2443-2455, October 2011.

[86] M. G. S. Sriyananda, and N. Rajatheva, “Analysis of Self Interference in a Basic FBMC System,” *IEEE 78th Vehicular Technology Conference*, Las Vegas, Nevada, USA, September 2013.

[87] H. Minn, P. Tarasak, and V. Bhargava, “OFDM frequency offset estimation based on BLUE principle,” *IEEE 56th Vehicular Technology Conference*, Vancouver, Canada, September 2002.

[88] A. J. Coulson, “Maximum likelihood synchronization for OFDM using a pilot symbol: analysis,” *IEEE Journal on Selected Areas in Communications*, vol. 19, no. 12, pp. 2495–2503, December 2001.

[89] M. Morelli, and U. Mengali, “An improved frequency offset estimator for OFDM applications,” *IEEE Communications Letters*, vol. 3, no. 3, pp. 75-77, March 1999.

[90] T. Ihalainen, A. Ikhlef, J. Louveaux, and M. Renfors, “Channel Equalization for Multi-Antenna FBMC / OQAM Receivers,” *IEEE Transactions on Vehicular Technology*, vol. 60, no. 5, pp. 2070-2085, June 2011.

[91] D. Roque, and C. Siclet, “Performances of Weighted Cyclic Prefix OFDM with Low-Complexity Equalization,” *IEEE Communications Letters*, vol. 17, no. 3, pp. 439-442, March 2013.

[92] X. Mestre, M. Majoral, and S. Pfletschinger, “An Asymptotic Approach to Parallel Equalization of Filter Bank Based Multicarrier Signals,” *IEEE Transactions on Signal Processing*, vol. 61, no. 14, pp. 3592-3606, July 2013.

[93] M. Caus, and A. I. Pérez-Neira, “Transmitter-Receiver Designs for Highly Frequency Selective Channels in MIMO FBMC Systems,” *IEEE Transactions on Signal Processing*, vol. 60, no. 12, pp. 6519-6532, December 2012.

[94] T. H. Stitz, T. Ihalainen, and M. Renfors, “Mitigation of Narrowband Interference in Filter Bank Based Multicarrier Systems,” *IEEE International Conference on Communications*, Istanbul, Turkey, June 2006.

[95] G. Ndo, H. Lin, and P. Siohan, “FBMC / OQAM equalization : Exploiting the imaginary interference,” *IEEE 23rd International Symposium Personal Indoor and Mobile Radio Communications*, Sydney, Australia, September 2012.

[96] K. Sathananthan, and C. Tellambura, “Probability of Error Calculation of OFDM Systems with Frequency Offset,” *IEEE Transactions on Communications*, vol. 49, no. 11, pp. 1884-1888, November 2001.

[97] N. C. Beaulieu, “The Evaluation of Error Probabilities for Intersymbol and Cochannel Interference,” *IEEE Transactions on Communications*, vol. 39, no. 12, pp. 1740-1749, December 1991.

[98] R. Zakaria, and D. Le Ruyet, “On Maximum Likelihood MIMO Detection in QAM-FBMC Systems,” *IEEE 21st International Symposium on Personal Indoor and Mobile Radio Communications*, Istanbul, Turkey, September 2010.

[99] M. Payaró, A. Pascual-Iserte, and M. R. Nájar, "Performance Comparison Between FBMC and OFDM in MIMO Systems Under Channel Uncertainty," *European Wireless Conference*, Lucca, Italy, April 2010.

[100] M. K. Simon, and M. -S. Alouini, "A Unified Approach to the Performance Analysis of Digital Communication over Generalized Fading Channels," *Proceedings of the IEEE*, vol. 86, no. 9, pp. 1860-1877, September 1998.

[101] M. D. Yacoub, "The $\kappa - \mu$ distribution and the $\eta - \mu$ distribution," *IEEE Antennas and Propagation Magazine*, vol. 49, no. 1, pp. 68-81, February 2007.

[102] H. Lin, C. Lele, and P. Siohan, "Equalization with Interference Cancellation for Hermitian Symmetric OFDM/OQAM systems," *IEEE International Symposium on Power Line Communications and Its Applications, 2008*, Jeju Island, Korea, April 2008.

[103] Z. Du, J. Cheng, and N. C. Beaulieu, "Accurate Error-Rate Performance Analysis of OFDM on Frequency-Selective Nakagami-m Fading Channels," *IEEE Transactions on Communications*, vol. 54, no. 2, pp. 319-328, February 2006.

[104] A. Papoulis, and S. U. Pillai, *Probability, Random Variables and Stochastic Processes*, McGraw-Hill Inc., 4th Edition, 2002.

[105] J. W. Craig, "A New, Simple and Exact Result for Calculating the Probability of Errors for Two Dimensional Signal Constellations," *IEEE Military Communications Conference*, Virginia, USA, November 1991.

[106] M. Caus, and A. I. Perez-Neira, "Multi-Stream Transmission for Highly Frequency Selective Channels in MIMO-FBMC / OQAM Systems," *IEEE Transactions on Signal Processing*, vol. 62, no. 4, pp. 786-796, February 2014.

[107] M. Luzio, R. Dinis, and P. Montezuma, "SC-FDE for Offset Modulations: An Efficient Transmission Technique for Broadband Wireless Systems," *IEEE Transactions on Communications*, vol. 60, no. 7, pp. 1851-1861, July 2012.

[108] H. Saeedi-Sourck, Y. Wu, J. W. M. Bergmans, S. Sadri, and B. Farhang-Boroujeny, "Complexity and Performance Comparison of Filter Bank Multicarrier and OFDM in Uplink of Multicarrier Multiple Access Networks," *IEEE Transactions on Signal Processing*, vol. 59, no. 4, pp. 1907-1912, April 2011.

[109] S. S. Soliman, and N. C. Beaulieu, "Exact Analysis of Dual-Hop AF Maximum End-to-End SNR Relay Selection," *IEEE Transactions on Communications*, vol. 60, no. 8, pp. 2135-2145, August 2012.

[110] A. M. Salhab, F. Al-Qahtani, S. A. Zummo, and H. Alnuweiri, "Exact Outage Probability of Opportunistic DF Relay Systems With Interference at Both the Relay and the Destination Over Nakagami-m Fading Channels,"

IEEE Transactions on Vehicular Technology, vol. 62, no. 2, pp. 920-927, February 2013.

[111] M. R. Bhatnagar, “On the Capacity of Decode-and-Forward Relaying over Rician Fading Channels,” *IEEE Communications Letters*, vol. 17, no. 6, pp. 1100-1103, June 2013.

[112] H. Ding, J. Ge, D. B. D. Costa, and Y. Guo, “Outage Analysis for Multiuser Two-Way Relaying in Mixed Rayleigh and Rician Fading,” *IEEE Communications Letters*, vol. 15, no. 4, pp. 410-412, April 2001.

[113] J. N. Laneman, D. N. C. Tse, and G. W. Wornell, “Cooperative Diversity in Wireless Networks : Efficient Protocols and Outage Behavior,” *IEEE Transactions on Information Theory*, vol. 50, no. 12, pp. 3062-3080, November 2004.

[114] T. Wang, F. Glineur, J. Louveaux, and L. Vandendorpe, “Weighted Sum Rate Maximization for Downlink OFDMA With Subcarrier-Pair Based Opportunistic DF Relaying,” *IEEE Transactions on Signal Processing*, vol. 61, no. 10, pp. 2512-2524, May 2013.

[115] X. J. Li, and P. H. J. Chong, “A medium access control scheme for TDD-CDMA cellular networks with two-hop relay architecture,” *IEEE Transactions on Wireless Communications*, vol. 8, no. 5, pp. 2280-2285, May 2009.

[116] F. He, Y. Sun, L. Xiao, X. Chen, C-Y. Chi, and S. Zhou, “Capacity Region Bounds and Resource Allocation for Two-Way OFDM Relay Channels,” *IEEE Transactions on Wireless Communications*, vol. 12, no. 6, pp. 2904-2917, June 2013.

[117] T. Liu, and C. Yang, “Spectral Efficiency Comparison Between MC-CDMA Two-Hop Relay Systems With Different Channel Information,” *IEEE Transactions on Vehicular Technology*, vol. 61, no. 8, pp. 3603-3614, October 2012.

[118] D. S. Michalopoulos, H. A. Suraweera, G. K. Karagiannidis, and R. Schober, “Amplify-and-Forward Relay Selection with Outdated Channel Estimates,” *IEEE Transactions on Communications*, vol. 60, no. 5, pp. 1278-1290, May 2012.

[119] A. Nosratinia, T. E. Hunter, and A. Hedayat, “Cooperative communication in wireless networks,” *IEEE Communications Magazine*, vol. 48, no. 10, pp. 74-80, October 2004.

[120] D. Zahavi, I. Beer-Sheva, and R. Dabora, “Capacity Theorems for the Fading Interference Channel With a Relay and Feedback Links,” *IEEE Transactions on Information Theory*, vol. 58, no. 8, pp. 5185-5213, August 2012.

[121] M. Benjillali, and L. Szczecinski, “Detect-and-forward in two-hop relay channels: a metrics-based analysis,” *IEEE Transactions on Communications*, vol. 58, no. 6, pp. 1729-1736, June 2010.

[122] M. O. Hasna, and M-S. Alouini, "A performance study of dual-hop transmissions with fixed gain relays," *IEEE Transactions on Wireless Communications*, vol. 3, no. 6, pp. 1963-1968, November 2004.

[123] D. Lee, Y. S. Jung, and J. H. Lee, "Amplify-and-Forward Cooperative Transmission with Multiple Relays Using Phase Feedback," *IEEE 64th Vehicular Technology Conference*, Montreal, Quebec, Canada, September 2006.

[124] Y. Li, and B. Vucetic, "On the Performance of a Simple Adaptive Relaying Protocol for Wireless Relay Networks," *IEEE 67th Vehicular Technology Conference*, Singapore, May 2008.

[125] I. Krikidis, J. S. Thompson, S. Mclaughlin, and N. Goertz, "Max-min relay selection for legacy amplify-and-forward systems with interference," *IEEE Transactions on Wireless Communications*, vol. 8, no. 6, pp. 1536-1276, June 2009.

[126] M. Dong, M. Hajiaghayi, and B. Liang, "Optimal Fixed Gain Linear Processing for Amplify-and-Forward Multichannel Relaying," *IEEE Transactions on Signal Processing*, vol. 60, no. 11, pp. 6108-6114, November 2011.

[127] Z. Hadzi-Velkov, D. S. Michalopoulos, G. K. Karagiannidis, and R. Schober, "On the Effect of Outdated Channel Estimation in Variable Gain Relaying: Error Performance and PAPR," *IEEE Transactions on Wireless Communications*, vol. 12, no. 3, pp. 1084-1097, March 2013.

[128] S. Mallick, M. M. Rashid, and V. K. Bhargava, "Joint Relay Selection and Power Allocation for Decode-and-Forward Cellular Relay Network with Channel Uncertainty," *IEEE Transactions on Wireless Communications*, vol. 11, no. 10, pp. 3496-3508, October 2013.

[129] W. Xiugang, and L-L. Xie, "On the Optimal Compressions in the Compress-and-Forward Relay Schemes," *IEEE Transactions on Information Theory*, vol. 59, no. 5, pp. 2613-2628, May 2013.

[130] Z. Zhang, W. Zhang, and C. Tellambura, "Cooperative OFDM Channel Estimation in the Presence of Frequency Offsets," *IEEE Transactions on Vehicular Technology*, vol. 58, no. 7, pp. 3447-3459, September 2009.

[131] S. C. Ng, W. Zhang, Y. Zhang, Y. Yang, and G. Mao, "Analysis of Access and Connectivity Probabilities in Vehicular Relay Networks," *IEEE Transactions on Selected Areas in Communications*, vol. 29, no. 1, pp. 140-150, January 2011.

[132] S. Sohaib, and D. K. C. So, "Asynchronous Cooperative Relaying for Vehicle-to-Vehicle Communications," *IEEE Transactions on Communications*, vol. 29, no. 1, pp. 1732-1738, May 2013.

[133] C-I. Kuo, S-H. Wu, and C-K. Tseng, "Robust Linear Beamformer Designs for Coordinated Multi-Point AF Relaying in Downlink Multi-Cell Networks," *IEEE Transactions on Wireless Communications*, vol. 11, no. 9, pp. 3272-3283, September 2012.

[134] Q Li, R. Q. Hu, Y. Qian, and W. Geng, "Cooperative communications for wireless networks: techniques and applications in LTE-advanced systems," *IEEE Transactions on Wireless Communications*, vol. 19, no. 2, pp. 1536-1284, April 2012.

[135] Y. Zou, Y-D. Yao, and B. Zheng, "Cognitive Transmissions with Multiple Relays in Cognitive Radio Networks," *IEEE Transactions on Wireless Communications*, vol. 10, no. 2, pp. 648-659, February 2011.

[136] Y. Zou, Y-D. Yao, and B. Zheng, "A Cooperative Sensing Based Cognitive Relay Transmission Scheme Without a Dedicated Sensing Relay Channel in Cognitive Radio Networks," *IEEE Transactions on Signal Processing*, vol. 59, no. 2, pp. 854-858, February 2011.

[137] K. T. Truong, P. Sartori, and R. W. Heath, "Cooperative Algorithms for MIMO Amplify-and-Forward Relay Networks," *IEEE Transactions on Signal Processing*, vol. 61, no. 5, pp. 1272-1287, March 2013.

[138] R. S. Ganesan, H. Al-Shatri, A. Kuehne, T. Weber, and A. Klein, "Pair-Aware Interference Alignment in Multi-User Two-Way Relay Networks," *IEEE Transactions on Wireless Communications*, vol. 12, no. 8, pp. 3662-3671, August 2013.

[139] Z. Pengcheng, K. Yu, and A. L. Swindlehurst, "Wireless Relay Communications with Unmanned Aerial Vehicles: Performance and Optimization," *IEEE Transactions on Aerospace and Electronic Systems*, vol. 47, no. 3, pp. 2068-2085, July 2011.

[140] N. Goddemeier, K. Daniel, and C. Wietfeld, "Role-Based Connectivity Management with Realistic Air-to-Ground Channels for Cooperative UAVs," *IEEE Transactions on Selected Areas in Communications*, vol. 30, no. 5, pp. 951-963, June 2012.

[141] A. Bletsas, H. Shin, and M. Z. Win, "Outage optimality of opportunistic amplify-and-forward relaying," *IEEE Communications Letters*, vol. 11, no. 3, pp. 261-263, March 2007.

[142] Z. K. M. Ho, and E. A. Jorswieck, "Instantaneous Relaying: Optimal Strategies and Interference Neutralization," *IEEE Transactions on Signal Processing*, vol. 60, no. 12, pp. 6655-6668, December 2012.

[143] Z. Zheng, L. X. Cai, R. Zhang, and X. Shen, "RNP-SA: Joint Relay Placement and Sub-Carrier Allocation in Wireless Communication Networks

with Sustainable Energy," *IEEE Transactions on Wireless Communications*, vol. 11, no. 10, pp. 3818-3828, October 2012.

[144] K. T. K. Cheung, Y. Shaoshi, and L. Hanzo, "Achieving Maximum Energy-Efficiency in Multi-Relay OFDMA Cellular Networks: A Fractional Programming Approach," *IEEE Transactions on Communications*, vol. 61, no. 7, pp. 2746-2757, July 2013.

[145] X. He, and A. Yener, "Cooperation With an Untrusted Relay: A Secrecy Perspective," *IEEE Transactions on Information Theory*, vol. 56, no. 8, pp. 3807-3827, August 2010.

[146] C. Jeong, I-M. Kim, and D. I. Kim, "Joint Secure Beamforming Design at the Source and the Relay for an Amplify-and-Forward MIMO Untrusted Relay System," *IEEE Transactions on Signal Processing*, vol. 60, no. 1, pp. 310-325, January 2012.

[147] J. E. McInroy, G. W. Neat, and J. F. O'Brien, "A robotic approach to fault-tolerant, precision pointing," *IEEE Robotics & Automation Magazine*, vol. 6, no. 4, pp. 24-31, 37, December 1999.

[148] H-C. Bui, H. Meric, J. Lacan, and M. Boucheret, "A Cooperative Network Coding Strategy for the Interference Relay Channel," *IEEE Wireless Communications Letters*, vol. 1, no. 5, pp. 456-459, October 2012.

[149] W. Zhang, M. Stojanovic, and U. Mitra, "Analysis of a Linear Multihop Underwater Acoustic Network," *IEEE Journal of Oceanic Engineering*, vol. 36, no. 4, pp. 961-970, October 2010.

[150] D. Mattera, and M. Tanda, "Blind Symbol Timing and CFO Estimation for OFDM / OQAM Systems," *IEEE Transactions on Wireless Communications*, vol. 12, no. 1, pp. 268-277, January 2013.

[151] T. Fusco, A. Petrella, and M. Tanda, "Data-Aided Symbol Timing and CFO Synchronization for Filter Bank Multicarrier Systems," *IEEE Transactions on Wireless Communications*, vol. 8, no. 5, pp. 2705-2715, May 2009.

[152] M. G. S. Sriyananda, and N. Rajatheva, "Performance of an Asymmetric and Asynchronous Decode-and-Forward FBMC Relay System," *IEEE Wireless Communications and Networking Conference*, Istanbul, Turkey, April 2014.

[153] M. -S. Alouini, and A. J. Goldsmith, "Capacity of Rayleigh Fading Channels Under Different Adaptive Transmission and Diversity-Combining Techniques," *IEEE Transactions on Vehicular Technology*, vol. 48, no. 4, pp. 1165-1181, July 1999.

[154] Y. Medjahdi, M. Terré, D. Le Ruyet, and D. Roviras, "On Spectral Efficiency of Asynchronous OFDM / FBMC based Cellular Networks," *IEEE 22nd International Symposium on Personal Indoor and Mobile Radio Communications*, Toronto, Canada, September 2011.

[155] A. Abdi, and M. Kaveh, “A space-time correlation model for multielement antenna systems in mobile fading channels,” *IEEE Journal on Selected Areas in Communications*, vol. 20, no. 3, pp. 550-560, April 2002.

[156] N. H. Vien, H. H. Nguyen, and T. Le-Ngoc, “Diversity Analysis of Smart Relaying,” *IEEE Transactions on Vehicular Technology*, vol. 58, no. 6, pp. 2849-2862, July 2009.

[157] N. H. Vien, and H. H. Nguyen, “Performance Analysis of Fixed-Gain Amplify-and-Forward Relaying With MRC,” *IEEE Transactions on Vehicular Technology*, vol. 59, no. 3, pp. 1544-1552, March 2010.

[158] R. Manna, R. H. Y. Louie, L. Yonghui, and B. Vucetic, “Cooperative Spectrum Sharing in Cognitive Radio Networks With Multiple Antennas,” *IEEE Transactions on Signal Processing*, vol. 59, no. 11, pp. 5509-5522, November 2011.

[159] S. Hussain, and X. N. Fernanado, “Closed-Form Analysis of Relay-Based Cognitive Radio Networks over Nakagami-m Fading Channels,” *IEEE Transactions on Vehicular Technology*, vol. 63, no. 3, pp. 1193-1203, March 2014.

[160] Z. Ding, M. Peng, and H-H. Chen, “A General Relaying Transmission Protocol for MIMO Secrecy Communications,” *IEEE Transactions on Vehicular Technology*, vol. 60, no. 11, pp. 3461-3471, November 2012.

[161] Z. Ding, and H. V. Poor, “A General Framework of Precoding Design for Multiple Two-Way Relaying Communications,” *IEEE Transactions on Signal Processing*, vol. 61, no. 6, pp. 1531-1535, March 2013.

[162] M. Dehghan, D. L. Goeckel, M. Ghaderi, and Z. Ding, “Energy Efficiency of Cooperative Jamming Strategies in Secure Wireless Networks,” *IEEE Transactions on Wireless Communications*, vol. 11, no. 9, pp. 3025-3029, September 2012.

[163] Z. Ding, K. K. Leung, D. L. Goeckel, and D. Towsley, “On the Application of Cooperative Transmission to Secrecy Communications,” *IEEE Journal on Selected Areas in Communications*, vol. 30, no. 2, pp. 359-368, February 2012.

[164] H. Bolcskei, M. Borgmann, and A. J. Paulraj, “Impact of the propagation environment on the performance of space-frequency coded MIMO-OFDM,” *IEEE Journal on Selected Areas in Communications*, vol. 21, no. 3, pp. 427-439, April 2003.

[165] Z. Zhang, and C. Tellambura, “The Effect of Imperfect Carrier Frequency Offset Estimation on an OFDMA Uplink,” *IEEE Transactions on Communications*, vol. 57, no. 4, pp. 1025-1030, April 2009.

[166] K. Lee, S-H. Moon, S. Kim, and I. Lee, "Sequence Designs for Robust Consistent Frequency-Offset Estimation in OFDM Systems," *IEEE Transactions on Vehicular Technology*, vol. 62, no. 3, pp. 1389-1394, March 2013.

APPENDIX 1 SUBCARRIER FILTER

It is very important to have a proper subcarrier filter for an FBMC system. In fact, this can be considered as the most important component of this particular physical layer communication technique. Localization property in both time and frequency domains and simplicity are among the foremost factors considered in filter selection.

APPENDIX 1.1 Subcarrier Filters

Different types of filters that can be used for FBMC, their characteristics, design principles and limitations are discussed in [20].

APPENDIX 1.2 PHYDYAS Filter

Out of two suitable filters PHYDYAS [24]-[26] and IOTA [27], [28], PHYDYAS NPR filter which is with smaller number of side lobes and spectral leakages, is used for this study (A1.1), (A1.4). The same filter is used as the transmit filter and as the receive filter. Overlapping factor, normalization factor, λth filter coefficient and half of the total number of subcarriers are represented by Λ, A, B_λ and $2M$ respectively. The parameters for the filter are set to $\Lambda = 4$, $B_1 = 0.9711100$, $B_2 = \frac{1}{\sqrt{2}}$ and $B_3 = 0.235147$ [24]-[26]. Symbol signaling interval is denoted by T_s.

APPENDIX 1.2.1 Continuous Domain Formulation

Continuous domain representation of the filter can be given as

$$f(t) = \begin{cases} 1 + 2\sum_{\lambda=1}^{\Lambda-1} (-1)^\lambda B_\lambda cos\left(\frac{2\pi\lambda t}{\Lambda T_s}\right) & 0 < t < \Lambda T_s \\ 0 & elsewhere \end{cases} . \tag{A1.1}$$

Filter Normalization Factor

For a higher accuracy, continuous domain filter $f(t)$ at time t is considered (A1.1) in determining the normalization factor,

$$\begin{aligned} A &= \int_0^{\Lambda T_s} [f(t)]^2 \, dt \\ &= 16T_s. \end{aligned} \tag{A1.2}$$

Then the normalized filter $p(k)$, $p(k) = \frac{1}{\sqrt{2A}} f(k)$ (power normalized to $1/2$) is given as

$$p(t) \quad = \quad \begin{cases} \frac{1}{\sqrt{2A}} \left[1 + 2 \sum_{\lambda=1}^{\Lambda-1} (-1)^{\lambda} B_{\lambda} cos \left(\frac{2\pi\lambda t}{\Lambda T_s} \right) \right] & 0 < t < \Lambda T_s \\ 0 & elsewhere \end{cases} . \quad \text{(A1.3)}$$

APPENDIX 1.2.2 Discrete Domain Formulation

Discrete domain formulation for the filter is given as

$$f[k] \quad = \quad \begin{cases} 1 + 2 \sum_{\lambda=1}^{\Lambda-1} (-1)^{\lambda} B_{\lambda} cos \left(\frac{2\pi\lambda k}{2\Lambda M} \right) & 1 \leq k \leq L_F - 1 \\ 0 & elsewhere \end{cases} . \quad \text{(A1.4)}$$

The length of the filter L_F is set to ΛM. Now the normalized filter $p[k]$, $p[k] = \frac{1}{\sqrt{2A}} f[k]$ (power normalized to $1/2$) can be presented as

$$p[k] \quad = \quad \begin{cases} \frac{1}{\sqrt{2A}} \left[1 + 2 \sum_{\lambda=1}^{\Lambda-1} (-1)^{\lambda} B_{\lambda} cos \left(\frac{2\pi\lambda k}{2\Lambda M} \right) \right] & 1 \leq k \leq L_F - 1 \\ 0 & elsewhere \end{cases} . \quad \text{(A1.5)}$$

The normalized filter in time-domain with $M = 32$ is given in Figure 27. Same filter in frequency domain, converted with Fourier transform on subcarrier $m = 32$ and two other adjacent subcarrier filters on $m - 1$ and $m + 1$ are given in Figure 28.

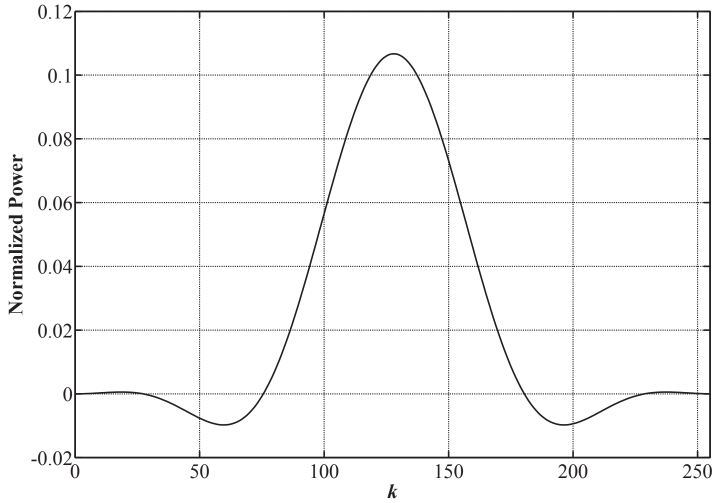

FIGURE 27 Normalized filter - Time domain

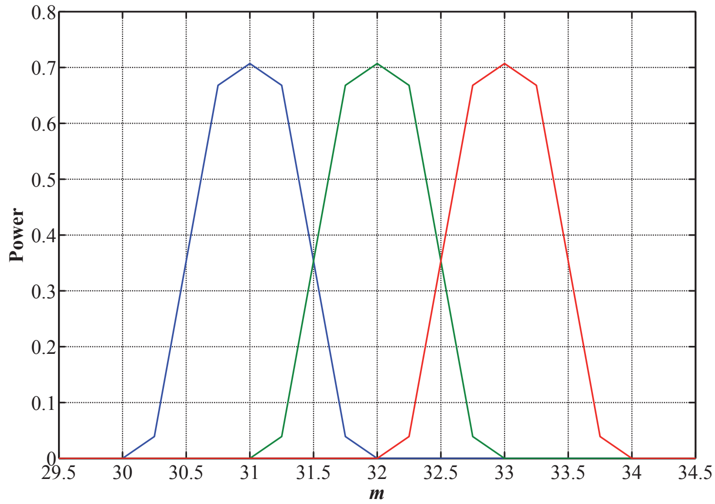

FIGURE 28 Normalized filter - Frequency domain

APPENDIX 2 SIMPLE DETECTION TECHNIQUE FOR FBMC

Many signal detection techniques for FBMC can be seen in the literature where most of them are with computationally complex multitap equalizers [90], [94], [106], [107]. Relatively higher implementation complexity associated with them can be observed. Lesser computationally complex simple single tap equalizers also can be seen as in [108].

APPENDIX 2.1 Introduction

A simple detection scheme that is with the same performance as the technique based on the minimum distance under synchronous and one-tap channel conditions is presented here.

APPENDIX 2.2 Detection Technique

Derivation is done in general for a SISO FBMC system operated in an asynchronous multipath channel. Here it is also assumed that the receive filter is same as the transmit filter. Considering the receive signal an asynchronous multipath channel after filtering as in (2.24),

$$\begin{aligned} y\left[m', n', \epsilon\right] &= 2\sum_{m=0}^{2M-1}\sum_{n=0}^{\infty} a_{m,n} e^{j\left(\psi_{m,n}-\psi_{m',n'}\right)} \sum_{l=0}^{L-1} h_l e^{-j\frac{2\pi(m+\epsilon)}{2M}l} \sum_{k=0}^{\infty} p\left[k-n'M\right] \\ &\quad .\, p[k-l-nM] e^{j\frac{2\pi}{2M}(m-m'+\epsilon)\left(k-\frac{L_F-1}{2}\right)} + \eta\,[k]. \end{aligned} \tag{A2.1}$$

Signal with the desired symbol is given as in (4.16) with $(m = m')$ and $(n = n')$,

$$\begin{aligned} y_a\left[m', n', \epsilon\right] &= 2a_{m,n} \sum_{l=0}^{L-1} h_l e^{-j\frac{2\pi(m+\epsilon)}{2M}l} \sum_{k=0}^{\infty} p[k-nM] \\ &\quad .\, p[k-l-nM] e^{j\frac{2\pi}{2M}(\epsilon)\left(k-\frac{L_F-1}{2}\right)}. \end{aligned} \tag{A2.2}$$

Let coefficient q_{FBMC} be defined as

$$q_{FBMC} = \frac{\left[\sum_{l=0}^{L-1} \hat{h}_l e^{-j\frac{2\pi(m+\epsilon)}{2M}l} \sum_{k=0}^{\infty} p[k-nM]p[k-l-nM] e^{j\frac{2\pi}{2M}(\epsilon)\left(k-\frac{L_F-1}{2}\right)}\right]^*}{\left|\sum_{l=0}^{L-1} \hat{h}_l e^{-j\frac{2\pi(m+\epsilon)}{2M}l} \sum_{k=0}^{\infty} p[k-nM]p[k-l-nM] e^{j\frac{2\pi}{2M}(\epsilon)\left(k-\frac{L_F-1}{2}\right)}\right|}. \tag{A2.3}$$

The phase compensated receive signal can be given by $q_{FBMC}y[m',n',\epsilon]$. Then the estimated receive real data symbol can be expressed as

$$\hat{a}_{m,n} = \Re\left\{\frac{q_{FBMC}y[m',n',\epsilon]}{2\left|\sum_{l=0}^{L-1}\hat{h}_l e^{-j\frac{2\pi(m+\epsilon)}{2M}l}\sum_{k=0}^{\infty}p[k-nM]p[k-l-nM]e^{j\frac{2\pi}{2M}(\epsilon)\left(k-\frac{L_F-1}{2}\right)}\right|}\right\}. \quad \text{(A2.4)}$$

The detection methodology is somewhat similar to EGC where it can be extended to FBMC systems with diversity receivers.